2008

TRANSLATIONAL REGULATORY MECHANISMS OF THE RAT AND HUMAN MULTIDRUG RESISTANCE PROTEIN 2

Yuanyuan Zhang
University of Kentucky, yzhang@uky.edu

ABSTRACT OF DISSERTATION

Yuanyuan Zhang

The Graduate School

University of Kentucky

2008

TRANSLATIONAL REGULATORY MECHANISMS OF THE RAT AND HUMAN MULTIDRUG RESISTANCE PROTEIN 2

ABSTRACT OF DISSERTATION

A dissertation submitted in partial fulfillment of the requirements for the degree of Doctor of Philosophy in the Graduate School at the University of Kentucky

By
Yuanyuan Zhang

Lexington, Kentucky

Director: Dr. Mary Vore, Professor of Toxicology

Lexington, Kentucky

2008

ABSTRACT OF DISSERTATION

TRANSLATIONAL REGULATORY MECHANISMS OF
THE RAT AND HUMAN MULTIDRUG RESISTANCE PROTEIN 2

Multidrug resistance protein 2 (MRP2) is the second member the C subfamily in the superfamily of adenosine triphosphate (ATP)-binding cassette (ABC) efflux transporters. MRP2 is a critical player for generation of bile acid-independent bile flow and biliary excretion of glutathione, glucuronate and sulfate conjugates of endo- and xenobiotics. Dysfunctional expression of MRP2 is associated with Dubin-Johnson Syndrome.

Pathological and physiological states or xenobiotics change the MRP2 expression level. Under some conditions, expression of the human MRP2 and rat Mrp2 proteins are regulated at the translation level. There are several transcription initiation sites in *MRP2/Mrp2* gene. The 5' untranslated regions (5'UTRs) of MRP2/Mrp2 contains multiple translation start codons. The focus of this study, therefore, was investigation of the translational regulatory mechanisms mediated by the upstream open reading frames (uORF) of MRP2/Mrp2.

Using *in vitro* translation assays and transient cotransfection assays in HepG2 cells, we showed that the rat uORF1 starting at position -109 (relative to the ATG of Mrp2) and the human uORF2 starting at position -105 (relative to the ATG of MRP2) are two major *cis*-acting inhibitors of translation among the rat and human multiple uORFs, respectively. Translational regulation mediated by the uORFs in the rat Mrp2 mRNA is a combined effect of the leaky scanning model and the reinitiation model, and also results from interaction of the multiple uORFs. In addition, by Ribonuclease Protection Assays (RPA), we detected multiple transcription initiation sites of *MRP2*/*Mrp2* gene in tissues. We also found that the relative abundance of the rat Mrp2 mRNA isoforms with different 5'UTRs differed in the rat liver, kidney, jejunum, ileum, placenta, and lung. This is the first study on the translational regulatory mechanisms of the *MRP2/Mrp2* gene.

KEYWORDS: Multidrug resistance protein 2 (MRP2), Translational regulation,

5’ Untranslated region (5’UTR), Upstream open reading frame (uORF), Transcription initiation sites.

Yuanyuan Zhang

August 15, 2008

TRANSLATIONAL REGULATORY MECHANISMS OF THE RAT AND HUMAN MULTIDRUG RESISTANCE PROTEIN 2

By

Yuanyuan Zhang

Mary Vore
Director of Dissertation

David Orren
Director of Graduate Studies

August 15, 2008

RULES FOR THE USE OF DISSERTATIONS

Unpublished dissertations submitted for the Doctor's degree and deposited in the University of Kentucky Library are as a rule open for inspection, but are to be used only with due regard to the rights of the authors. Bibliographical references may be noted, but quotations or summaries of parts may be published only with the permission of the author, and with the usual scholarly acknowledgments.

Extensive copying or publication of the dissertation in whole or in part also requires the consent of the Dean of the Graduate School of the University of Kentucky.

A library that borrows this dissertation for use by its patrons is expected to secure the signature of each user.

Name	Date

DISSERTATION

Yuanyuan Zhang

The Graduate School

University of Kentucky

2008

TRANSLATIONAL REGULATORY MECHANISMS OF THE RAT AND HUMAN MULTIDRUG RESISTANCE PROTEIN 2

DISSERTATION

A dissertation submitted in partial fulfillment of the requirements for the degree of Doctor of Philosophy in the Graduate School at the University of Kentucky

By

Yuanyuan Zhang

Lexington, Kentucky

Director: Dr. Mary Vore, Professor of Toxicology

Lexington, Kentucky

2008

ACKNOWLEDGEMENTS

The following dissertation, while an individual work, benefited from contributions of many people. I owe my gratitude to all those people who have made this dissertation possible and because of whom my graduate experience has been one that I will cherish forever.

First, my deepest gratitude is to my advisor, Dr. Mary Vore, for her generous time and commitment. I have been amazingly fortunate to have her as my mentor who exemplifies the excellence in scholarship to which I aspire as a scientist. Throughout my doctoral work, Dr. Vore encouraged me to develop independent thinking and research skills. She continually and greatly assisted me with scientific writing and presentation skills. Her patience and support helped me overcome crisis situations and finish this dissertation.

Next, I wish to thank the complete Dissertation Committee, and outside reader, respectively: Dr. Charlotte Kaetzel, Dr. Daret St. Clair, Dr. Hsin Sheng Yang, Dr. Stephen Zimmer who unfortunately passed away, and Jeffrey Moscow. Each individual provided insights that guided and challenged my thinking, substantially improving the finished product.

Finally, I extend many thanks to my current and previous colleagues and friends, especially Dr. Wei Li, Dr. Phil Gerk, Dr. Marcie Wood, Dr. Bret Jones, Dr. Paiboon Jungsuwadee, Dr. Tianyong Zhao, Dr. Aldo Mottino, and fellow graduate students Ruth Wooton-Kee, Vandana Megaraj, Donna Coy, Antony Athippozhy. I thank them for the many valuable discussions and insights to this work, and for

providing help with my presentation skills. I would like to thank Tim Hoffman and Baoxiang Yan for being so organized and helpful in the laboratory.

In addition, I have received invaluable support from my family members, although all of them are living in China. To my parent, Ming Yue and Suying Ma, thank you for the love, encouragement and continuous support for me to pursue higher education. I am grateful to my sister, Fang Yue, and her family for supporting and taking care of my parents. I also appreciate the financial support of my aunt, Hongyi Zhang, and her family for all of my education. And last, but not least, I owe special thanks to my fiancé, Jeffrey Bernardo, for his love and tolerance and for encouraging me to finish the writing. He and his mom give me another home in this country.

TABLE OF CONTENTS

Acknowledgments……iii

List of Tables..……vii

List of Figures……...viii

List of Files……x

Chapter One: Introduction……1

Chapter Two: Translational Regulation of Rat Multidrug Resistance Protein 2 (Mrp2) Expression is Mediated by Upstream Open Reading Frames (uORFs) in the 5' Untranslated Region (UTR)……..……....18

Background…….…….18

Materials and Methods..……...21

Results……..……26

Conclusions……..31

Chapter Three: Determination of Sequence Dependence of the Translational Inhibitory Effect Exerted by uORF1 and Investigation Regarding Expression of Its Encoded Peptide (Pep56) in Rat issues……...41

Background…….…….41

Materials and Methods.……...44

Results……..……..50

Conclusions……...54

Chapter Four: Translational Regulation of Human Multidrug Resistance Protein 2 (MRP2) is Mediated by the 5' Untranslated Regions……..69

Background……..……..69

Materials and Methods..……72

Results……..…….……..…77

Conclusions……..……81

Chapter Five: Discussion……..……..…95

Appendices……..……...117

Appendix A: List of Abbreviations……..……...……...…117

Appendix B: Ribonuclease Protection Assay (RPA)…….……118

Appendix C: *In Vitro* Translation Assay……..……..123

Appendix D: Site-directed Mutagenesis……..….125

Appendix E: The First Strand of cDNA Preparation……...126

Appendix F: Online Programs……..……..127

References……..……128

Vita……..139

LIST OF TABLES

Table 2.1. Primers used for PCR amplification of the rat *Mrp2* 5'UTR cDNAs….40

Table 3.1. Primers used in site-directed mutagenesis for determination of sequence dependence ……66

Table 4.1. Primers used in site-directed mutagenesis for construction of human MRP2 5'UTRs fused T7 luciferase vectors..……..……..…..94

LIST OF FIGURES

Figure 1.1. Schematic representation of eukaryotic translation initiation.……17

Figure 2.1. Construction of fusion plasmids…….……...32

Figure 2.2. Identification of transcription initiation sites of the *Mrp2* gene and the relative abundance in rat tissues by RPA……....34

Figure 2.3. The relative abundance of transcription initiation sites of the *Mrp2* gene in neonatal rat tissues and adults by RPA…….……..…….....35

Figure 2.4. Effect of the Mrp2 5'UTRs on expression of the luciferase reporter gene in HepG2 cell transient cotransfection assays…….....37

Figure 2.5. Effect of the Mrp2 5'UTRs on translation efficiency of the luciferase reporter transcript by *in vitro* translation assays……...38

Figure 2.6. *In vitro* expression in the Transcription/Translation coupled system……..39

.

Figure 3.1. Schematic representation of construction of plasmids……...56

Figure 3.2. Sequence dependence of uORF1 on translation by *in vitro* translation assays……..……...58

Figure 3.3. Determination of the *cis*- or *trans*-acting effect of uORF1 on translation by *in vitro* translation assay……..……...60

Figure 3.4. Expression of Pep56 in the Transcription/Translation coupled system……..62

Figure 3.5. Detection of Pep56 in the rat liver and kidney by Western Blot…...63

Figure 3.6. Titration with the antigen peptide…….....….64

Figure 3.7. Immunoprecipitation of the rat kidney homogenate with PAS……..65

Figure 4.1. The cDNA sequence of the 5'UTR and the schematic representation of organization of uORFs of the human MRP2……...…83

Figure 4.2. Detection by RPA of transcription initiation sites of MRP2 and the relative abundance in the human liver and HepG2 cells. ……..……..……85

Figure 4.3. Effect of the human MRP2 5'UTRs on expression of the luciferase gene in HepG2 cells in transient cotransfection assays……....86

Figure 4.4. Effect of the human MRP2 5'UTRs on translation efficiency of the luciferase transcript by *in vitro* translation assays……..…….88

Figure 4.5. Determination of sequence dependence of uORF2 on translation by *in vitro* translation assays……..……...90

Figure 4.6. Determining whether uORF2 acts as a *cis*- or *trans*- regulator on translation by *in vitro* translation assay……..…...92

Figure 5.1. The hypothetical mechanic model of uORFs-mediated translational regulation of the rat Mrp2 mRNA……..……114

LIST OF FILES

DissertationYuanyuanZhang.pdf	2.17MB

CHAPTER ONE

INTRODUCTION

Multidrug resistance protein 2 (MRP2, also ABCC2) is the second member identified of the 12 transporters of the C subfamily in the superfamily of adenosine triphosphate (ATP)-binding cassette (ABC) efflux transporters [1]. It is also termed the canalicular multispecific organic anion transporter (cMOAT) and canalicular multidrug resistance protein (cMRP2) [2, 3]. Forty eight ABC transporters have been identified in human beings, and grouped into seven subfamilies designated from A to G, based on the amino acid sequence similarity and phylogeny. Human MRP2 and rat Mrp2 are integral plasma membrane proteins and are exclusively expressed in the apical membrane of polarized cells of human and rat liver [2, 4, 5], kidney proximal tubules [6, 7], small intestine [8-10], human colon [9, 11], gallbladder [12], bronchi [9, 11], and placenta [13, 14]. The human hereditary disorder, Dubin-Johnson Syndrome, is characterized by conjugated hyperbilirubinemia and is associated with the absence of expression of the functional MRP2 in the canalicular membrane of hepatocytes [2, 15]. Expression of Mrp2 is absent in the natural animal models of Dubin-Johnson Syndrome: the Groningen yellow/transport deficient Wistar rat (GY/TR$^-$) and the Eisai hyperbilirubinemic Sprague-Dawley rat (EHBR). This is due to 1bp deletion in the *Mrp2* gene that results in introduction of a premature stop codon in the mRNA and subsequent degradation of the transcript [4, 16, 17]. Like MRP1, MRP2/Mrp2 are predicted by computational analysis to contain three membrane-spanning domains (MSD0, MSD1, and MSD2) consisting of 17 transmembrane

helices. There are two highly conserved nucleotide-binding domains, NBD1 and NBD2, following MSD1 and MSD2, respectively [4, 18, 19]. Further, the extracellular localization of the amino terminus of human MRP2 is confirmed by immunofluorescence studies [19, 20].

Generation of bile flow is dependent on active transport of osmotically active solutes across the canalicular membrane of hepatocytes into the canaliculi. The two major solute contributors to bile are bile salts and glutathione (GSH). Because of its localization and substrate specificity, MRP2/Mrp2 is considered to be a critical player for generation of bile acid-independent bile flow. It is exclusively present on the canalicular membrane of hepatocytes, and excretes GSH and conjugates of glutathione, glucuronide, and sulfate into bile. In addition to the conjugated bile acids, substrates of MRP2/Mrp2 include organic anions of endogenous and exogenous origin, such as leukotriene C_4, 2,4 dinitrophenyle-S-glutathione (DNP-SG), and estradiol-17β-D-glucuronide ($E_2$17G).

Regulation of MRP2/Mrp2 expression

Expression of MRP2/Mrp2 is also tissue-specific and regulated by drug treatments and diseases. Regulation of *MRP2/Mrp2* expression occurs at all levels: transcription, post-transcription, translation, and post-translation (e.g., endocytic retrieval from the apical membrane).

Transcriptional regulation. Kauffmann et. al sequenced the 5'-flanking region of the rat *Mrp2* gene (-1073 to -14 bp with respect to the translation start site). They characterized two regions that mediate constitutive expression of *Mrp2*: 17

bp at position -317 to -290 and 37 bp at position -250 to -214. The first region contains an inverted CCAAT element, which is the core sequence of the Y-Box. The second region is a GC-Box, which is a binding site for the transcription factor, specificity protein (Sp1). The regulatory mechanism of constitutive expression of the *Mrp2* gene is very similar to *MRP1* or members of the *Mdr1* family. Other putative binding sites for transcription factors found by computational analysis are several glucocorticoid responsive elements (GREs) and peroxisome proliferators responsive elements (PPREs), as well as activator protein 1 (AP1), C-repeat binding factor (CBF), CCAAT-enhancer binding protein α (C/EBPα), enhancer factor I A (EFIA), hepatic nuclear factor 1 (HNF1), c-Myb, polyomavirus enhancer A binding protein-3 (PEA3), and Sp1 [21].

The 2.7 kb 5'-flanking region of the human *MRP2* gene in a human placental genomic library has also been sequenced [22]. A positive regulatory element is localized in the -431 to -258 bp region that contains the transcription factor binding site of C/EBPβ. Comparison of the 5'-flanking regions between human and rat shows 51% nucleotide sequence identity. Both contain two elements, hepatic nuclear factor 1 (HNF1) and upstream stimulatory factor (USF)-like element, which are predicted by computational programs [22].

Expression of the *Mrp2* gene in rat hepatocytes is inducible by a variety of carcinogenic and chemotherapeutic agents, such as 2-acetylaminofluorene (2-AAF), cisplatin, phenobarbital, ethiny estradiol and cyclohemixide [21]. The mRNA levels of MRP2/Mrp2 are up-regulated in human and rat hepatoma cell lines (HepG2 and FAO cells, respectively), following treatment of agonists of the

farnesoid X-activated receptor (FXR), the pregnane X receptor (PXR), and the constitutive androstane receptor (CAR). In the rat 5' flanking region of the *Mrp2* gene, an unusual 26 bp sequence at position -401 to -376 is identified to contain two copies of the AGTTCA hexad organized as an ER-8. PXR, CAR or FXR bind to ER-8 as a heterodimer with the retinoid X receptor α (RXRα) [23].

Expression of both Mrp2 mRNA and protein is reduced in the cholestatic rat liver induced by bile duct ligation or endotoxin [24-26]. This down-regulation induced by endotoxin is partly due to up-regulated expression of the inflammatory cytokine interleukin-1β (IL-1β). IL-1β is reported to down-regulate the heterodimer of retinoic acid receptor α (RARα)/RXRα, resulting in down-regulation of *Mrp2* promoter activity [27, 28]. In HepG2 cells, IL-1β represses expression of the *MRP2* gene because it inactivates binding of the interferon regulatory factor (IRF3) to the interferon stimulatory response element (ISRE) on the *MRP2* promoter [29].

Endocytic retrieval from the apical membrane. Transporter function is also regulated at the post-translation level due to trafficking of MRP2/Mrp2 protein between the canalicular membrane and a peri-canalicular pool of vesicles. Mrp2 is retrieved into intracellular structures following isolation and culture of rat hepatocytes, and resorted into the apical membrane in a time-dependent fashion, which is consistent with changes in transport activity [30]. The trafficking of Mrp2 protein and changes in transport activity are confirmed in sandwich-cultured rat hepatocytes [31].

This trafficking is inducible. Phalloidin, a potent mushroom hepatotoxin and cholestatic agent, induces significant internlization of Mrp2 along with other canalicular proteins. The induced retrieval coincides with decreased bile flow and decreased biliary excretion of Leukotriene (LTC_4), an Mrp2 substrate [32]. Treatment of rats with lipopolysaccharide (LPS) causes endocytic retrieval of Mrp2 along with cholestasis [33, 34]. Finally, a single dose of estradiol-17β-D-glucuronide ($E_2$17G) induces a potent dose-dependent and reversible inhibition of bile flow in the rat. This coincides with a rapid endocytic internalization of Mrp2 and with subsequent spontaneous exocytic insertion of Mrp2 into the apical membrane [35].

Retrieval of the hepatic MRP2 in human beings is also reported in several studies. Percutaneous transhepatic biliary drainage (PTBD) is a treatment to reduce hyperbilirubinemia in patients with obstructive cholestasis. In the liver biopsy specimens of cholestatic patients who were poorly drained, fuzzy immunostaining of MRP2, which indicates internalization from the canalicular membrane, is observed, in contrast to the linear and intense immunostaining outlining the canalicular membrane domain in the liver of control subjects, which indicates canalicular membrane localization. This correlates with the impaired bilirubin conjugate and bile acid secretion [36]. Moreover, hepatic MRP2 immunostaining is broadened and irregular in non-icteric primary biliary cirrhosis (PBC) stage III, while a thin and clear line on the canalicular membrane is seen in controls. This indicates re-distribution of MRP2 localization from the canalicular membrane into intracellular structures of the hepatocytes in PBC-III patients [37].

Many studies have addressed the mechanisms of altered localization of MRP2/Mrp2 in the cholestatic liver. Cyclic AMP stimulates microtubule-dependent transport of vesicles [38]. $E_2$17G induces endocytic retrieval of hepatic Mrp2 in rats. But treatment of dibutyryl-cyclic AMP (DBcAMP) preceding $E_2$17G attenuates this retrieval and accelerates re-distribution of Mrp2 into the canalicular membrane along with restoration of bile flow. In contrast, prior administration of colchicine that disrupts microtubules, blocks the actions of DBcAMP [39]. The data indicate involvement of microtubule in Mrp2 trafficking.

Radixin is a cross-linker between actin filaments and plasma membrane proteins. Radixin knockout mice show a loss of Mrp2 from the canalicular membrane and develop conjugated hyperbilirubinemia [40]. In the rat models of intrahepatic and extrahepatic cholestasis, along with endocytic retrieval of hepatic Mrp2, the colocalization of Mrp2 and radixin is disturbed. Phosphorylated radixin shown by fluorescence markedly decreases in both intra- and extrahepatic cholestasis in rats, indicating an important role of the reduced phosphorylated radixin in the endocytic retrieval of Mrp2 in cholestasis [41]. That is, inactivation of radixin may weaken anchorage of Mrp2 in the canalicular membrane [41]. Disturbed colocalization of MRP2 and radixin as well as endocytic retrieval of MRP2 is detected by immunofluorescence in various human cholestatic liver diseases [42]. The mechanisms of disturbed interaction between radixin and Mrp2/MRP2 in cholestasis are still unclear. But radixin is essentially involved in maintaining the canalicular localization of Mrp2, since

down-regulated radixin by iRNA induces dissociation of Mrp2 from the canalicular membrane and down-regulates Mrp2 function [43].

Translational regulation. Under some conditions, expression of MRP2/Mrp2 undergoes translational regulation. Hepatic Mrp2 protein is expressed 50% less in the pregnant rat liver than in the control rat, even though the mRNA level is unchanged [44-46]. Ethinylestradiol (EE2) decreases the Mrp2 protein markedly in the rat liver, but the mRNA does not change. Moreover, treatment with EE2 does not affect the relative abundance of the three Mrp2 mRNA transcripts that contain different 3'-untranslated regions (UTR) [26]. In cultured H4IIE cells, a rat hepatoma cell line, EE2 treatment also caused a significant decrease in the Mrp2 protein in contrast to an increase in the Mrp2 mRNA level [21]. Conversely, hepatic Mrp2 protein in rats treated with pregnenolone 16α-carbonitrile (PCN) increases 2-3 fold, while the mRNA level is not changed [46, 47]. Together, the data show a poor association between the Mrp2 protein and mRNA, indicating that under these conditions and treatments, Mrp2 protein expression is under post-transcriptional regulation.

To investigate the mechanism of post-transcriptional regulation of Mrp2 expression, our lab previously analyzed Mrp2 synthesis and degradation in 19- and 20-day pregnant rats, and PCN-treated rats as well as in control female rats. [^{35}S]cysteine/methionine and [^{14}C]$NaHCO_3$ were administered into rats to study the rate of synthesis and the degradation half-life of Mrp2 protein, respectively. The measured degradation half-lives of ^{14}C-labeled Mrp2 are not significantly different in control, pregnant, and PCN-treated rats (27, 36, and 22 h,

respectively). However, the rate of incorporation of ^{35}S into hepatic Mrp2 is the highest in the PCN-treated rats relative to that in the control rats. The initial rate of synthesis in the pregnant rats could not be obtained because of the very low level of incorporation of ^{35}S into Mrp2 protein. Additionally, polysomal distribution analysis of hepatic Mrp2 mRNA in the control, pregnant, and PCN-treated female rats showed that 1) more Mrp2 mRNA transcripts are associated with polysomes in the PCN treated rats; 2) more Mrp2 mRNA transcripts are associated with a single ribosome in the pregnant rats. In both cases, no major change is observed in relative distribution of the Mrp2 mRNA 5'UTRs. Therefore, post-transcriptional regulation in the control, pregnant, and PCN-treated rats occurs not through degradation of Mrp2 protein, but through the rate of Mrp2 protein synthesis, indicating translational regulation of rat Mrp2 protein [46].

Moreover, along the small intestine in rats, expression of Mrp2 protein is maximal in the duodenum and jejunum, and decreases gradually to 5% of the maximum in the terminal ileum, whereas there is no significant decrease of the Mrp2 mRNA level in the terminal ileum compared to that in the duodenum/jejunum [48].

Several studies show that expression of human hepatic MRP2 protein also undergoes translational regulation. No changes in the MRP2 mRNA levels are observed in patients with icteric inflammatory cholestasis, but the MRP2 protein levels are markedly reduced as shown by immunolabeling [49]. In one experimental model, cholestasis is induced by enodotoxin or lipopolysaccharide (LPS). The acute phase response of liver to LPS treatment is initiated by

producing pro-inflammatory cytokines such as TNF-α, IL-1 β, and IL-6, as well as anti-inflammatory cytokines such as IL-10 [50]. LPS treatment of human liver slices impairs expression of MRP2 protein, with the mRNA level unchanged and no intracellular vesicles containing MRP2 observed by immunofluorescence [51]. Finally, HepG2 cells treated with TNF-α or IL-1β showed no significant changes in the MRP2 mRNA level [52]. There are no studies on the mechanisms of translational regulation of human MRP2 to date

Translational regulatory mechanisms

There are many factors controlling translation of mRNA in eukaryotic cells, such as microRNA, mRNA binding proteins, translation initiation factors, and intrinsic characteristics of mRNA (5' and 3' untranslated regions (UTRs), secondary structures, etc.). Here, we will discuss the 5'UTR as a regulatory factor in translation.

5' Untranslated region mediated translational regulation. The 40S ribosomal subunit binds with Met-tRNA/eIF2-GTP and other eukaryotic initiation factors (eIFs), and thus the 43S pre-initiation complex is formed (Figure 1.1.). According to the scanning model of translation (shown in Figure 1.1.), the 43S complex attaches to the 5' 7-methylguanosine (5' m7G) capped site of an mRNA, and recruits more eIFs (eIF4B, eIF4F, etc.), generating the 48S complex. The 48S complex migrates linearly along the mRNA in the 5' → 3' direction until it encounters the first translation initiation codon (ATG). Once the first AUG is base paired with Met-tRNA in an optimal context, the 48S complex stops and

translation initiation factors are released from the initiation complex. The 60S ribosomal subunit joins the 40S subunit. Thus translation is initiated at the first AUG and the proceeds with the elongation stage [53]. This is also called the first-AUG rule. The regulators of translation initiation include: 1) 7-methylguanosine (m7G) capped structure at the 5' end. All cellular and most viral mRNAs have 5' m7G capped ends [54]. Interaction between the 5' m7G cap and eIF4E strongly promotes ribosome binding with mRNA [55, 56], and translational efficiency of an mRNA without a 5' m7G cap is reduced more than 10-fold in *in vivo* experiments. 2) The context sequence flanking the AUG. Kozak et. al [53] found the optimal context for translation initiation in eukaryotic cells: GCCRCCatgG (named Kozak Motif). The critical nucleotides in the Kozak Motif are the purine in position -3 and the G in position +4 (where the A in AUG is numbered +1). Mutation of the nucleotides at these two positions strongly reduces translational efficiency. 3) The length and the secondary structure of the 5' leading region prior to the first AUG. Usually, a longer 5' leader is thought to slow down translation initiation since the scanning 40S subunit needs more time to migrate from the end to the first AUG. But one report showed that the distance of >1000 nt from the 5' end to the first AUG does not reduce the translational efficiency [57]. Kozak argues that the length of 5'-leader prior to the first AUG is irrelevant in terms of translation initiation [58]. However, a long 5'-leader sequence usually contains a secondary structure. A stable stem-loop secondary structure formed by base pairing in the leader sequence is inhibitory by blocking access of the 40S subunit to the AUG [59-61].

The 5' leader sequence prior to the ATG (we use cDNA codon, ATG, instead of AUG in following text) of the main open reading frame (ORF) is commonly called the 5' untranslated region (5'UTR). Here, we call the ATGs present in the 5'UTR as upstream ATGs. It is estimated that at least 10% of human 5'UTRs contain upstream ATGs. According to the first ATG rule, the 48S subunits recognize the first ATG by base pairing while scanning. Downstream ATGs only can be recognized through two mechanisms. First is context-dependent leaky scanning, in which the 48S subunits bypass the first ATG present in an unfavorable context and proceed to advance to the downstream ATGs. Second is reinitiation following translation of upstream open reading frames (uORFs). The translational machineries efficiently recognize the upstream ATGs and translate the uORFs. But after finishing translation of the uORFs, the translational machineries do not dissociate from mRNA strands, but remain bound on the mRNA strands and continue scanning until encountering the next ATG where they initiate translation again. The best studied example of uORFs as translational regulators is the general control protein *GCN4* gene, which demonstrates the orchestrated effect of multiple uORFs on translational regulation.

The GCN4 [62] protein of the yeast *Saccharomyces cerevisiae* is a transcriptional activator of amino acid biosynthetic genes. Translation of the GCN4 mRNA is derepressed in amino acid-deprived cells. The derepression is the orchestrated effect of the four short uORFs (named uORF1-4) in GCN4 mRNA and phosphorylation of eukaryotic initiation factor 2 (eIF-2). These four

uORFs determine where initiation, re-initiation, and leaky scanning of the translation complex occur from the capped end to the GCN4 ATG. In an amino acid-rich medium, ribosomes translate uORF1 and reinitiate primarily at uORF4, but are unable to access the GCN4 ATG. In amino acid-deprived cells, ribosomes still translate uORF1, but bypass uORF2 through uORF4 and reinitiate at the GCN4 ATG instead. The fact that the GCN4 synthesis is due to reinitiation at the GCN4 ATG following translating uORF1 has been demonstrated by two experiments. First, when uORF1 is elongated to overlap the encoding region of GCN4, GCN4 expression is abolished. Second, GCN4 expression is reduced as uORF1 is moved progressively closer to the GCN4 ATG, which is consonant with Kozak's finding that reinitiation efficiency at the downstream ATG is reduced as the distance from the upstream ATG to the downstream ATG is gradually decreased [63]. Therefore, uORF4 and the GCN4 ORF are competitors for the scanning ribosomes after translating uORF1. The level of the active form of eIF2 determines whether uORF4 or GCN4 captures the ribosomes more efficiently. In conclusion, GCN4 expression in derepression conditions is a result of two mechanisms: reinitiation after uORF1 translation and leaking scanning of uORF2-4.

uORF-encoded peptide mediated translational regulation. In addition to the mechanisms of leaking scanning and reinitiation, a mechanism by which uORFs modulate translation depends on the properties of the peptide encoded by the uORFs. Missense mutations in the uORFs interfere with its control function. In

this mechanism, translational regulation is dependent on the amino acid sequence of the encoded peptide by a uORF [64].

A uORF-encoded peptide can cause ribosome stalling. The arginine attenuator peptide (AAP) is encoded by an evolutionarily conserved uORF. This uORF is present in the 5'UTRs of both *S. cerevisiae* CPA1 and *N. crassa* arg-2 mRNAs. In the presence of arginine, expression of both CPA1 and arg-2 mRNA is repressed. The investigation of the underlying mechanism shows that the scanning ribosomes translate the uORF of AAP first and the newly synthesized AAP then causes the ribosomes to stall at the termination codon. As a result, the ribosomes are blocked from reaching the main ORF of CPA1 and arg-2 mRNAs. In contrast, in the absence of arginine, the AAP uORFs are bypassed by most scanning ribosomes (leaking scanning), and the main ORFs are translated. Therefore, a uORF regulates translation of a downstream cistron not only through reinitiation, but also through stalling ribosomes [65, 66].

The ribosome stalling model resembles that exerted by the 22-codon uORF2 of human cytomegalovirus gpUL4 and the 6-codon uORF of *S*-adenosylmethionine decarboxylase (AdoMetDC). Mutants of these uORFs abolish the ribosome stalling, resulting in failure to inhibit translation of the downstream main ORF. The inhibitory effect of the uORFs on the gpUL4 and AdoMethDC mRNAs is eliminated when the terminal codons of the uORFs are removed. This suggests that the nascent peptides translated from the uORFs interfere with the translation termination reaction. Further studies showed that the affected step occurs prior to peptidyl-tRNA hydrolysis [67-70]. Raney and Morris

experimentally detected an intermediate in the termination process of translation of the uORF, the complete nascent peptide linked to the tRNA. They also show that association of this complex with the ribosome is regulated by levels of polyamine.

Several studies have successfully detected uORF-encoded peptides *in vitro* and *in vivo*. The glucocorticoid receptor (GR) mRNA contains five uORFs (uORF1-5). Among them, only the peptide encoded by uORF2 is detected by immunoblotting analysis in the *in vitro* translation reaction and in liver cells. Moreover, disruption of uORF2 abolishes synthesis of this peptide and also GR, suggesting that the peptide may be involved in translation of GR [71]. The hexapeptide (sequence MAGDIS) encoded by the uORF of AdoMetDC is also detected as a product of *in vitro* translation reaction by HPLC, following a series of purification steps [72]. In addition, four novel small uORF-encoded peptide (<100 amino acids in length) were recently detected using high-resolution nanoflow liquid chromatography coupled with electrospray inonization tandem mass spectrometry. Three peptides are encoded by uORFs that overlap the downstream main ORFs and the other peptide is encoded by a uORF that terminates prior to the main ORF [73]. To date, the mechanism by which uORF-encoded peptides *trans*-regulate translation of the downstream main ORFs is still unclear.

Research Objectives

MRP2/Mrp2 plays an important role in bile formation, detoxification, and drug disposition (absorption and elimination). Dysfunctional MRP2 expression results in Dubin-Johnson syndrome in human beings and changes in MRP2/Mrp2 expression are also involved in all types of cholestasis. Changes in MRP2/Mrp2 protein expression occur at the translation level under some conditions (pregnancy, PCN treatment, etc.) as well as the transcription level. To date, there have been no studies to investigate the mechanisms of translational regulation of MRP2/Mrp2. The work presented here characterized the uORFs of the human MRP2 and rat Mrp2 mRNAs as translational regulators in *in vitro* systems. Therefore, the uORF-mediated translational regulation provides a possible mechanic model that future studies could use to investigate the translational regulation of MRP2/Mrp2 protein expression under certain conditions, such as pregnancy, cholestasis, or PCN treatment.

In Chapter Two, the studies were focused to investigate the hypothesis that the 5'UTRs of rat Mrp2, particularly the upstream ATGs, modulate translation. We compared the effect of multiple 5'UTRs of the rat Mrp2 mRNA on translation of the luciferase gene. Four ATGs are present in the longest 5'UTR (-213 nucleotides relative to the Mrp2 ATG) of Mrp2. It is shown that the ATG at position -109 inhibited translation dramatically, compared with other ATGs.

In Chapter Three, we continued to study the mechanism by which the uORF at position -109 of rat Mrp2 inhibited translation. In order to test whether the inhibitory effect exerted by this uORF was sequence-dependent, we compared

the translational efficiencies of the native and frame-shifted sequences in *in vitro* translation assays. We also tried to detect the presence of the peptide encoded by the uORF at position -109 in tissues (liver and kidney).

In Chapter Four, we extended the research to investigation the hypothesis that the 5'UTRs of human MRP2 mediate translational regulation. The 5'UTRs of the human mRNA are more complicated; the longest 5'UTR contains seven upstream ATGs. Here, we investigated the effect of the 5'UTRs, particularly the upstream ATGs, on translation in transiently transfected HepG2 cells and *in vitro* translation. Finally, we examined the sequence-dependence of translational effects exerted by the uORF at position -105 (relative to the ATG of MRP2).

FIGURE AND LEGEND

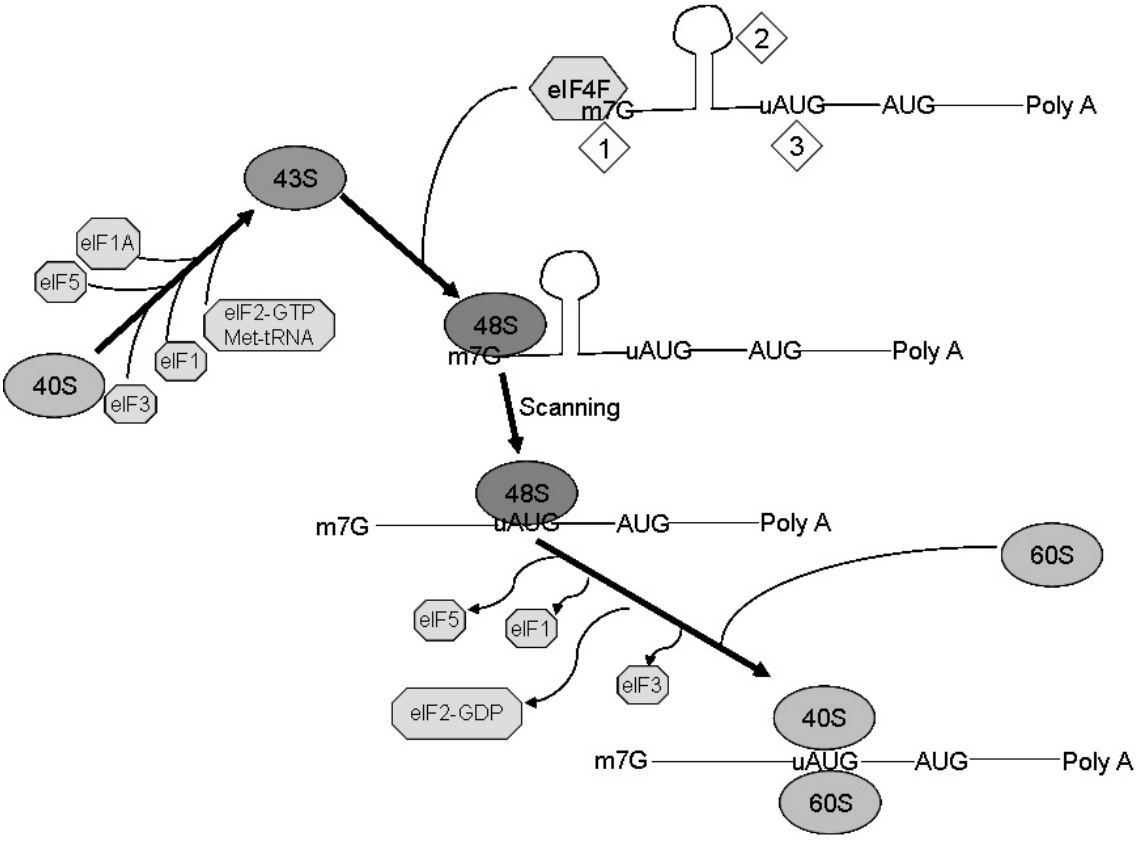

Figure 1.1. Schematic representation of eukaryotic translation initiation. The three factors of an mRNA controlling translation initiation are marked in the picture with the diamond shape, 1) m7G capped 5' end, 2) stable stem-loop secondary structures, and 3) upstream translation initiation sites ATGs.

CHAPTER TWO

TRANSLATIONAL REGULATION OF RAT MULTIDRUG RESISTANCE PROTEIN 2 (MRP2) IS MEDIATED BY UPSTREAM OPEN READING FRAMES (UORFS) IN THE 5' UNTRANSLATED REGION (UTR)

BACKGROUND

Multidrug resistance protein 2 (rat Mrp2 or human MRP2), a member of the ATP-binding cassette gene superfamily of transport proteins, is present in the apical membrane of hepatocytes, enterocytes and renal proximal tubules. Mrp2 protein mediates efflux of organic anions such as glutathione, glucuronide and sulfate conjugates against a concentration gradient from hepatocytes into bile [16, 19, 74, 75], and also contributes to bile flow by mediating canalicular excretion of glutathione (GSH) [76].

Regulation of Mrp2 expression has been characterized primarily at the transcriptional level in rats and mice. Exposure to activators of nuclear receptors, such as Nrf2, CAR and PXR, increases Mrp2 protein expression in rat primary hepatocyte cultures [23], while studies in mice have shown that CAR and Nrf2 agonists, but not PXR agonists, increase Mrp2 mRNA expression [77, 78], supporting the importance of transcriptional regulation. However, in the rats treated with pregnenolone-16α-carbonitrile (PCN), a PXR agonist, hepatic Mrp2 mRNA expression is unchanged, whereas Mrp2 protein expression is increased 2-3 fold [46, 79, 80]. Ethinylestradiol treatment markedly decreases Mrp2 protein in the rat liver, while Mrp2 mRNA remains unchanged [26]. Similarly, hepatic Mrp2 protein in the pregnant rat is significantly decreased by 50%, while Mrp2

mRNA is unchanged [44, 45]. Along the rat small intestine, Mrp2 protein is decreased by 90% in the distal ileum relative to that in the jejunum, whereas Mrp2 mRNA does not change significantly [48]. The inconsistency between the changes in Mrp2 mRNA and protein expression indicates that under some conditions, rat Mrp2 protein expression undergoes post-transcriptional regulation.

Post-transcriptional regulation of protein expression can occur through changes in mRNA stability, in the rate of protein degradation, or in the rate of protein synthesis. The minimal changes in Mrp2 mRNA expression in female control, pregnant and PCN-treated rats argue against significant differences in Mrp2 mRNA stability as likely to contribute to the mechanism of translation of rat Mrp2 that could account for the 4-5-fold differences in Mrp2 protein expression among these groups. We recently showed that altered rates of hepatic Mrp2 protein degradation cannot explain the differences in its protein expression in control, pregnant and PCN-treated rats, whereas decreased and increased rates of Mrp2 protein synthesis were observed in pregnant and PCN-treated rats, respectively [46]. In the present studies, we therefore focused on the potential mechanism of translational regulation of Mrp2 protein synthesis.

Accumulating evidence indicates that upstream open reading frames (uORFs) are important regulators of mRNA translation [64, 81, 82], which can be explained by the ribosomal scanning model. Translation of a downstream main open reading frame (ORF) of a gene by ribosomes occurs through leaky scanning of any ATGs in the 5' untranslated region (5'UTR) when the sequence around the upstream ATGs is suboptimal [53], or through reinitiation when the

translation machinery is not dissociated from the mRNA chain after termination of translation of uORFs [64]. We identified four transcription initiation sites in rat hepatic Mrp2 cDNA that occur at -213, -163, -132, and -98, where the ATG of the Mrp2 coding gene is numbered +1, +2, and +3 [46] (Figure 2.1.A.). In the present study, we fused these Mrp2 5'UTRs upstream of the luciferase reporter gene and investigated their effect on luciferase expression in HepG2 cells in transient expression assays and on the translation efficiency of the luciferase transcript in *in vitro* translation assays. We also used ribonuclease protection assay (RPA) to identify transcription initiation sites in the rat liver, kidney and small intestine, and during postnatal development. We found that these tissues utilize different Mrp2 transcription initiation sites, and that translation from these transcripts is greatly influenced by the presence of the uORF at -109 nucleotides.

MATERIALS AND METHODS

Materials

α-^{32}P-UTP (800 Ci/mmol) and ^{35}S-methionine (1000 Ci/mmol) were obtained from Perkin Elmer Life and Analytical Sciences (Boston, MA). Unless otherwise noted, all other chemicals were of analytical grade and of cell culture grade from Sigma Chemical Co. (St. Louis, MO), Invitrogen™ life technologies (Carlsbad, CA), Roche Diagnostics (Indianapolis, IN) and Fisher Scientific (Pittsburgh, PA). Restriction enzymes were obtained from Invitrogen and Promega (Madison, WI).

Animals

Adult female Sprague Dawley rats whose weights were 215±25 g were obtained from Harlan Industries (Indianapolis, IN). The rats had free access to water and food and were maintained on an automatically timed 12-h light/12-h dark cycle. All experimental protocols involving animals were approved by the Institutional Animal Care and Use Committee of the University of Kentucky, and conducted following National Institutes of Health guidelines for the care and use of laboratory animals. In order to determine postnatal changes, female pups were separated from moms at indicated times after birth, and tissues were immediately removed and frozen in liquid nitrogen until isolation of RNA.

Ribonuclease protection assay (RPA)

The neonatal and control (adult) rat liver, kidney, placenta, lung, and small intestine were removed immediately after decapitation and frozen in liquid

nitrogen. Total RNA was isolated using TRIzol™ reagent (Invitrogen) following the manufacturer's instructions.

The luciferase control vector (Promega) was fused at cloning sites Hind III and BamH I with the Mrp2 5'UTR cDNA sequence starting at -1 to -214 relative to the ATG (numbered as +1, +2, and +3) of the Mrp2 coding region. A double-stranded 280 bp fragment containing the T7 promoter and the Mrp2 5'UTR was purified after the fusion luciferase vector was digested with Pvu II and BamH I. The α-^{32}P-UTP labeled Mrp2 probe was prepared according to the instructions of the MAXIscript T7 kit (Ambion, Austin, TX), using the 280 bp fragment as template. RPA was performed following the procedure of the RPA III kit (Ambion). Briefly, total RNA was incubated with the Mrp2 probe in the mixture containing 0.5 M ammonium acetate and 2.5 volumes of ethanol. Following co-precipitation of the probe with total RNA after incubation at -80°C for 90 min, the RNA pellet was washed once with 75% ethanol and dissolved in hybridization solution. The hybridization reaction was incubated at a decreasing temperature from 56°C to 36°C at the rate of 2°C per 2 hr. The single-stranded RNA was digested by RNAse A/T1 mix at 37°C for 1 hr. The fragments protected from RNAse digestion were identified by electrophoresis on 6% urea-PAGE gel.

Plasmid construction

The Mrp2 5'UTR cDNA is shown in Figure 2.1.A. The cDNA sequences of the Mrp2 5'UTRs (Figure 2.1.B.), L, M1, M2, and S1, were PCR amplified using the forward primers TRF1, TRF2, TRF3, and TRF4, respectively (Table 2.1). The

reverse primer for L and M1 PCR amplification was CONR (Table 2.1). The reverse primer for amplifying both M2 and S1 was T7R1 (Table 2.1). The fragments were ligated upstream of the ATG of the firefly luciferase reporter gene into the pGL3 control vector (Promega) for transient co-transfection assays in HepG2 cells, and into the T7 control vector (Promega) for *in vitro* translation assays.

The cDNA sequences of the 5'UTRs, deL, deM, and S2, were PCR amplified using forward primers TRF1, TRF2, and TRF5, respectively, and the reverse primer TRRR that deleted 1 nucleotide from T7R1 (Table 2.1). These fragments were fused in the T7 control luciferase vector. As a result, ATG1 (at position -109) is in-frame with the luciferase reporter gene ORF.

uORFs were disrupted by introducing a point mutation into start codons, ATG→AAG, using the corresponding wildtype constructs as templates. The point mutations of the nucleotides T at -148 and -108 to A were termed "a" and "b", respectively; and the mutation of the Kozak motif flanking the ATG at -109 termed "c" (Figure 2.1.B.). All mutagenesis was performed according to the manufacturer's instructions of the Quick-Change Site-Directed Mutagenesis Kit (Stratagene, La Jolla, CA). All plasmids were confirmed by sequencing.

HepG2 cell transient co-transfection assays

HepG2 cells were cultured in DMEM/F12 (1:1) medium supplemented with 10% charcoal-stripped fetal bovine serum (Hyclone Laboratories, Logan, UT), 3.58 mM glutamine, 55 μg/ml gentamycin, and 1 μg/ml insulin (Invitrogen). One

day before transfection, culture medium was replaced by phenol red-free DMEM supplemented with 10% charcoal stripped FBS, glutamine, and gentamycin. The plasmids (1 μg) were transfected by the ProFectin mammalian transfection system-calcium phosphate (Promega) into HepG2 cells, together with 30 ng of pSV40-Ren (Promega) as an internal control for transfection efficiency. After 5-6 h incubation, the transfection medium was replaced with maintenance medium. Cells were harvested 24 h later for measurement of the firefly and *Renilla reniformis* luciferase activities by the Dual-luciferase reporter assay system (Promega). The firefly luciferase activity was normalized to *Renilla reniformis* luciferase activity.

In vitro **translation assays**

The tested Mrp2 5'-UTR-luciferase constructs were linearized by Pvu II and Sac I. The capped and α-^{32}P-UTP-labeled firefly luciferase transcripts that were fused with Mrp2 5'UTRs, were synthesized *in vitro* with the Pvu II-Sac I fragments as templates, according to the manufacturer's instructions of mMESSAGE mMACHINE T7 kit (Ambion). Transcription efficiency was quantified by scintillation counting of α-^{32}P-UTP incorporation into RNA. The integrity and size of the luciferase transcripts were verified by formaldehyde-agarose gel electrophoresis. The luciferase protein was synthesized from the capped luciferase transcripts *in vitro*, according to the manufacturer's procedure of the Rabbit Reticulocyte Lysate System (Promega). Briefly, 0, 2, 4, 10, or 20 ng of the luciferase transcript was added to a reaction mixture. The translation

reaction was immediately incubated at 30 °C for 60 min and terminated by moving onto ice. The firefly luciferase activity was measured by the Luciferase Assay System (Promega) according to the manufacturer's instructions.

In vitro expression in the Transcription/Translation coupled system

The TnT quick Transcription/Translation coupled system (Promega) was used to translate the luciferase protein using tested constructs as templates. According to the manufacturer's instructions, a reaction mixture (50 µl) containing 40 µl of TnT Master Mix and 2 µl of ^{35}S-methionine were incubated at 30 °C for 90 min. The translated products were separated on 4-20% gradient denaturing SDS-PAGE and data processed using the STORM 840 Phosphoimager (Molecular Dynamics).

Data analysis

RPA bands were quantified by densitometry using Quantity One 1-D Analysis Software (Bio-Rad). Linear regression analysis was performed by GraphPad Prism 4.0.

RESULTS

Identification of rat Mrp2 transcription initiation sites and the relative abundance in rat tissues by RPA

Four transcription initiation sites have been identified at position -213, -163, -132, and -98 in the 5'UTR of the rat hepatic Mrp2 mRNA cDNA (Figure 2.1.A.) [46]. We investigated the transcription initiation sites in the various rat tissues to determine if their use might be tissue-specific. The four transcription initiation sites were detected in the rat liver, with the site at position-98 as the primary site, and the one at position -132 as the secondary site (Figure 2.2.). The transcription initiation sites in other tissues were different from that in the liver. In the placenta and kidney, the primary site was located at position -132 and the secondary site was at position -98, while other sites were barely detected. The primary site in the lung was at position -98, while other transcription initiation sites not detected. In the jejunum, the primary and secondary sites were located at position -98 and -132, but located at position -132 and -98 in the ileum, respectively, while other sites not detected.

We next investigated whether utilization of the transcription initiation sites might vary with age. In the liver, the ratio of expression of the transcript starting at position -132 to the one starting at position -98 was 0.73 ± 0.06 at Day 0, increased to 1.06 ± 0.10 at Day 10, and then decreased to 0.80 ± 0.03 in the adult (Figure 2.3.A.). In the kidney, the ratio was similar at Day 0 and Day 6 (≈ 4), and increased to 13.4 ± 1.2 in adulthood (Figure 2.3.B.). In the jejunum, the ratio was 1.2 ± 0.19 at Day 0, increased to 1.5 ± 0.02 at Day 20, and then decreased

to 0.87 ± 0.1 in the adult (Figure 2.3.C.). In the ileum, the ratio was very similar from Day 0 to adulthood (0.70 – 0.85) (Figure 2.3.D.). The data indicated that the changes in expression of Mrp2 transcripts with age were relatively minor compared to those among the tissues.

Effect of the rat Mrp2 5'UTRs on expression of the luciferase reporter gene in the transiently transfected HepG2 cells

In order to determine whether the various 5'UTRs differentially influenced Mrp2 protein expression, the effect of Mrp2 5'UTRs on expression of the firefly luciferase reporter gene was determined in the transiently transfected HepG2 cells. Fusion plasmids were constructed by inserting Mrp2 5'UTRs into the pGL3 control vector immediately upstream of the luciferase reporter gene. In addition, the wildtype 5'UTRs were altered by disruption of ATG1 at position -109 and ATG2 at position -149 to determine the influence of uORF1 and uORF2 on protein expression. Fusion plasmids were transiently cotransfected individually with pSV40-Ren into HepG2 cells, and the firefly luciferase activity normalized to the *Renilla* luciferase activity of cell extracts.

When normalized to the ratio of Firefly/*Renilla* luciferase of the pGL3 control vector that is without any Mrp2 5'UTR (=1) (Figure 2.4.A., B.), the luciferase activities of L (the -213 nt transcript), L^{b} (L with a single mutation at ATG1 to AAG), and L^{a+b} (L with double mutations at ATG1 and ATG2 to AAG) were 0.39, 0.8, and 0.93, respectively. Similarly, those of M1 (the -163 nt transcript), $M1^{b}$ (M1 with a single mutation at ATG1 to AAG), and $M1^{a+b}$ (M1 with double

mutations at ATG1 and ATG2 to AAG) were 0.23, 0.96, and 0.90, respectively. Therefore, L (the -213 nt transcript) decreased the luciferase activity about 60% relative to the control pGL3 vector ($p<0.001$), whereas disruption of ATG1 in L (L^b) increased the luciferase activity 2-fold relative to L ($p<0.001$). Disruption of the both ATG1 and ATG2 (L^{a+b}) slightly increased the luciferase activity in comparison to L^b ($p>0.05$). The wildtype M1 (the -163 nt transcript) expressed the lowest luciferase activity (25% of pGL3, $p<0.001$) (Figure 2.4.B.). Disruption of ATG1 in M1 ($M1^b$) increased the luciferase activity 3-fold compared to M1 ($p<0.001$), whereas disruption of both ATG1 and ATG2 ($M1^{a+b}$) slightly decreased the luciferase activity compared to $M1^b$ ($p<0.001$). Taken together, these data implied that uORF1 was more important in regulation of expression compared to uORF2.

Effect of the rat Mrp2 5'UTRs on translation efficiency of the luciferase transcript by *in vitro* translation assays

Since the luciferase protein expression in HepG2 cells required both transcription and translation processes, we next investigated the influence of various rat Mrp2 5'UTRs on translation efficiency of mRNA. The capped luciferase transcripts were prepared using Pvu II-Sac I fragments as templates in which Mrp2 5'UTRs were located immediately upstream of the luciferase coding region. The capped luciferase transcripts were added to the rabbit reticulocyte lysate system to determine the effect of 5'UTRs on translation efficiency under conditions of linearity with respect to transcript concentration. Translation

efficiency was calculated from the linear relationship between the luciferase activities and mRNA concentrations.

Translation efficiencies of the capped luciferase mRNAs with S1 (-98 nt), M2 (-132 nt), and L (-213 nt) were 67-, 37-, and 15-fold higher than that of M1 (-163 nt) ($p<0.0001$, Figure 2.5.A.). We investigated contribution of uORFs to the differences in translation efficiency of the various transcripts. Mutation of ATG1 to AAG in the -213 nt transcript (L^b) increased translation efficiency 3-fold, whereas mutation of ATG2 to AAG in the -213 nt transcript (L^a) decreased translation efficiency 80%, compared to the wildtype L ($p<0.0001$, Figure 2.5.B.). Compared to that of M1 (-213 nt), the translation efficiency of $M1^b$ containing mutation of ATG1 to AAG increased 31-fold ($p<0.0001$), while the translation efficiency of $M1^a$ containing mutation of ATG2 to AAG increased 6-fold ($p=0.0026$) (Figure 2.5.C.). Compared to the -132 nt transcript (M2), a single mutation at ATG1 to AAG in M2 ($M2^b$) increased translation efficiency 4-fold ($p<0.0001$), while disruption of the Kozak motif of uORF1 in M2 ($M2^c$) increased translation efficiency only 1.7-fold ($p=0.001$, Figure 2.5.D.).

In vitro expression in the Transcription/Translation coupled system

The effect of uORF1 on translation efficiency suggested that ATG1 serves as a translation start site. To determine if translation could be initiated at uORF1, we inserted Mrp2 5'UTRs into the T7 control vector in such a way that ATG1 was in-frame with the luciferase ORF. When the plasmids containing deL and deM1 were used as templates, a peptide of a higher molecular weight was observed in

the Transcription/Translation coupled system (Lanes 1 and 5 in Figure 2.6.). The higher molecular weight peptide was not observed when the plasmid containing S2 was used as template (Lane 3), or when uORF1 in deL and deM1 was disrupted (Lanes 2 and 4, Figure 2.6.). Detection of a higher molecular weight peptide of the plasmids containing uORF1 indicated that ATG1 can be used as an efficient translation initiation site.

CONCLUSIONS

For the first time, we demonstrate by RPA that the transcription initiation sites at position -213, -163, -132, and -98 (Figure 2.1.A.) were differentially used in the rat liver, kidney, small intestine, lung and placenta (Figure 2.2.) and that their use varied little with age in the liver, kidney, and jejunum and ileum (Figure 2.3.). In the jejunum, the primary and secondary transcription initiation sites were at position -98 and -132, respectively, whereas in the ileum, the primary and secondary sites were at position -132 and -98, respectively. In the kidney, the site at position -132 predominated, with other sites under detectable limits. In the liver, the site at position -98 was the primary site.

This study also showed for the first time that Mrp2 5'UTRs were involved in translational regulation. uORF1 at position -109 had an inhibitory effect on translation. Disruption of uORF1 abolished the inhibitory effect of wild type 5'UTRs (-213, -163, and -132 nt) on translation of the luciferase reporter gene in HepG2 cell transient transfection assays (Figure 2.4.) and *in vitro* translation assays (Figure 2.5.). The evidence that luciferase protein with a higher molecular weight was observed when uORF1 was fused in-frame with the luciferase ORF (Figure 2.6.) suggested that translation was efficiently initiated at uORF1.

FIGURES AND LEGENDS

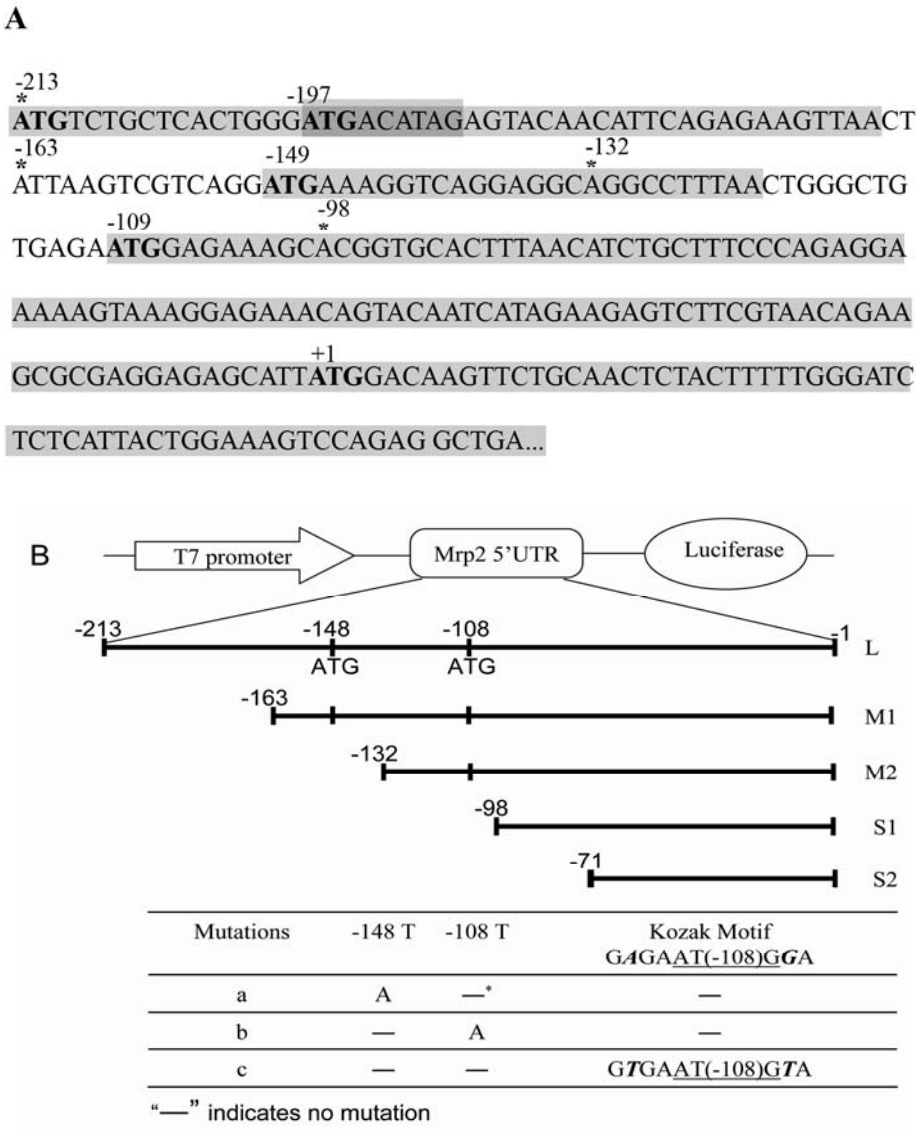

Mutations	-148 T	-108 T	Kozak Motif GAGAAT(-108)GGA
a	A	—*	—
b	—	A	—
c	—	—	GTGAAT(-108)GTA

"—" indicates no mutation

Figure 2.1. Construction of fusion plasmids. A. The full cDNA sequence of 5'UTR of the rat *Mrp2* gene. The ATGs are in bold and the gray-shaded sequences represent their uORFs**.** The ATG of the rat *Mrp2* gene is numbered as +1, +2, and +3 and its ORF is termed ORF0. The upstream ATGs are located at position -109, -149, -197, and -213 and termed ATG1, ATG2, ATG3, and ATG4, respectively. Accordingly, the uORFs are termed uORF1, uORF2,

uORF3, and uORF4. uORF1 from position -109 to +62 contains 57 codons; uORF2 from position -149 to -123, 9 codons; uORF3 from position -197 to -189, 3 codons; and uORF4 from position -213 to -166, 16 codons. uORF4 is in-frame with ORF0 and uORF1-3 are out-of-frame with ORF0. Transcription initiation sites at position -213, -163, -132, and -98 are marked with asterisks. **B. Schematic representation of the fusion Mrp2 5'UTR-luciferase constructs.** The inserts shown were fused in the pGL3 control vector or in the T7 luciferase control vector between the T7 promoter and the luciferase ORF. Mrp2 5'UTRs are shown as the lines to scale. The point mutations in the 5'UTRs are listed in the table. The italicized nucleotides were mutated to disrupt uORF1 and uORF2 or Kozak motif of uORF1: "a", mutation of the nucleotide T at position -148 to A; "b", mutation of the nucleotide T at position -108 to A; "c", mutation of both the nucleotides A at position -112 and G at -106 to T.

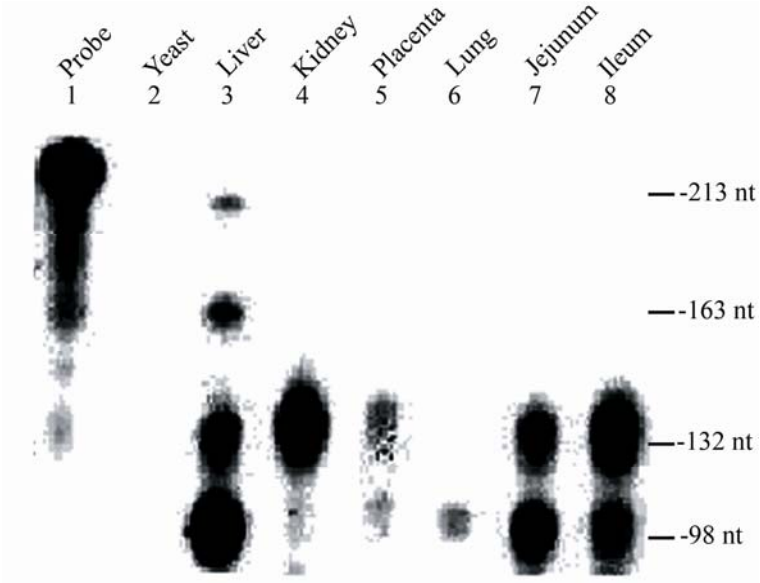

Figure 2.2. Identification of transcription initiation sites of the *Mrp2* gene and the relative abundance in rat tissues by RPA. The α-^{32}P-UTP-labeled Mrp2 probe of 280 nucleotides contains the Mrp2 5'UTR from position -1 to -214. Total RNA was incubated with the probe. Following hybridization, the single strand RNA was degraded by RNAse A/T1 Mix. The fragments protected from RNAse digestion were identified by electrophoresis on 6% urea-PAGE gel. Mrp2 probe (lane 1) is the product of 20 μg of yeast without RNAse treatment.

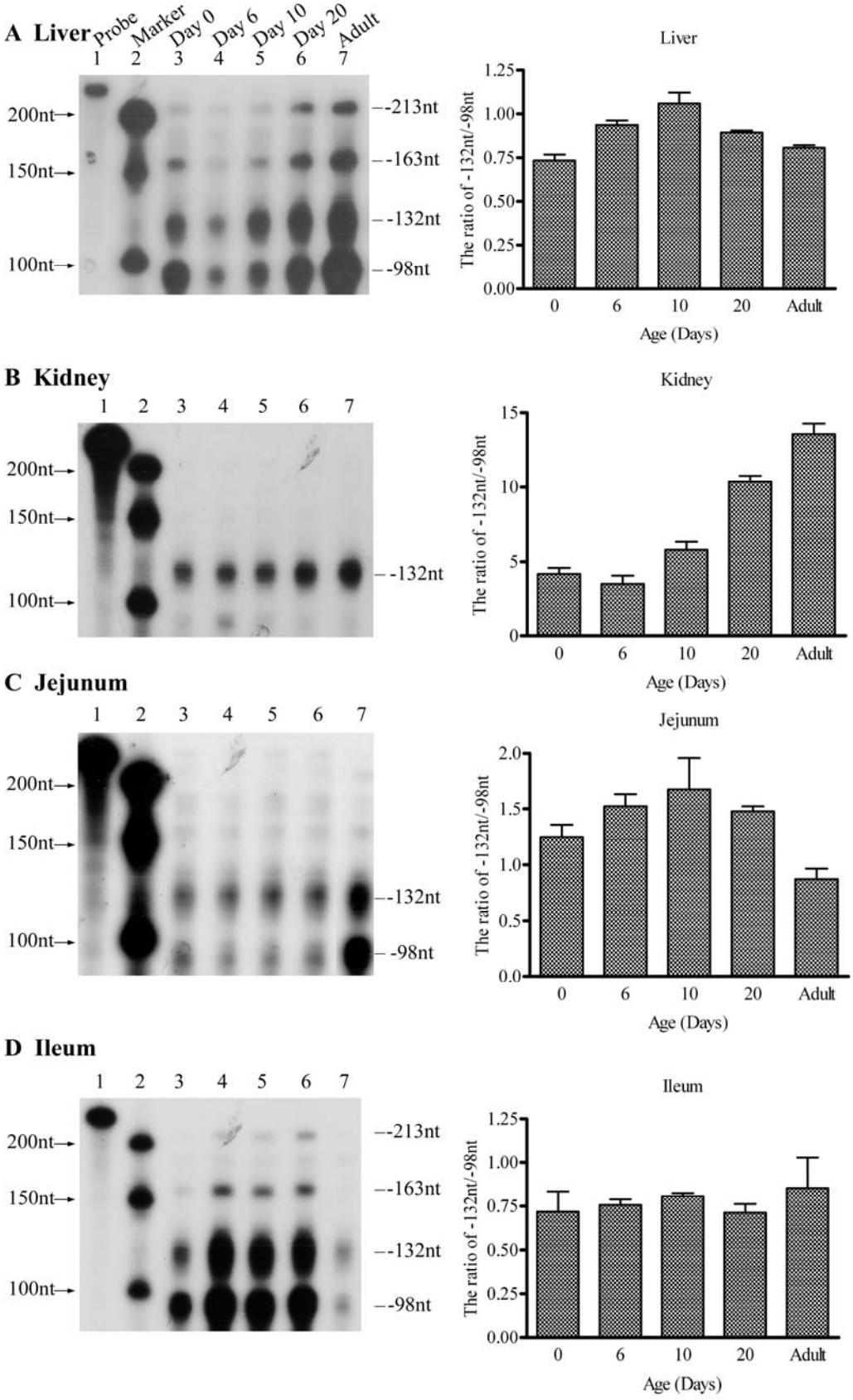
A Liver
Probe
Marker
Day 0
Day 6
Day 10
Day 20
Adult
1 2 3 4 5 6 7
200nt
150nt
100nt
--213nt
--163nt
--132nt
--98nt
Liver
The ratio of -132nt/-98nt
1.25
1.00
0.75
0.50
0.25
0.00
0 6 10 20 Adult
Age (Days)
B Kidney
1 2 3 4 5 6 7
200nt
150nt
100nt
--132nt
Kidney
The ratio of -132nt/-98nt
15
10
5
0
0 6 10 20 Adult
Age (Days)
C Jejunum
1 2 3 4 5 6 7
200nt
150nt
100nt
--132nt
-98nt
Jejunum
The ratio of -132nt/-98nt
2.0
1.5
1.0
0.5
0.0
0 6 10 20 Adult
Age (Days)
D Ileum
1 2 3 4 5 6 7
200nt
150nt
100nt
--213nt
--163nt
--132nt
--98nt
Ileum
The ratio of -132nt/-98nt
1.25
1.00
0.75
0.50
0.25
0.00
0 6 10 20 Adult
Age (Days)

Figure 2.3. The relative abundance of transcription initiation sites of the *Mrp2* gene in neonatal rat tissues and adults by RPA. Rat pups were decapitated at day 0, 6, 10, 20, and adulthood. The liver, kidney, jejunum, and ileum were taken, frozen in liquid nitrogen, and stored at -80°C until isolation of total RNA. Liver RNA (10 µg) and 20 µg of kidney, jejunum, and ileum RNA were used. Mrp2 probe (lane 1) is the product of 10 µg of yeast RNA without RNAse treatment. The figure shown is a representative of three experiments. The histograms represent the ratio of the transcript starting at position -132 to the one at position -98 obtained, and represented as mean ± SD of three independent experiments.

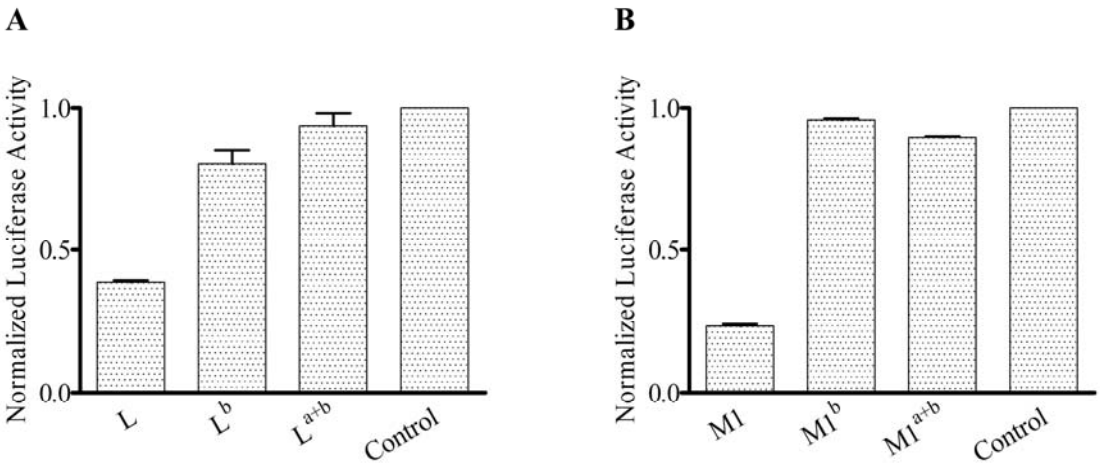

Figure 2.4. Effect of Mrp2 5'UTRs on expression of the luciferase reporter gene in HepG2 cell transient cotransfection assays. Mrp2 5'UTR-luciferase constructs were cotransfected with pSV40-Ren into HepG2 cells. After 24 hours, the firefly and *Renilla reniformis* luciferase activities were measured. The effect of various 5'UTRs (A. L, -213 nt; B. M1, -163 nt) on luciferase expression is represented as the ratio of the firefly luciferase activity to *Renilla reniformis* luciferase activity. The assays were performed in triplicate. The data are normalized to the Luc/Ren ratio of the pGL3 control vector and represented as mean ± SEM. This work was done by Dr. Wei Li in the laboratory. The data were performed One-Way ANOVA and followed with Bonferroni's pairwise comparison.

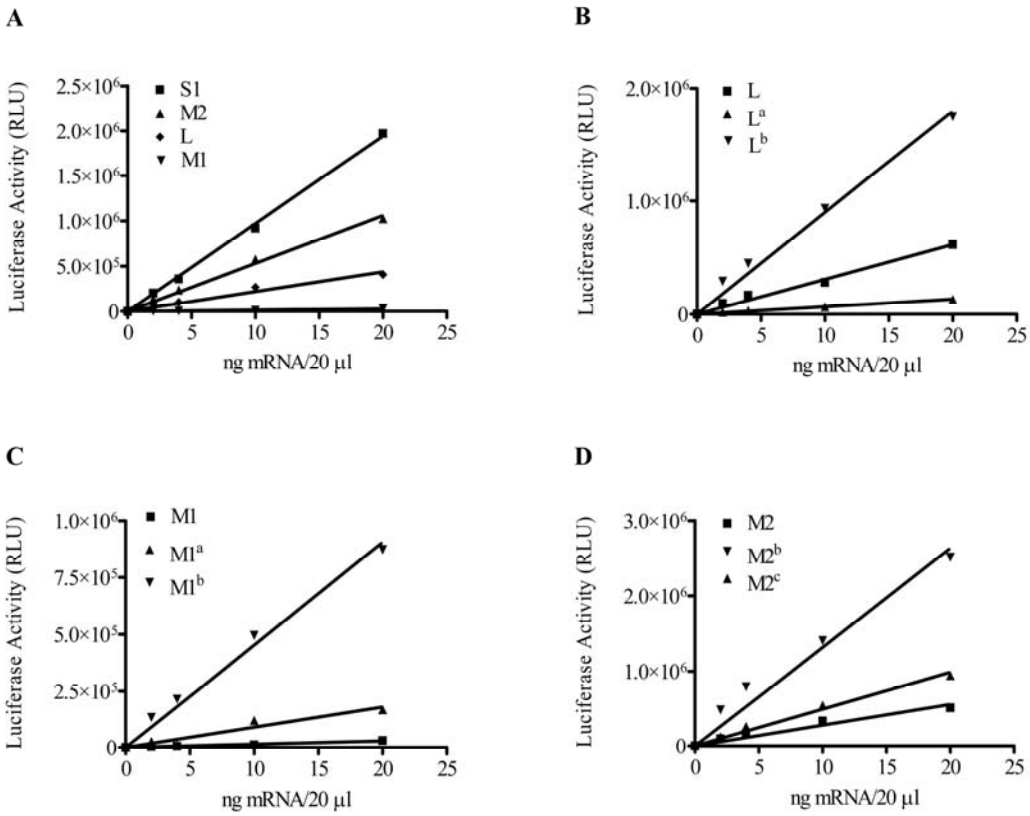

Figure 2.5. Effect of Mrp2 5'UTRs on translation efficiency of the luciferase reporter transcript by *in vitro* translation assays. Mrp2 5'-UTR-luciferase constructs were linearized by restriction enzymes Pvu II and Sac I. The fragments of Pvu II-Sac I were used as templates to synthesize the capped, Mrp2 5'UTRs-fused luciferase transcripts. The luciferase transcripts (0, 2, 4, 10, or 20 ng) were added to a rabbit reticulocyte lysate mixture. The translation reaction was incubated at 30°C for 60 min and terminated on ice. The lines represent the relationship of luciferase activities with respect to transcript concentrations. The statistical significance of the difference in the slopes was tested by GraphPad Prism 4.0. **A.** Translation of the 5'UTRs; **B.** L and its mutants; **C.** M1 and its mutants; **D.** M2 and its mutants.

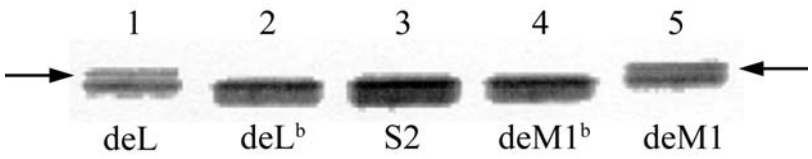

Figure 2.6. *In vitro* expression in the Transcription/Translation coupled system. The rat Mrp2 5'UTR cDNA sequences were inserted into control T7 luciferase vector to make ATG1 in-frame with the luciferase ORF. The 5'UTRs of deL and deM1 contain ATG1 while S2 does not. The point mutation of ATG1→AAG disrupted uORF1 in deL and deM1, obtaining deL^{b} and deM1^{b} constructs. These constructs were used in the Transcription/Translation coupled system. The translated products were separated on 4-20% gradient SDS-PAGE. Data were processed using STORM 840 Phosphoimager. This work was done by Dr. Wei Li in the laboratory.

Table 2.1 Primers used for PCR amplification of the rat *Mrp2* 5'UTR cDNAs

Name	Sequence (5'-3')	cloning site
TRF1	5' gg<u>aagctt</u>atgtctgctcactggga 3'	Hind III
TRF2	5' gg<u>aagctt</u>attaagtcgtcaggatga 3'	Hind III
TRF3	5' tca<u>aagctt</u>aggcctttaactgggctg 3'	Hind III
TRF4	5' gga<u>aagctt</u>acggtgcactttaacatctg 3'	Hind III
TRF5	5' gg<u>aagctt</u>agaggaaaaagtaaaggag 3'	Hind III
CONR	5' acc<u>ccatgg</u>taatgctctcctcgcgc 3'	Nco I
T7R1	5' ggg<u>gatcc</u>gaatgctctcctcgcgc 3'	BamH I
T7R2	5' ttt<u>ggatcc</u>aatgctctcctcgcg 3'	BamH I
TRRR	5' ggg<u>gatcc</u>aatgctctcctcgcgc 3'	BamH I

The cloning sites are underlined.

CHAPTER THREE

DETERMINATION OF THE SEQUENCE DEPENDENCE OF TRANSLATIONAL INHIBITORY EFFECT EXERTED BY UORF1 AND INVESTIGATION REGARDING EXPRESSION OF ITS ENCODED PEPTIDE (PEP56) IN RAT TISSUES

BACKGROUND

Several studies show that nascent peptides encoded by uORFs mediate regulation of translation [64]. This mechanism depends on the amino acid sequence of the encoded peptide. At present, at least six eukaryotic mRNAs have been found in which translation is repressed by their uORFs in a sequence-dependent way [64].

S-Adenosylmethionine decarboxylase (AdoMetDC) is a key regulated enzyme in the biosynthesis of the polyamines spermidine and spermine. The mRNA of AdoMetDC contains a single short uORF encoding a peptide: MAGDIS [64]. Missense but not synonymous mutation of each codons shows that repression of translation exerted by this uORF encoding MAGDIS stringently requires the codons at positions 4 and 5. No amino acid substitution of the naturally occurring aspartic acid at codon 4 yields a full suppression of translation. Only valine could substitute productively for isoleucine at codon 5 [68, 69].

Retinoic acid receptor-β2 (RARβ2) mRNA has a complex 5'UTR. Among the five uORFs, uORF4 of RARβ2 mRNA encodes a translational inhibitory peptide.

Missense mutations show that the amino acids at position 5, 6, 12, and 13 of this peptide are critical for translational inhibition of uORF4 [83].

The human cytomegalovirus (CMV) virion glycoprotein gpUL4 mRNA contains three uORFs. Using deletion, frameshifting, and missense substitution of the amino acids of the encoded peptide of uORF2, Degnin et al [84, 85] found that uORF2 exerts translational inhibition in an amino acid sequence dependent way. They also reported that this peptide acts in a *cis*-dependent manner.

Although conserved sequences are not found in these peptides encoded by uORFs or in the nucleotide sequences of uORFs, it is believed that a uORF-encoded peptide can cause ribosome stalling by association with RNA or proteins of the scanning ribosomes so as to inhibit their function [64].

We have demonstrated by point mutation in Chapter Two that uORF1 at position -109 (shown in Figure 2.1A) of the rat Mrp2 mRNA down-regulates translation of the downstream main ORF and the scanning ribosomes efficiently recognize ATG1 at position -109 and initiate translation of uORF1. Therefore, we next investigated the role of the nascent peptide encoded by uORF1 in controlling translation of the downstream main ORF.

Since uORF1 in the rat Mrp2 mRNA encodes a 56 amino acid peptide. It is unrealistic to mutate, at least initially, each single codon to determine the amino acid sequence dependence. Therefore, logically, we first divided the peptide into three segments: first segment (rF), middle segment (rM), and last segment (rL) (shown in Figure 3.1.), each of which encodes 22 amino acids. After the middle and last segments were found to have stronger inhibitory effect on translation in

in vitro translation assays, we further confirmed this by studying the frame-shifted mutants of the middle and last segments. To narrow down the amino acid range that would be critical to the inhibitory effect of uORF2, the combined amino acid segments of the middle and last segments were further divided into three pieces each of which contained 11 codons: r11aa_1, r11aa_2, and r11aa_3 (shown in Figure 3.1.). Finally, the translational efficiencies of the nature and frame-shifted sequences of uORF1 (r56 and Δr56, shown in Figure 3.1.) were examined in *in vitro* translation assays. We also investigated whether uORF1 at position -109 is a *cis*- or *trans*-acting regulator of translation *in vitro*. In addition, we also expressed the peptide encoded by uORF2 of the rat Mrp2 mRNA in the TnT system, and also tried to detect this peptide in the rat liver and kidney.

MATERIALS AND METHODS

Materials

L-^{35}S-Methionine was purchased from Amersham (UK), and protein A/G Plus-agarose was from Santa Cruz. PAS is a rabbit polyclonal antibody to a 17 amino-acid epitope (SAFPEEKUKEKQYNHRR) of the peptide of 56 amino acids encoded by uORF1 (Pro-Sciences) (named Pep56). The construct pET21_Pep56 was prepared by EnzyMax by cloning the sequence of uORF1 into the expression vector pET21. Expression of Pep56 tagged with 6xHis at the N-terminal (molecular weight: 7.2 kDa) was induced by IPTG in *E. Coli*. Pep56-His was used as the positive control of Pep56 in the following work.

Plasmid construction

A schematic representation of the fusion luciferase constructs used is shown in Figure 3.1. All inserts were fused between the T7 promoter and the luciferase ORF at the Hind III restriction site. Using the pair of primers of pepF/pepR (all primers are shown in Table 3.1.), the sequence from position -109 to +92 was PCR-amplified from the genomic cDNA library prepared from the rat liver, and cloned into the luciferase T7 control vector, obtaining the plasmid rMrp2_56. The nucleotides GTGAGA were inserted into rMrp2_56 before ATG1 with the primers KoF/KoR to maintain the Kozak motif intact, thus obtaining the plasmid r56. The plasmid Δr56 was prepared by frame-shifting uORF1 according to the following sequence: 1) A potential stop codon formed after frame-shifting was deleted by mutation of T at position -38 to C with the primers MutF/MutR; 2) A frame-shifting

mutation was performed by deletion of the nucleotides GA after ATG1 following insertion of the nucleotides AA before TGA of uORF1 with the pairs of primers DelF/DelR and InsF/InsR, respectively.

The plasmid rF was obtained by deletion of the sequence from position -43 to +61 with the plasmid rMrp2_56 as template and then by insertion of the nucleotides GTGAGA before ATG1, using two pairs of primers of rFna/rRna and KoF/KoR, respectively. Thus, the insert rF contained the first 22 codons of uORF1.

The plasmid rM was prepared by sequential deletion of the sequences from position -104 to -42 and from position +16 to +61 nt from the plasmid r56, using two pairs of primers, M1F/M1R and M2F/ M2R, respectively. Thus the insert rM contains the middle 22 codons of uORF1. Frame-shifting prepared the plasmid ∆rM through sequential deletion of two adenosines after ATGGAG and insertion of two adenosines before TGA, using two pairs of primers of delMF/delMR and insMF/insMR, respectively. The plasmid rL was prepared by deleting the sequence from position -104 to -2 from the plasmid r56 with the pair of primers of LF/LR. The insert rL contains the last 22 codons of uORF1, but overlaps the sequence of rM. The plasmid ΔrL was prepared by deletion of an adenosine after ATGGAG and insertion of an adenosine before TGA, using two pairs of primers of delLF/delLR and insLF/insLR, respectively.

With a pair of primers M3F/M3R, the sequence from position -10 to +61 was deleted from the plasmid rM to obtain r11aa_1. The plasmid r11aa_2 was prepared by deletion of the sequences from position -104 to -13 and +24 to +61

from the plasmid r56, using two pairs of primers of M4F/M4R and M5F/M5R, respectively. The plasmid r11aa_3 was constructed by deletion of the sequences from position -104 to +23 from the plasmid r56, using the pair of primers of M6F/M6R. Each of the obtained inserts of r11_1, _2, and _3 contains 11 codons.

The plasmid r56_LucAAG was obtained by mutation of the ATG of the luciferase gene to AAG to disrupt the luciferase ORF, using the plasmid r56 as template and the pair of primers MutLucF/MutLucR.

In all of these constructed plasmids, the sequences upstream of the start codon and downstream of the stop codon were maintained as in the native *Mrp2* gene. All primers used are listed in Table 3.1. Mutagenesis was performed according to the manufacturer's instructions of Quick-Change Site-Directed Mutagenesis Kit (Stratagene, La Jolla, CA). All plasmids were confirmed by forward sequence sequencing reactions.

In vitro **translation assays**

The template of about 1.8 kbp was obtained by linearizing each tested fusion luciferase construct with restriction enzymes Pvu II and Sac I. The capped-end luciferase transcripts were prepared and randomly labeled by α-^{32}P-UTP by *in vitro* transcription reactions. To quantify the RNA yield, incorporation efficiency of α-^{32}P-UTP into RNA was determined by scintillation counting. Free nucleotides in the reaction mixture were removed using NucAway™ Spin Columns (Ambion). The luciferase transcripts (0, 2, 4, 10, 20, and 40 ng) were added to the reaction mixtures and incubated at 30 °C for 60 min and terminated on ice. The firefly

luciferase activity was measured by the Luciferase Assay System (Promega) according to the manufacturer's instructions. The best linear fit of the relationship between luciferase activities and mRNA concentrations was determined using GraphPad Prism 4.0. The slopes of these lines represent translation efficiencies.

Expression of Pep56 in the Transcription/Translation coupled system (TnT system).

pcDNA3.1-r56aa was obtained by cloning the fragment from position -122 to +67 into the pcDNA3.1 vector (Invitrogen) at the Hind III and Xho I restriction sites. The TnT quick Transcription/Translation coupled system (Promega) was used to translate Pep56. According to the manufacturer's instructions, a reaction mixture (50 µl) containing 40 µl of TnT Master Mix, 2 µl of ^{35}S-methionine, 1 µg of pcDNA3.1 or pcDNA3.1_r56aa was incubated at 30 °C for 60 min. The reaction (1 or 2 µl) products were loaded and separated on 16% Tricine gel (Invitrogen). The gel was dried for 1 h at 80ºC and then developed at -80ºC for two weeks.

Western Blot

Female Sprague Dawley rats (weight=200-250 g) were sacrificed to obtain kidney and liver tissues. Tissues were homogenized in lysis buffer with a Dounce homogenizer. Cytosolic fraction was obtained by sequential centrifugation of homogenate at 9,000 g at 4°C for 20 min and 100, 000 g at 4°C for 60 min. Protein concentrations were determined by means of the Bio-Rad protein assay. Samples were boiled in 2x Tricine SDS sample buffer (Invitrogen) at 90°C for 3

min before being loaded on a 16% Tricine gel. Proteins were transferred to Protran® nitrocellulose filters by electrophoresis in transfer buffer for 2 hrs. Filters were incubated with PAS (1:200 in 1xT TBS with 5% milk) at 4°C overnight. After washing twice with 1x T-TBS at room temperature for 15 min, the secondary antibody (peroxidase-conjugated anti-rabbit IgG, 1:5000 in 1xT-TBS buffer with 5% milk) was incubated with filters at room temperature for 1 hr. Then filters were washed twice again and developed using the Amersham enhanced chemiluminescence detection system.

Titration with the antigen peptide

The rat kidney homogenate (100 µg) and 0.1 µg of the positive control peptide (Pep56-His) were run on a 16% Tricine gel and transferred onto Protran® nitrocellulose filters. Before the Protran filter was incubated with the primary antibody, the antibody (PAS) was incubated with the 17-amino acid antigen peptide (0, 10, 100, 1000 ng) at 4°C for 3 hr, rotating on an end-to-end rotator. The Protran filter was then incubated with the secondary antibody (peroxidase-conjugated anti-rabbit IgG) and developed using the Amersham enhanced chemiluminescence detection (ECL) system.

Immunoprecipitation

Rat kidney homogenate (100 µg protein) was incubated with 120 µl RIPA buffer and 3 or 6 µg PAS at 4°C overnight on an end-to-end rotator. The next day, 40 or 60 µl of Protein A/G Plus-agarose was added into the mixtures with 3

or 6 µl PAS, respectively, and incubated at 4°C overnight on an end-to-end rotator. The pellets were collected by centrifugation at 2500 rpm at 4°C for 5 min and then gently washed 4 times with RIPA buffer. After the final wash, supernatants were carefully aspirated and discarded. The pellets were resuspended in 20 µl of 2x Tricine SDS sample buffer and boiled at 90°C for 3 min. Then beads were spun down at 2500 rpm for 5 min and the supernatants were loaded in a 16% Tricine gel for Western blot analysis.

RESULTS

Effect of the amino acid sequence of uORF1 on translation efficiency of the luciferase transcript in *in vitro* translation assays

We have shown that ATG1 has an inhibitory effect on translation (Figure 2.5.) and that it was able to be recognized efficiently by ribosomes since a longer luciferase protein was translated in the TnT system (Figure 2.6.). The next investigation was focused on determining whether this inhibitory translation is dependent on the amino acid sequence encoded by uORF1. We cloned uORF1, either intact or in 3 segments containing 22 or 11 amino acids into the control T7 luciferase vector. We investigated whether the peptide and these segments might affect translation of the luciferase transcript. All segments shared the same ATG and its Kozak motif sequence, and the same stop codon and its downstream sequence as shown in Figure 3.1.

When the sequence of uORF1 was divided into three segments (rF, rM, and rL), each of which encodes 22 amino acids, translation efficiencies of rM and rL were 1.6- and 2.6–fold lower than that of rF ($p<0.0001$), while the translation efficiency between rM and rL was similar ($p=0.0014$) (Figure 3.2.A.). When the amino acid sequence of rM was scrambled by frame-shifting, translation efficiency of ΔrM was 5.7-fold higher than that of the native rM ($p<0.0001$, Figure 3.2.B.). Similarly, ΔrL increased translation efficiency 5.3-fold compared to rL ($p<0.0001$, Figure 3.2.C.). Thus, the amino acids of Pep56 without the first 22 amino acids contributed more to the translational inhibitory effect. Therefore, the sequence of the last 34 codons was further divided into three pieces (shown in

Figure 3.1.). Each of the three sequential pieces encodes 11 or 12 amino acids. Translation efficiencies of r11aa_1, r11aa_2 and r11aa_3 were essentially the same (p=0.0019, Figure 3.2.D.). Finally, the translation efficiency of the luciferase transcript with the sequence of uORF1 (r56) was 1.29-fold higher than that with the frame-shifted sequence (Δr56) (p=0.00015, Figure 3.2.E.).

Is the effect of uORF1 *cis*- or *trans*- acting?

We have shown that uORF1 exerted a translational inhibitory effect when present upstream of the luciferase reporter transcript, and its encoded Pep56 was expressed in the Transcription/Translation coupled system. In this experiment, we further investigated whether uORF1 is a *cis*- or *trans*- factor on translation.

The luciferase ORF was disrupted in the plasmid r56_LucAAG. The luciferase transcript alone or both the luciferase transcript along with the r56_LucAAG transcript (0, 2, 4, 10, 20, and 40 ng of each) were added into the *in vitro* translation reaction mix. After incubation at 30ºC for 1 hr and termination on ice, the luciferase activities were measured. The translation efficiency of T7Luc_ctrl in the presence of r56_LucAAG was 97% of that in the absence of r56_LucAAG (p=0.91, Fig3.3.). Therefore, there was no difference shown in translational efficiency between the luciferase transcripts alone or together with the r56_LucAAG transcript. That is, uORF1 did not have a *trans*-acting effect on translation through its encoded peptide (Fig3.3.).

In vitro expression of Pep56 in the Transcription/Translation coupled system

To determine if translation can efficiently initiate at ATG1, terminate at the stop codon at position +62, and express Pep56 (MW: 6.8 kDa), the plasmid pcDNA3.1-r56aa containing the segment from position -122 and +67 was incubated with the TnT reaction mixture and the newly synthesized peptide was labeled in the presence of L-^{35}S-Methionine. A peptide was observed at 6.8 kDa in the lane of pcDNA3.1_r56aa, with no bands showing in the lane of the control plasmid pcDNA3.1 (Figure 3.4.).

Detection of Pep56 expression in the rat kidney and liver

We have shown that Pep56 was able to be expressed *in vitro.* We therefore questioned whether Pep56 is expressed *in vivo*. The theoretical molecular weight of Pep56 is 6.8 kDa. PAS was used as the primary antibody in Western blot analysis and Pep56-His was used as the positive control (Figure 3.5.). Although there was no band observed at 6.8 kDa, a peptide (about 14 kDa) was detected in the kidney homogenate at a higher level than in the liver homogenate, but was not found in the cytosolic fraction of either kidney or liver.

Two more experiments were performed to determine whether the 14 kDa peptide might be an oligomer of Pep56. In the first experiment, titration of PAS with the antigen peptide (Figure 3.6.) showed that this band disappeared when 10 ng of the antigen peptide was pre-incubated with PAS, in line with the fact that the positive control was titrated out gradually by antigen peptide (10, 100, and

1000 ng). Second, in the experiment of immunoprecipitation (Figure 3.7.), when 3 µg of PAS and 40 µl of Protein A/G were used (lane 2-5), the band of 14 kDa did not appear in the pull-down products (lane 2 and 4) or their supernatants (lane 3 and lane 5) of either kidney homogenate alone (lane 2 and 3) or in the presence of the positive control (lane 4 and 5), even though the positive control was successfully immunoprecipitated by PAS (lane 4). When 6 µg of PAS and 60 µl of Protein A/G were used (lane 6-9), the band appeared but was not able to be seen separately from non-specific bands in the immunoprecipitated products (lane 6 and 8), and it didn't appear in the supernatants (lane 7 and 9) of either kidney homogenate alone (lane 6 and 7) or in the presence of the positive control (lane 8 and 9). More Pep56-His was immunoprecipitated in the mixture of the positive control plus kidney homogenate by 6 µg of PAS and 60 µl of Protein A/G (lane 8) than by 3 µg of PAS and 40 µl of Protein A/G (lane 4).

CONCLUSIONS

To investigate whether the translational inhibition exerted by uORF1 at position -109 was dependent on its encoded amino acid sequence, uORF1 was divided into three segments (rF, rM, and rL) each of which encodes 22 amino acids. The data showed that rM and rL inhibited translation more efficiently than rF (Figure 3.2.A), suggesting that the amino acids in the segments of rM and rL were critical for translational inhibition exerted by uORF1 at position -109. This was further confirmed by the 5-6-fold higher translation efficiencies of the frame-shifted sequences of ∆rM and of ∆L, compared to those of the native segments of rM and rL (Figure 3.2.B and C), respectively. However, when we narrowed down the amino acid range by further dividing the last 34-codon segment into three pieces (r11aa_1, r11aa_2, and r11aa_3), there was no difference observed in translation efficiency between r11aa_1, r11aa_2, and r11aa_3 (Figure 3.2.D). Also, when we finally examined the full-length 56 amino acid peptide, we observed no difference in the translation efficiencies between the native and altered amino acid sequences of uORF1 (r56 and Δr56, respectively) (Figure 3.2.E). Therefore, the last 34 amino acids in uORF1 work together in inhibiting translation.

Further, the translational inhibition exerted by uORF1 was demonstrated not to be *trans*-acting (Figure 3.3.B.), indicating that these amino acids may stall the scanning of ribosomes before the translation of uORF1 is finished, even though the peptide encoded by uORF1, Pep56 (MW=6.5 kDa), was expressed in the

TnT system (Figure 3.5.). However, we were unable to detect Pep56 in the rat liver or kidney.

FIGURES AND LEGENDS

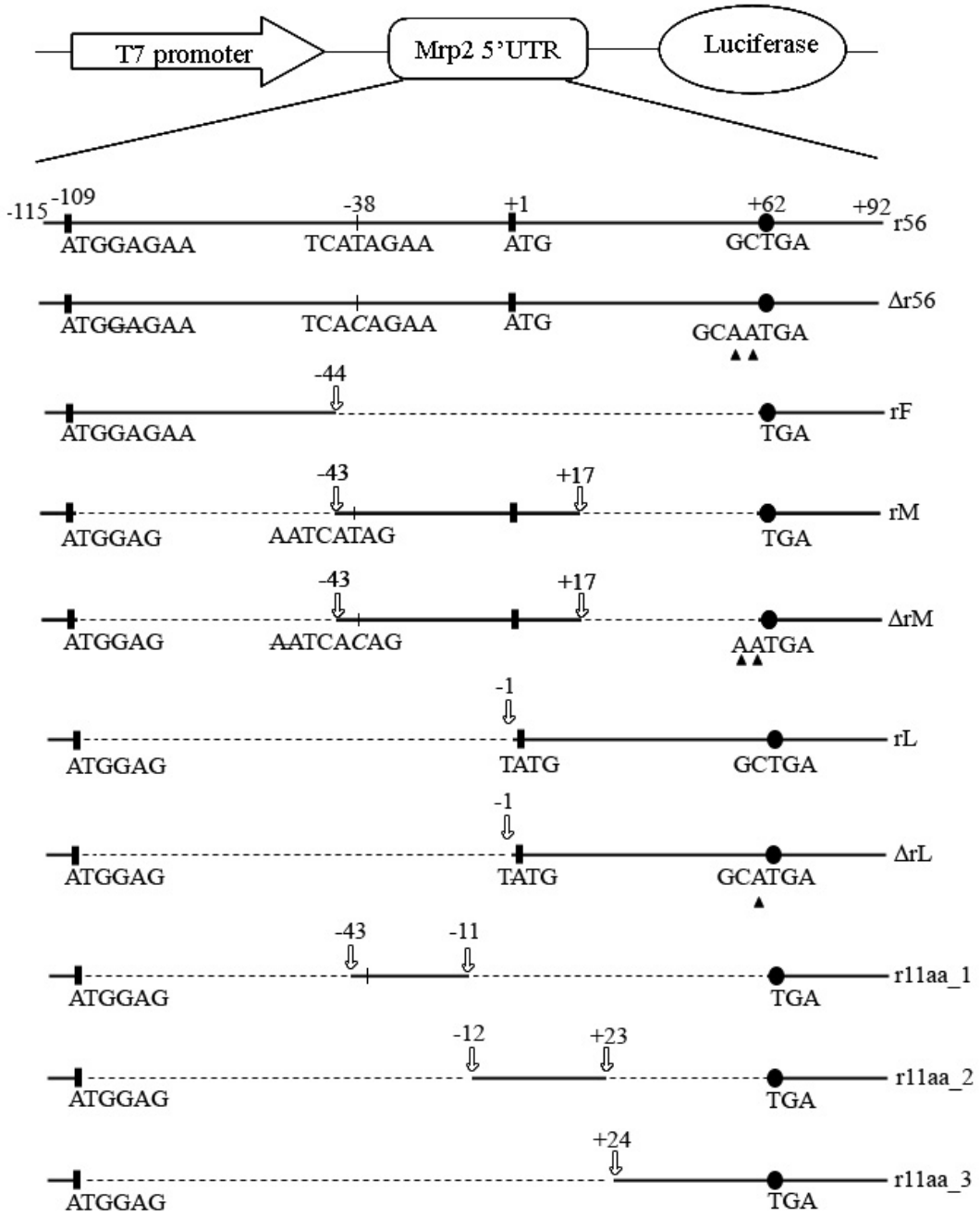

Figure 3.1. Schematic representation of construction of plasmids. All constructs shown were used to investigate the sequence dependence of uORF1 on translation. Inserted sequences are shown as bold solid lines to scale and dashed lines represent the deleted sequences. All inserts shown were fused in

the T7 luciferase control vector between the T7 promoter and the luciferase coding region at the Hind III restriction site. Solid bars represent start codons and solid circle stop codons. The point mutations are shown as italic. The strike-through nucleotides (like ~~AA~~) present the deleted ones. Inserted nucleotides are indicated by solid triangles underneath the nucleotides. The unfilled arrows point to the ligation locations. r56 is the native sequence from position -115 to +92. Δr56 is the scrambled sequence obtained by frame-shifting r56. The insert of rF from position -115 to -44 encodes the first 22 amino acids of Pep56; rM from position -43 to +17, the middle 22 amino acids; rL from position -1 to +61 nt, the last 22 amino acids but shares amino acids with rM. ΔrM is a frame-shifted sequence of rM, and ΔrL a frame-shifted sequence of rL. The inserts of r11aa_1, r11aa _2, and r11aa _3 were obtained by dividing the sequence from position -43 to +61 into three fragments each of which encodes 11 or 12 amino acids. All of these constructs share the same start codon and its upstream sequence, and the same stop codon and its downstream sequence.

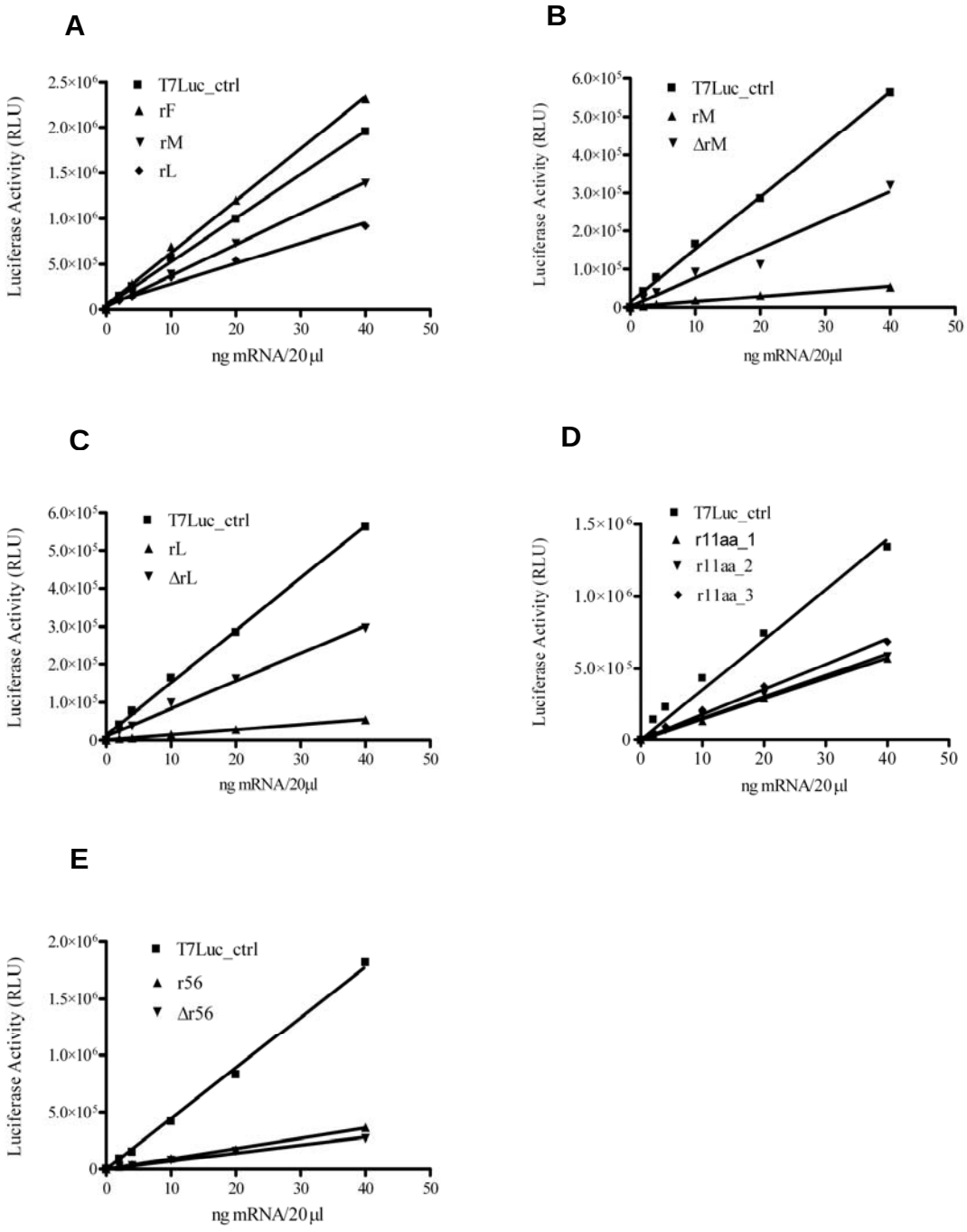

Figure 3.2. Sequence dependence of uORF1 on translation by *in vitro* translation assays. The capped fusion luciferase transcripts (2, 4, 10, 20, and 40 ng) were added to the reaction mixtures and incubated at 30ºC for 1 hr and then terminated on ice. The luciferase activity was measured. The straight lines

are the best fit of the relationship between luciferase activities and mRNA concentrations. The slopes represent translation efficiencies. This graph is a representative of two experiments. The statistical significance of the difference between the slopes was tested by GraphPad Prism 4.0.

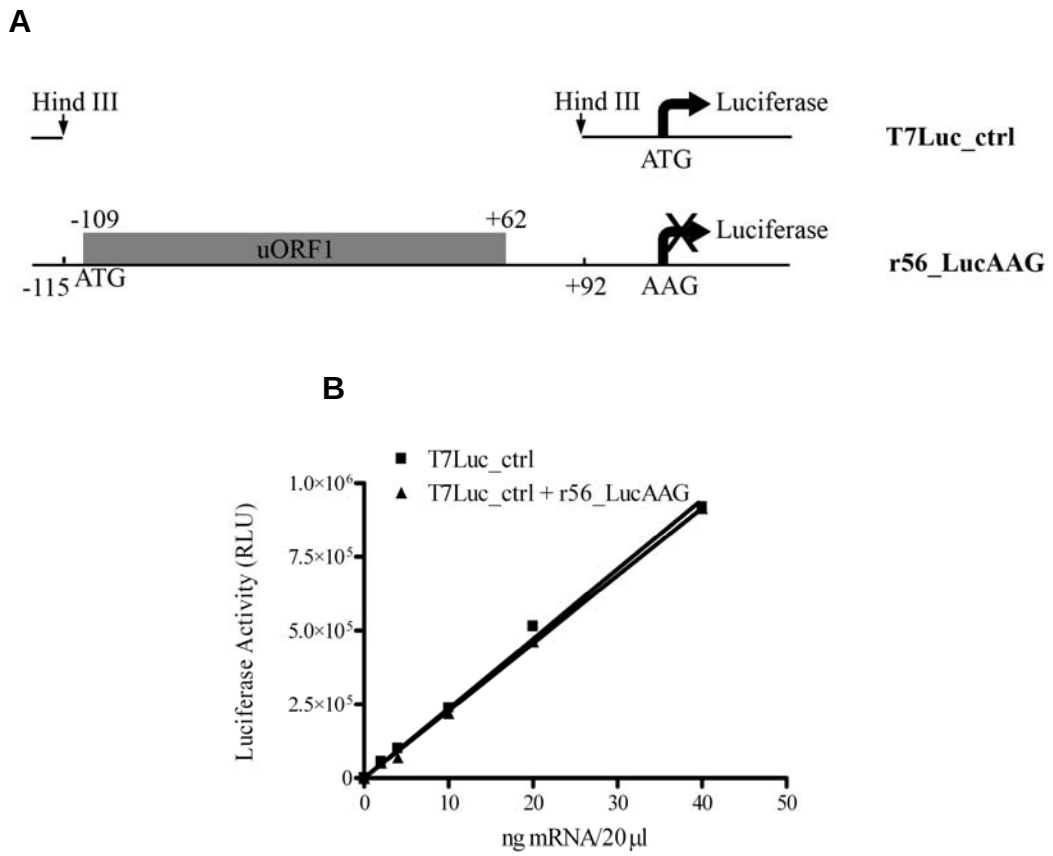

Figure 3.3. Determination of the *cis*- or *trans*-acting effect of uORF1 on translation by *in vitro* translation assay. A. Schematic representation of the plasmid constructs. The sequence of position -115 to +92 of the rat Mrp2 5'UTR cDNA was inserted at Hind III restriction enzyme site in the T7 luciferase control vector (T7Luc_ctrl). The luciferase ORF in the plasmid r56_LucAAG was disrupted by mutation of the ATG of the luciferase gene to AAG. **B.** *In vitro* translation assays. The luciferase control transcript alone or together with the transcript of r56_LucAAG (2, 4, 10, 20, and 40 ng of each) were added to reaction mixtures and incubated at 30ºC for 1 hr and then terminated on ice. The luciferase activity was measured. The straight lines are the best fit of the relationship between luciferase activities and mRNA concentrations. The slopes

represent translation efficiencies. The statistical significance of the difference between the slopes was tested by GraphPad Prism 4.0.

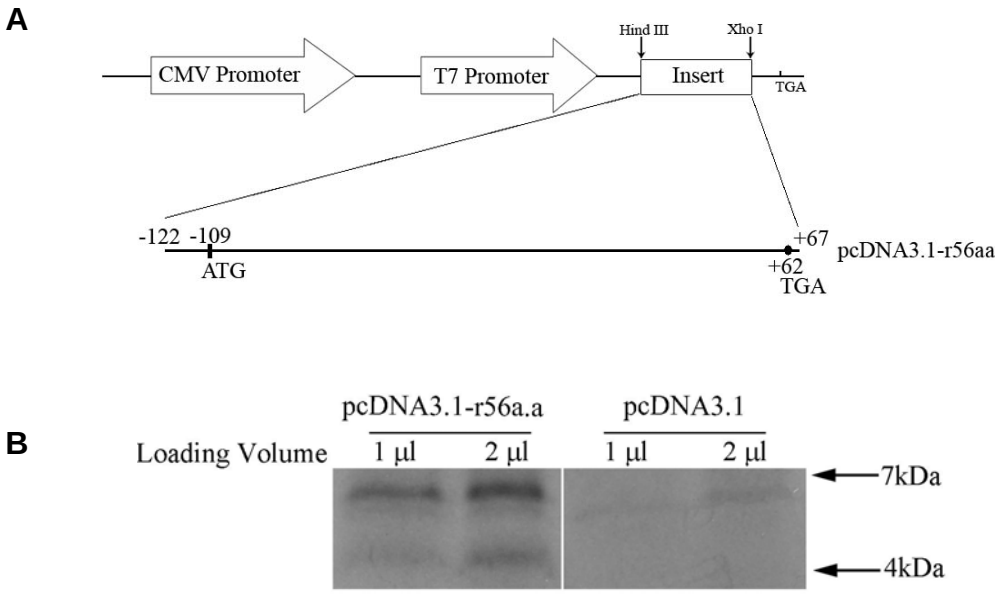

Figure 3.4. Expression of Pep56 in the Transcription/Translation coupled system. A. The schematic representation of pcDNA3.1-r56aa constructs. The sequence from position -122 to +67 was cloned into the pcDNA3.1 vector at the Hind III and Xho I restriction sites. **B.** Expression of Pep56 in the TnT system. The control pcDNA3.1 vector (1 µg) or the pcDNA3.1-r56aa vector (1 µg) was added into the TnT reaction mixtures that contained L-^{35}S-Methionine and incubated at 30ºC for 1 hr. The reaction products (1 or 2 µl) were run on a 16% Tricine gel. This is representative of two experiments.

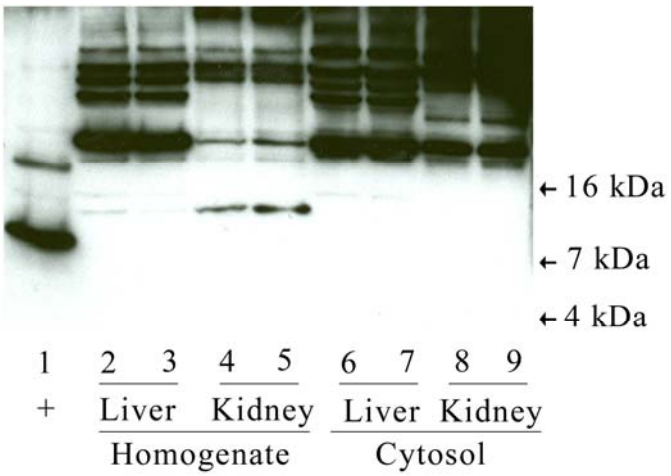

Figure 3.5. Detection of Pep56 in the rat liver and kidney by Western Blot. The homogenates (100 µg of each) and the cytosol (78 µg of each) of liver and kidney were loaded on 16% Tricine gel for western blot analysis. Lane 1 is the positive control, Pep56-His (0.1 µg). Lane 2 and 3, the liver homogenate; Lane 4 and 5, the kidney homogenate; Lane 6 and 7, the liver cytosol; and Lane 8 and 9, the kidney cytosol. The protein ladders are indicated by arrows.

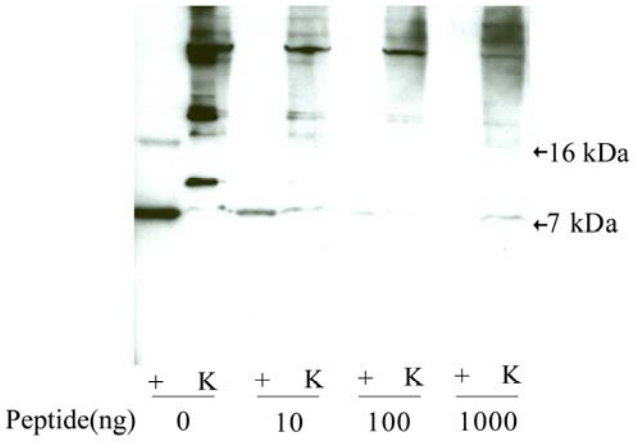

Figure 3.6. Titration with the antigen peptide. The rat kidney homogenate (100 µg) and 0.1 µg of Pep56-His were run on 16% Tricine gel and transferred onto Protran® nitrocellulose filters. Before incubated with the filter, the primary antibody of PAS (1:200 in T-TBS) was incubated with the 17-amino acid antigen peptide (10, 100, 1000 ng) at 4°C for 3 hr. “K” represents the kidney homogenate and “+” represents Pep56-His.

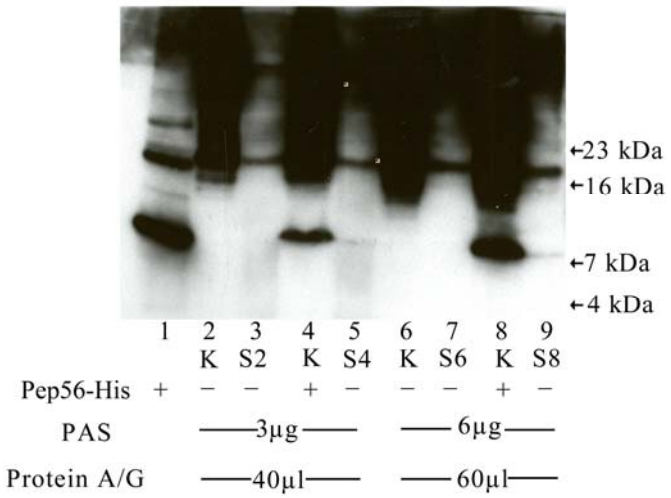

Figure 3.7. Immunoprecipitation of the rat kidney homogenate with PAS. The rat kidney homogenate (1000 μg) was used in immunoprecipitation and pull-down products was run on a 16% Tricine gel. “K” represents the kidney homogenate (1000 μg). Pep56-His (0.1 μg) was used in this experiment. S2, S4, S6, and S8 are supernatants of the lanes 2, 4, 6, and 8, respectively, after immunoprecipitation. Lanes 2-5 were all pulled down with 3 μg of PAS and 40 μl of Protein A/G plus agarose. Lanes 6-9 were pulled down with 6 μg of PAS and 60 μl of Protein A/G plus agarose. The protein ladders were indicated by arrows.

Table 3.1. Primers used in site-directed mutagenesis for determination of sequence dependence

Primers	Sequence	constructs
pepF	5’atcaagcttatggagaaagcacg3’	rMrp2_56
pepR	5’atcaagcttagaacagtttgctca3’	
KoF	5’ctatagggagacccaagcttgtgagaatggagaaagcacggtgca3’	r56 &rF
KoR	5’tgcaccgtgctttctccattctcacaagcttgggtctccctatag3’	
MutF	5’ggagaaacagtacaatcacagaagagtcttcgtaacag3’	∆r56
MutR	5’ctgttacgaagactcttctgtgattgtactgtttctcc3’	
DelF	5’gacccaagcttatggaaagcacggtg3’	
DelR	5’caccgtgctttccataagcttgggtc3’	
InsF	5’gaaagtccagaggcaatgacctgcctctttg3’	
InsR	5’caaagaggcaggtcattgcctctggactttc3’	
rFna	5’gctttcccagaggaaaaagtaaaggagaaacagtactgacctgcctctttgttttgagcaaactgttctaag3’	rF
rRna	5’cttagaacagtttgctcaaaacaaagaggcaggtcagtactgtttctcctttacttttttcctctgggaaagc3’	
M1F	5’cactatagggagacccaagcttgtgagaatggagaatcatagaagagtcttcgtaacagaagc3’	rM
M1R	5’gcttctgttacgaagactcttctatgattctccattctcacaagcttggtctccctatagtg3’	

M2F	5’cgaggagagcattatggacaagttctgcaatgacctgcctctttg ttttgagcaaactgttc3’	
M2-R	5’gaacagtttgctcaaaacaaagaggcaggtcattgcagaactt gtccataatgctctcctcg3’	
LF	5’cgactcactatagggagacccaagcttgtgagaatggagtatg gacaagttctgcaactctacttttttgggatctctc3’	rL
LR	5’gagagatcccaaaaagtagagttgcagaacttgtccatactcc attctcacaagcttgggtctccctatagtgagtcg3’	
delMF	5’cccaagctttgtagaatggagtcacagaagagtcttcgtaac3’	ΔrM
delMR	5’gttacgaagactcttctgtgactccattctacaaagcttggg3’	
insMF	5’agagcattatggacaagttctgcaaaatgacctgcctcttt3’	
insMR	5’aaagaggcaggtcattttgcagaacttgtccataatgctct3’	
delLF	5’ccaagcttgtgagaatggagttggacaagttctgca3’	ΔrL
delLR	5’tgcagaacttgtccaactccattctcacaagcttgg3’	
insLF	5’ggaaagtccagaggcatgacctgcctctttg3’	
insLR	5’caaagaggcaggtcatgcctctggactttcc3’	
M3F	5’catagaagagtcttcgtaacagaagcgcgatgacctgcctcttt gttttgagcaaactgttc3’	11aa_1
M3R	5’gaacagtttgctcaaaacaaagaggcaggtcatcgcgcttctgt tacgaagactcttctatg3’	
M4F	5’ctatagggagacccaagcttgtgagaatggagggagagcatt atggacaagttctgcaactc3’	11aa_2

M4R	5’gagttgcagaacttgtccataatgctctccctccattctcacaagcttgggtctccctatag3’	
M5F	5’gagcattatggacaagttctgcaactctactgacctgcctctttgtttttgagcaaactgttc3’	
M5R	5’gaacagtttgctcaaaacaaagaggcaggtcagtagagttgcagaacttgtccataatgctc3’	
M6F	5’ctatagggagacccaagcttgtgagaatggagtttttgggatctctcattactggaaagtcc3’	11aa_3
M6R	5’ggactttccagtaatgagagatcccaaaaactccattctcacaagcttgggtctccctatag3’	
MutLucF	5’gcccggatccaaaaggaagacgccaaaaac3’	r56_LucAAG
MutLucR	5’gtttttggcgtcttccttttggatccgggc3’	

CHAPTER FOUR

TRANSLATIONAL REGULATION OF HUMAN MULTIDRUG RESISTANCE PROTEIN 2 (MRP2) IS MEDIATED BY THE 5' UNTRANSLATED REGIONS

BACKGROUND

Studies in patients and human liver tissues have shown that expression of human hepatic MRP2 protein undergoes post-transcription regulation. A poor correlation between the human MRP2 mRNA levels and protein has been observed in patients with icteric inflammatory cholestasis [49] and in LPS treated human liver slices [51]. In the cancerous kidney cortex tissue of clear-cell renal cell cancer (CCRCC) and non-CCRCC patients, a significantly decreased MRP2 protein was observed compared to that in the normal cortex tissues, but the mRNA level of MRP2 did not confirm this [86]. Expression of human MRP2 protein is reduced by obstructive cholestasis in the intestine, while the level of mRNA is not affected [87]. There are no studies on the mechanisms of translational regulation of the human *MRP2* gene to date

The 5' flanking region of the human *MRP2* gene was first sequenced by Tanaka et. al [22], who identified three initiation sites of transcription (at position -247, -204, and -99 relative to the ATG of human MRP2), based on the 5' rapid amplification capped end assay (5'RACE) [22]. One of the similarities between Mrp2 and MRP2 mRNAs is the presence of multiple upstream translation start sites (ATGs) in the 5'UTRs, although the human MRP2 mRNA is more complex in terms of uORFs that rat. The cDNA sequence of the longest 5'UTR and the organization of uORFs of the human *MRP2* gene are shown in Figure 4.1. There

are seven upstream ATGs in the cDNA sequence of the longest 5'UTR at position -74, -105, -137, -146, -173, -180, and -199 (relative to the ATG of human MRP2), which are termed ATG1, ATG2, ATG3, ATG4, ATG5, ATG6, and ATG7, respectively. Accordingly, the uORFs of these ATGs are termed as uORF1, uORF2, uORF3, uORF4, uORF5, uORF6, and uORF7. Only one upstream ATG in the human MRP2 5'UTR, ATG2 (at position -105), has a perfect Kozak motif (A at position -3 and G at +4 relative to ATG2). However, unlike uORF1 at position -109 in the rat Mrp2, the human uORF2 at position -105 is in-frame with, but terminates prior to the coding region of MRP2 (termed ORF0). uORF6 is also in-frame with uORF2 and ORF0. uORF1, 3, 4, and 5 are in the same frame, but out-of-frame with ORF0. uORF7 is out-of-frame with both ORF0 and uORF1. Among these seven uORFs, uORF1 is unusually long (103 codons) and overlaps ORF0. uORF3 and uORF4 share the same stop codon, and the start codon of uORF4 is immediately adjacent to the stop codon of uORF5. Therefore, uORF7 overlaps with uORF6 and uORF5, uORF4 overlaps uORF3 and uORF2, and uORF2 overlaps uORF1. The organization of these uORFs is shown in Figure 4.1.B.

In the rat Mrp2 5'UTR cDNA sequence, only uORF1 at position -109 among all four uORFs is flanked by a perfect Kozak Motif. We have demonstrated in Chapter Two and Three that 1) uORF1 exerts an strong inhibitory effect on translation; 2) this translational inhibition is not *trans*-acting; and 3) uORF1 can be successfully expressed in the *in vitro* system [88]. Here, we studied the 5'UTRs-mediated mechanisms of translational regulation of human MRP2 and

focused on the role of uORF2 at position -105 in translational regulation. We investigated the effect of the 5'UTRs, particularly the upstream ATGs, on translation in the transiently transfected HepG2 cells and *in vitro* translation. In addition, we examined sequence dependence of translational effects exerted by uORF2 at position -105. Finally, we also investigated expression of the MRP2 mRNA isoforms in the liver and HepG2 cells using ribonuclease protection assay.

MATERIALS AND METHODS

Materials

α-^{32}P-UTP (800 Ci/mmol) was obtained from Perkin Elmer Life and Analytical Sciences (Boston, MA). Unless otherwise noted, all other chemicals were of analytical grade and of cell culture grade from Sigma Chemical Co. (St. Louis, MO), Invitrogen™ Life Technologies (Carlsbad, CA), Roche Diagnostics (Indianapolis, IN), and Fisher Scientific (Pittsburgh, PA). Restriction enzymes were obtained from Invitrogen, NewEngland Biolab, and Promega (Madison, WI).

Ribonuclease protection assay (RPA)

Total RNA of the human liver was purchased from Ambion, and total RNA from HepG2 cells was isolated using TRIzol (Invitrogen), according to the manufacture's protocol. A fragment of a T7 luciferase vector containing the human MRP2 5'UTR sequence was purified from agarose gel after digestion with Pvu II and BamH I restriction enzymes. This fragment was used as a template to prepare the MRP2 probe by *in vitro* transcription, and was randomly labeled with α-^{32}P-UTP. The RPA was performed following the procedures of the RPA III Kit (Ambion). Briefly, total RNA (20 µg) was incubated at -80°C for 90 min with the MRP2 probe in the 20 µl mixture containing 0.5 M ammonium acetate plus 2.5 volumes of ethanol. Following coprecipitation, the RNA pellet was washed once with 75% ethanol and dissolved in the hybridization solution (in RPA III Kit). The hybridization reaction mixture was incubated at a gradient annealing temperature from 56°C to 36°C at a rate of 2°C per 2 hr. After the hybridization reaction, the

single-stranded RNA was digested by RNAse A/T1 mix at 37°C for 1 hr. The fragments protected from RNAse digestion were identified by electrophoresis on 6% urea-PAGE gels.

Plasmid construction

The cDNA sequence of the human MRP2 5'UTR is shown in Figure 4.1.A. Schematic representations of the MRP2 5'UTR luciferase fusion constructs are shown in Figure 4.3.A. (based on the pGL3 control vector) and Figure 4.4.A. (based on the T7 luciferase control vector). All primers are listed in Table 4.1.

The constructs from the pGL3 control vector were used in transient co-transfection assays in HepG2 cells. The fragments of Hu-L (-247 nt), Hu-M (-204 nt), and Hu-S (-99 nt) were cloned into the pGL3 control vector between the SV40 promoter and the luciferase coding frame.

The constructs from the T7 luciferase control vector were used in *in vitro* translation assays. The fragments of hM- and hS- 5'UTR were cloned into the T7 luciferase control vector at Hind III restriction site between the T7 promoter and the luciferase coding region. The plasmid of hmutM was prepared by mutation of ATG2 to AAG to disrupt uORF2 using the plasmid of hM as template.

To determine whether the inhibitory regulation of translation of the ATG2 is dependent on the amino acid sequence of uORF2, the native sequence from position -111 to -1 and the frame-shifted uORF2 sequence were cloned into the T7 luciferase control vector. The native sequence from position -111 to -1 was PCR-amplified by the pair of primers hF/hR (Table 4.1) using the plasmid Hu-M

as template. Both of hF and hR contained a Hind III restriction site. After digestion by Hind III, the fragment and the T7 luciferase control vector were ligated with T4 ligase, obtaining the plasmid MRP2_22. The plasmid ΔMRP2_22 was constructed by frame-shifting uORF2 in the plasmid MRP2_h22 through 1) deletion of the T at position -101 after ATGG with the primers of hFdel/hRdel; 2) insertion of an A before the stop codon TAA at position -39 using the primers hFins/hRins; and then 3) disruption of the ATG1 at position -74 by mutation to ATA using the primers of hFmut/hRmut. The plasmids h22 and Δh22 were obtained by cloning a spacer sequence from position -143 to -112 between the capped site and ATG2 in the plasmids MRP2_22 and ΔMRP2_22, using the pair of primers of hFex/hRex, and the pair of primers of ΔhFex/ΔhRex, respectively. Thus, neither of the plasmids of h22 or Δh22 contained ATG3 at position -137.

The luciferase ORF and uORF2 were disrupted in the plasmid h22 by a site-directed point mutation with MutLucF/MutLucR and h105aagF/h105aagR, respectively, obtaining the plasmids h22_LucAAG and h22_105AAG.

All mutagenesis was performed according to the manufacturer's instructions of Quick-Change Site-Directed Mutagenesis Kit (Stratagene, La Jolla, CA). All the plasmids were confirmed by sequencing.

Transient co-transfection assays in HepG2 cells

HepG2 cells were cultured in DMEM/F12 (1:1 medium) supplemented with 10% charcoal-stripped fetal bovine serum (Hyclone Laboratories, Logan, UT), 3.58 mM glutamine, 55 μg/ml gentamycin, and 1 μg/ml insulin (Invitrogen). One

day before transfection, the culture medium was replaced by phenol red-free DMEM supplemented with 10% charcoal stripped FBS, glutamine and gentamycin. The plasmids (1 μg) (Hu-L, -M, and -S) were transfected by the ProFectin mammalian transfection system-calcium phosphate (Promega) into HepG2 cells together with 30 ng pSV40-Ren (Promega) used as an internal control for transfection efficiency. After 5-6 hr incubation, the transfection medium was replaced with the maintenance medium. Cells were harvested 24 hr later for measurement of the firefly and *Renilla reniformis* luciferase activities by the Dual-luciferase reporter assay system (Promega). The firefly luciferase activity was normalized to *Renilla reniformis* luciferase activity.

In vitro translation assays

Each of the tested luciferase fusion constructs was linearized by digestion with Pvu II and Sac I. The PvuII-SacI fragments of about 1.8 kbp were used as templates to prepare luciferase fusion transcripts that were randomly labeled with α-^{32}P-UTP. Transcription efficiency was quantified by scintillation counting. Free nucleotides in the reaction mixture were washed out by running through NucAway™ Spin Columns (Ambion). The luciferase transcripts (0, 2, 4, 10, 20, and 40 ng) were added to the reaction mixture and incubated at 30 °C for 60 min. The reactions were terminated on ice. The firefly luciferase activity was measured by the Luciferase Assay System (Promega) according to the manufacturer's instructions. The lines are the best linear fit of the relationship

between luciferase activities and mRNA concentrations whose slopes represent translation efficiencies.

RESULTS

Identification of human MRP2 transcription initiation sites in the human liver and HepG2 cells by RPA

Three transcription initiation sites of the human *MRP2* gene are reported to be located at position -247, -204, and -99 nt relative to the ATG of the human *MRP2* gene by a study of 5' rapid amplification of cDNA ends [22] (shown in Figure 4.1.A.). The transcription initiation sites and the relative abundance of these MRP2 mRNA transcripts were investigated by RPA in the human liver and HepG2 cells. All reported transcription initiation sites were detected in the human liver and HepG2 cells. The distribution patterns in the liver and HepG2 cells were very similar (Figure 4.2.). There were other bands in addition to the reported transcription initiation sites, which might also be transcription initiation sites or could be degradation products. The transcript with the -247 nt-5'UTR was expressed at a very low level in both the liver and HepG2 cells, compared to the -204 nt- and -99 nt-transcripts, both of which were expressed at a similar level.

Effect of the human MRP2 5'UTRs on expression of the luciferase reporter gene in transient cotransfection assays in HepG2 cells

To investigate the influence of the 5'UTRs of the human MRP2 gene on translation, the three 5'UTR sequences (Hu-L, Hu-M, and Hu-S, shown in Figure 4.3.A.) were fused immediately upstream of the luciferase coding gene in the pGL3 control vector. Fusion plasmids were transiently co-transfected individually with pSV40-Ren into HepG2 cells. The ratios of the firefly luciferase activity

relative to *Renilla* luciferase activity were normalized to that of the pGL3 control vector (the ratio of the pGL3 control vector is one).

The normalized ratios of the plasmids of Hu-L and Hu-M were 1.16 and 1.23, respectively (Figure 4.3.B.), while that of the plasmid of Hu-S was 3.67. Thus, the 5'UTRs of Hu-L and Hu-M inhibited expression of the luciferase reporter gene about 66% in comparison to Hu-S ($p<0.001$), suggesting the presence of an inhibitory element.

Effect of the human MRP2 5'UTRs on the translation efficiency of the luciferase transcript in *in vitro* translation assays

We investigated the regulatory role of the human MRP2 5'UTRs on translation *in vitro*. The capped luciferase fusion transcripts obtained by *in vitro* transcription contained MRP2 5'UTRs immediately upstream of the luciferase ORF (Figure 4.4.A.). The transcripts (0, 2, 4, 10, 20, and 40 ng) were added to the rabbit reticulocyte lysate and the reaction mixtures were incubated at 30ºC for 1 hr. After incubation, the luciferase activity was measured.

The translation efficiency of hS was 8.2-fold higher than that of hM ($p<0.0001$) (Figure 4.4.B.). The translation efficiency of hmutM containing the mutation of ATG2 at position -105 to AAG increased 4.4-fold ($p<0.0001$), compared to that of hM, but was still less than that of hS.

Sequence dependence of uORF2 on translation in *in vitro* translation assays.

Since it was shown that ATG2 exerted an inhibitory effect on translation and is flanked by a perfect Kozak motif, we next investigated whether the translational inhibition is dependent on the amino acid sequence of uORF2. Two plasmids were constructed, one, h22, containing the native amino acid sequence of uORF2, and the other, ∆h22, containing the frame-shifted sequence of uORF2 (Figure 4.5.A.). *In vitro* transcription-prepared mRNAs from the two plasmids (0, 2, 4, 10, 20, and 40 ng) were added to the rabbit reticulocyte lysate mixture to determine their translational efficiencies.

Translational efficiency of ∆h22 was only 1.26 times higher than that of h22 ($p=0.002$, Figure 4.5.B.) Thus, the inhibitory translation executed by ATG2 is not dependent on the amino acid sequence of uORF2

Determining if uORF2 is a *cis*- or *trans*-acting regulator on translation by *in vitro* translation assay.

Using the plasmid of h22 as template, uORF2 in the plasmid h22_105AAG and the ORF of the luciferase in the plasmid h22_LucAAG were disrupted, respectively, by point mutations of ATG2 at -105 and the ATG of the luciferase ORF to AAG. The transcript of h22_LucAAG (0, 2, 4, 10, 20, and 40 ng) was incubated with the same amounts (0, 2, 4, 10, 20, and 40 ng, respectively) of the transcript of h22_105AAG or T7Luc_ctrl in *in vitro* translation assays.

The translation efficiency of the plasmid h22 was 57% of that of T7Luc_ctrl, while that of h22_105AAG was 1.12-fold higher than that of T7Luc_ctrl. The construct h22_105AAG with disruption of ATG2 increased the translation efficiency of h22 2-fold ($p<0.0001$), bringing it to the level of T7Luc_ctrl. The data indicate that uORF2 *cis*-inhibits translation of the luciferase mRNA. The translation efficiency of h22_105AAG incubated together with h22_LucAAG was 89% of that of h22_105AAG. The presence of h22_LucAAG did not change the translation efficiency of h22_105AAG ($p=0.1111$). The level of T7Luc-ctrl translation when incubated with h22_LucAAG was 95% of that when incubated without h22_LucAAG. The presence of h22_LucAAG did not change the translation efficiency of T7Luc-ctrl ($p=0.347$). This indicated that h22_LucAAG did not exert a *trans*-acting inhibitory effect on translation (Figure 4.6.).

CONCLUSIONS

First, by means of ribonuclease protection assays (RPA), this study not only confirmed (Figure 4.2) the transcription initiation sites at position -247, -204, and -99 in the liver and HepG2 cells, but also found that the distribution patterns of these sites in the liver and HepG2 cells were similar. The amount of -247 nt was much less, compared to -204 and -99 nt. In addition, bands other than the three reported sites were also present. Further 5'RACE studies are needed to determine if these bands represent transcription initiation sites.

Second, the upstream uORF2-7 between position -204 and -99 also can inhibit translation in transiently cotransfected HepG2 cells either individually or in concert (Figure 4.3), because Hu-S (-99 nt) exhibited a 3.5-fold greater luciferase activity relative to Hu-L (-247 nt) and Hu-M (-204 nt). More studies are needed to examine their effects. However, uORF2 at position -74 appears not play an important role when present alone in hS.

Third, uORF2 was more critical to the inhibitory effect than other uORFs, since it alone contributed about 50% of the inhibitory effect. Deletion of uORF2 (at position -105) in hM (hmutM) increased translation efficiency 4.4-fold in comparison to hM *in vitro* translation assays (Figure 4.4.). At the same time, the translation efficiency of hS was 8.2-fold higher than that of hM.

Finally, the translation inhibition exerted by uORF2 at position -105 was not dependent on the amino acid sequence of the encoded peptide. Furthermore, this effect was *cis*-, not *trans*-acting. Thus, there was not any difference observed in translation efficiency between the native and altered amino acid sequences of

uORF2. Further, coincubation of h22_LucAAG in *in vitro* translation reactions, which should express the peptide encoded by uORF2, did not change translation efficiency of T7Luc_ctrl or h22_105AAG.

FIGURES AND LEGENDS

Figure 4.1. The cDNA sequence of the 5'UTR and the schematic representation of organization of uORFs of the human MRP2. A. The cDNA sequence of the human MRP2 5'UTR. The three transcription initiation sites at position -247, -204, and -99 are marked with asterisks. The ATG start codons are in bold. The ATG of the *MRP2* gene is termed ATG0 and the nucleotides of ATG0 are numbered as +1, +2, and +3. Relative to ATG0, the upstream start codons at position -74, -105, -137, -146, -173, -180, and -199, are termed ATG1, ATG2, ATG3, ATG4, ATG5, ATG6, and ATG7, respectively. Accordingly, the

upstream open reading frames of these ATG are named uORF1 -7. The uORFs are grey-shaded. uORF1 from position -74 to +234 contains 103 codons; uORF2 from -105 to -39, 23 codons; uORF3 from -137 to -98, 13 codons; uORF4 from -146 to -98, 16 codons; uORF5 from -173 to -147, 9 codons; uORF6 from -180 to -174, 2 codons; and uORF7 from -199 to -164, 12 codons. **B.** Schematic representation of the organization of the uORFs of the human MRP2. The arrow at +1 is the start codon of the human MRP2 mRNA. The rectangles represent the uORFs on the MRP2 mRNA strand to scale. The same color filled rectangles are in-frame with each other. uORF2 and uORF 6 are in-frame with ORF0; uORF1, uORF3, uORF4. uORF5 are all in the same reading frame, but out-of frame with ORF0. uORF7 is out-of frame with both ORF0 and with uORF1.

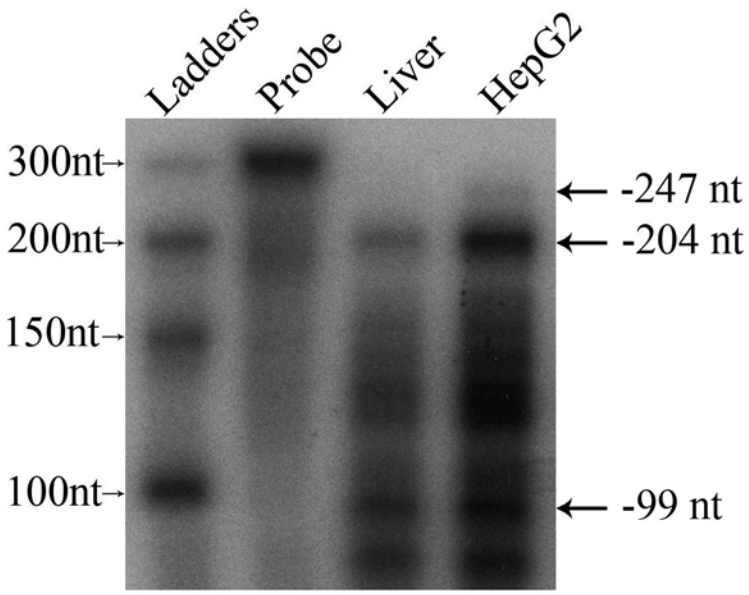

Figure 4.2. Detection by RPA of transcription initiation sites of MRP2 and their relative abundance in the human liver and HepG2 cells. RNA markers (100, 150, 200, and 300 nt) were prepared by *in vitro* transcription. Probe, 20 µg of yeast RNA; human liver RNA, 10 µg; HepG2 cells RNA, 10 µg. The picture is a representative of three experiments.

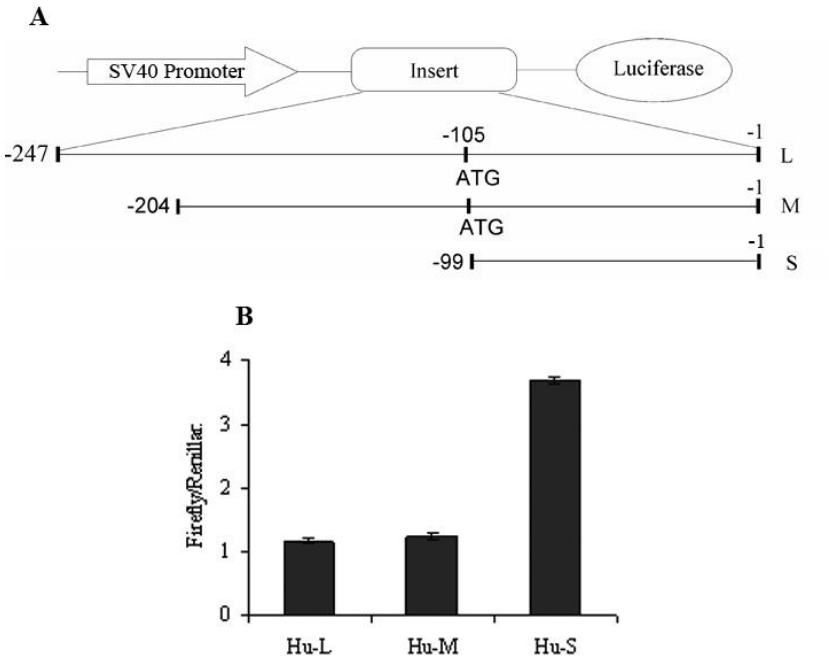

Figure 4.3. Effect of the human MRP2 5'UTRs on expression of the luciferase gene in HepG2 cells in transient cotransfection assays. A. Schematic representation of the MRP2 luciferase constructs used. The inserts (L, M, and S) shown were cloned into the pGL3 vector between the SV40 promoter and the luciferase ORF. The inserts are shown as the lines to scale. Only ATG2 is marked. **B.** The luciferase activity following transient cotransfection assays in HepG2 cells. The human MRP2 5'UTR-luciferase constructs were cotransfected with pSV40-Ren into HepG2 cells. After 24 hours, the firefly and *Renilla reniformis* luciferase activities were measured. The effect of the 5'UTRs on luciferase expression is represented as the ratio of the firefly luciferase activity to *Renilla reniformis* luciferase activity. The assays were performed in triplicate. The data are presented as mean ± SEM and normalized to the Luc/Ren ratio of the pGL3 control vector. This work was done by Dr. Wei Li in the laboratory. The

data were performed One-Way ANOVA and followed with Bonferroni's pairwise comparison.

A

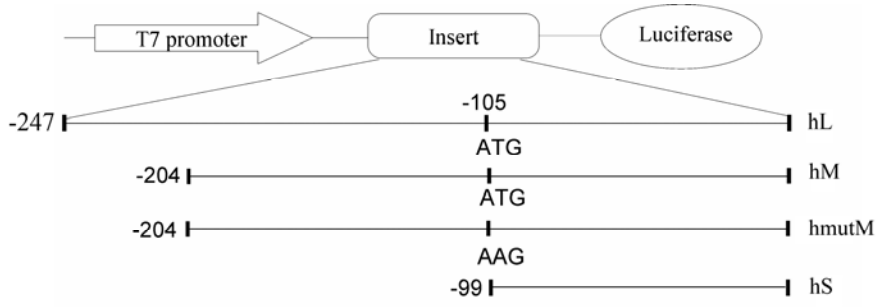

B

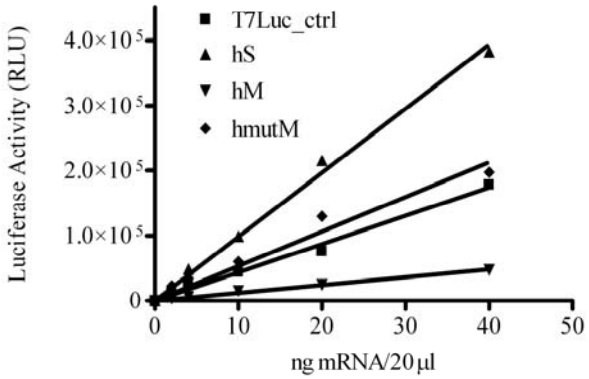

Figure 4.4. Effect of the human MRP2 5'UTRs on translation efficiency of the luciferase transcript by *in vitro* translation assays. A. Schematic representation of MRP2 5'UTR luciferase fusion constructs. The inserts shown as the lines to scale were cloned into the T7 luciferase vector between the T7 promoter and the luciferase ORF. Only ATG2 is marked. **B.** *In vitro* translation assays. The end-capped, MRP2 5'UTRs-fused luciferase transcripts (0, 2, 4, 10, 20, and 40 ng) were added to the rabbit reticulocyte lysate mixture. Translation reactions were carried out at 30°C for 60 min and then terminated on ice. The firefly luciferase activity was measured. The lines are the best fit of the relationship between luciferase activities and mRNA concentrations. The slopes

represent translation efficiencies. The statistical significance of the difference between the slopes was tested by GraphPad Prism 4.0.

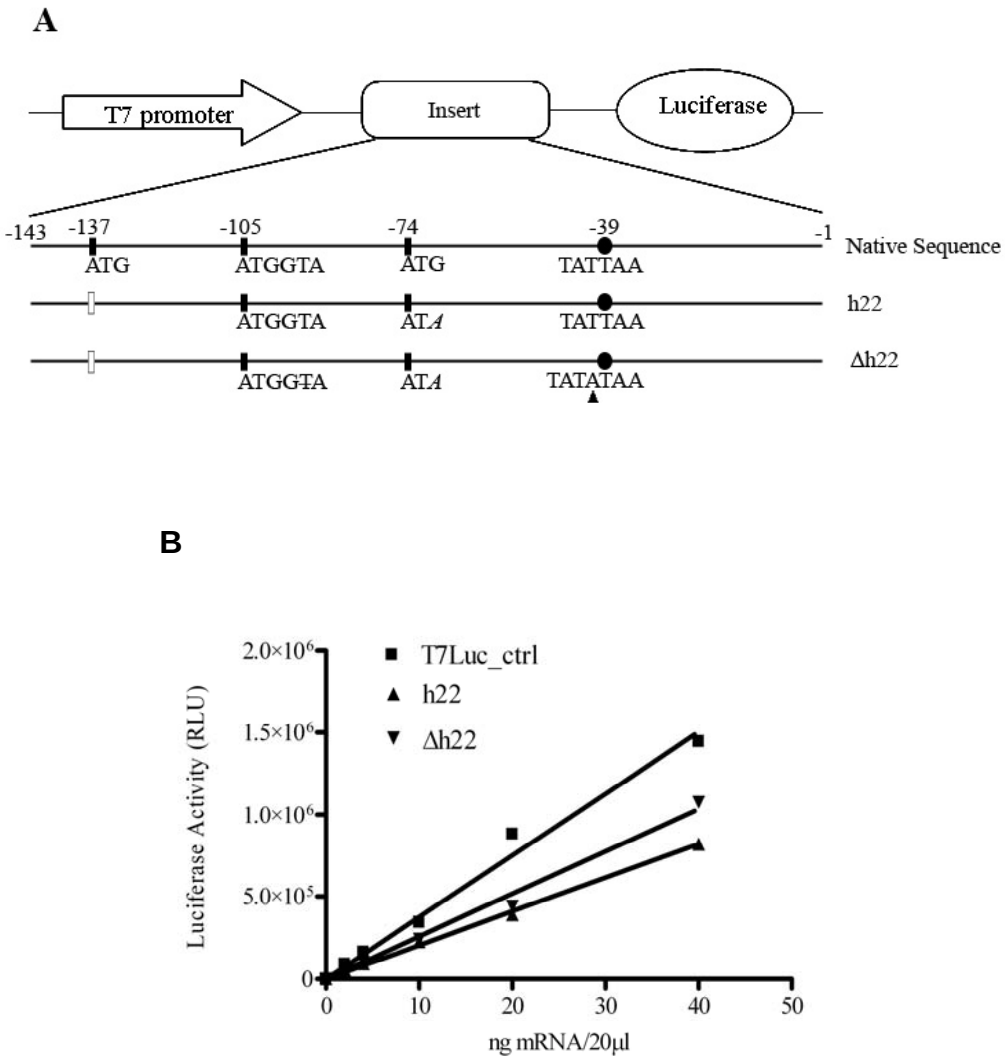

Figure 4.5. Determination of sequence dependence of uORF2 on translation by *in vitro* translation assays. A. Schematic representation of luciferase fusion constructs. The inserts were fused into the T7 luciferase control vector between the T7 promoter and the luciferase coding gene. The native sequence from position -143 to -1 is shown as the line with the start codons shown as solid bars at position -137, -105, and -74 and the stop codon shown as a solid circle at position -39. The plasmid h22 was constructed by point mutation of ATG1 at position -74 to ATA and deletion of ATG3 at position -137 (open bar) using the

plasmid with the native sequence as template. With the purpose of frame-shifting uORF2, the plasmid Δh22 was constructed by deleting T, shown as strikethrough (T̶ in ATGGT̶A), and inserting an A (shown as solid triangle underneath) before the stop codon TAA at position -39. **B.** *In vitro* translation assays. The capped fusion luciferase transcripts obtained by *in vitro* transcription (0, 2, 4, 10, 20, and 40 ng) were added to the rabbit reticulocyte lysate reaction mixtures and incubated at 30ºC for 1 hr and then terminated on ice. The luciferase activity was measured. The lines are the best fit of the linear relationship between luciferase activities and mRNA concentrations. The slopes represent translation efficiencies. This graph is representative of two experiments. The statistical significance of the difference between the slopes was tested by GraphPad Prism 4.0.

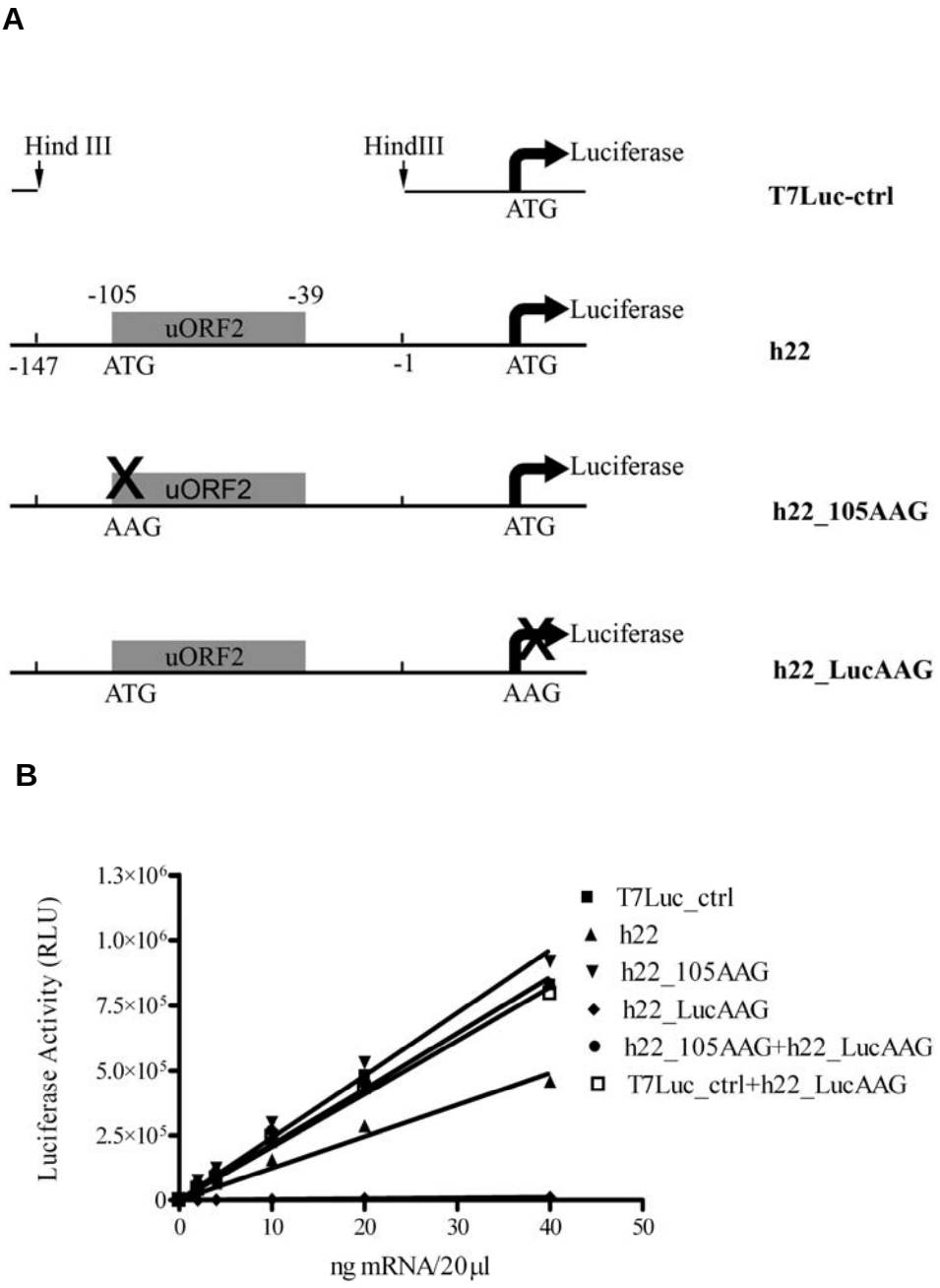

Figure 4.6. Determining whether uORF2 acts as a *cis*- or *trans*- regulator on translation by *in vitro* translation assay. A. Schematic representation of the plasmid constructs. The sequence of position -147 to -1 of the human MRP2 5'UTR cDNA was inserted at Hind III restriction enzyme site in the T7 luciferase control vector (T7Luc_ctrl). The plasmid h22 is the same one shown in Figure

4.5. uORF2 was disrupted in the plasmid h22_105AAG by mutation of ATG2 at position -105 to AAG, and the ORF of the luciferase in the plasmid h22_LucAAG was disrupted by mutation of the ATG of the luciferase gene to AAG. **B.** *In vitro* translation assays. The transcripts (0, 2, 4, 10, 20, and 40 ng) prepared by *in vitro* transcription were added to the rabbit reticulocyte lysate reaction mixtures and incubated at 30ºC for 1 hr and then terminated on ice. The luciferase activity was measured. The lines are the best fit of the linear relationship between luciferase activities and mRNA concentrations. The slopes represent translation efficiencies. The statistical significance of the difference between the slopes was tested by GraphPad Prism 4.0.

Table 4.1. Primers used in site-directed mutagenesis for construction of human MRP2 5'UTRs fused T7 luciferase vector

Primers	Sequences	Constructs
hF	5'ggacaagcttatcagaatggtagataattcctg3'	MRP2_22
hR	5'ggtaagcttgattcctggactgcgtc3'	
hFins	5'caacacaatcatatataatagaagagtcttcgttcc3'	ΔMRP2_22
hRins	5'ggaacgaagactcttctattatatatgattgtgttg3'	
hFmut	5'cctgttccactttctttgataaaacaagtaaag3'	
hRmut	5'ctttacttgttttatcaaagaaagtggaacagg3'	
hFdel	5'ccaagcttatcagaatggagataattcctg3'	
hRdel	5'caggaattatctccattctgataagcttgg3'	
hFex	5'ctcactatagggagacccaagcttgttgggaaaggtcatcc tttacggagaacatcagaatggtagataattcctgttc3'	h22
hRex	5'gaacaggaattatctaccattctgatgttctccgtaaaggat gacctttcccaacaagcttgggtctccctatagtgag3'	
ΔhFex	5'ctcactatagggagacccaagcttgttgggaaaggtcatcc tttacggagaacatcagaatggagataattcctgttc3'	Δh22
ΔhRex	5'gaacaggaattatctccattctgatgttctccgtaaaggatg acctttcccaacaagcttgggtctccctatagtgag3'	
MutLucF	5'gcccggatccaaaaggaagacgccaaaaac3'	h22_LucAAG
MutLucR	5'gtttttggcgtcttccttttggatccgggc3'	
h105aagF	5'cctttacggagaacatcagaaaggtagataattcttgttc3'c	h22_105AAG
h105aagR	5'ggaacaggaattatctacctttctgatgttctccgtaaagg3'	

CHAPTER FIVE

DISCUSSION

Based on prediction, 30-40% of eukaryotic mRNAs contain uORFs [89], [90]. Some uORFs, although not all, serve as important regulatory elements of transcript-specific translational regulation [58, 64, 66, 91-95]. Evidence shows that expression of both human MRP2 and rat Mrp2 undergo translational regulation. Moreover, one of the similarities between Mrp2/MRP2 mRNAs is the multiple upstream translation initiation sites present in the 5'UTRs, although the human MRP2 mRNA is more complicated in terms of the number of uORFs. The studies presented here are focused on the mechanisms by which the uORFs of Mrp2/MRP2 regulate translation. Here we discuss the conclusions drawn from these studies.

Before discussion, it is important to point out two considerations in these studies. First, because all cellular and most viral mRNAs have 7-methylguanosine capped (m7G) 5' ends [54] and translation of mRNAs with capped 5' ends is far more efficient than those without such capped 5' ends [96], the RNAs used in *in vitro* translation assays all have m7G-capped end structures, and were prepared by *in vitro* transcription using mMESSAGE mMACHINE T7 kit (Ambion). Second, we used the luciferase gene, a reporter gene, instead of the *Mrp2/MRP2* gene, to investigate translational regulation, because the cDNA sequences of Mrp2/MRP2 mRNAs are too large (about 4.5 kbp) for efficient translation in this *in vitro* system.

ATG1 at position -109 in the rat Mrp2 5'UTR functions as an inhibitory element in controlling translation.

In the rat *Mrp2* gene, there are transcription initiates at several different sites (position -213, -163, -132, and -98) (Figure 2.1.A.). The existence of the four transcripts of Mrp2 mRNA that differ in the length of the 5'UTRs was confirmed by RPA in the rat liver (Figure 2.2.). There are four upstream ATGs (ATG1-4 at position -109, -149,-197, and -213, respectively) present in the cDNA sequence of the longest 5'UTR. Thus, the four mRNA isoforms embrace different numbers of upstream ATGs. The ATG4 (at position -213) is in-frame with the Mrp2 ORF, while the others are out-of-frame. uORF1 starting at ATG1 (at position -109) overlaps the Mrp2 ORF, while the other uORFs terminate prior to the Mrp2 ATG.

First of all, we investigated the effect of the 5'UTRs on translation by cloning the sequences from the 5' ends to position -1 prior to the ATG of the luciferase gene in the luciferase control vector (Figure 2.1.B.). The data in the transiently transfected HepG2 cells (Figure 2.3.) indicate that the L (-213 nt), and M1 (-163 nt) 5'UTRs contain inhibitory elements for expression of the luciferase gene in HepG2 cells. But the inhibitory effect is not exerted by the length of the 5'UTRs, because the luciferase activities of the luciferase mRNAs containing 5'UTRs of L^{a+b} (deletion of ATG1 at position -109 termed "a", and deletion of ATG2 at position -149 termed "b"), L^{b}, $M1^{a+b}$, and $M1^{b}$ are about the same level as the luciferase control mRNA that does not contain any 5'UTR (Figure 2.3.) This is consistent with the report that the distance of >1000 nucleotides from the 5' end to the first ATG alone does not reduce the translational efficiency [57]. The data

also confirm the results of the analysis of the 5'UTR folding by the computer program-mFold: there is not a secondary structure formed in the Mrp2 5'UTRs that is stable enough to block ribosome scanning and slow down the translation. Another reason supporting the absence of a stable secondary structure is that the G+C richness is <50% in the L-, M1-, and M2-5'UTRs. Usually, a long and G+C rich 5'UTR will form a stable secondary structure and slow down translation. In fact, the translational inhibition is exerted by the upstream ATGs, since deletion of the ATGs in L, M1, and M2 increased their luciferase activities both in the transfected HepG2 cells and *in vitro* translation assays.

To be accurate, it is ATG1, not ATG2, in the Mrp2 5'UTRs that exerts the inhibitory effect on translation. There are four, three and two ATGs present in the L-, M1-, and M2-5'UTRs, respectively. In the transiently cotransfected HepG2 cells (Figure 2.4.), the single deletion of ATG1 in the L- and M1-5'UTRs abolished the majority of the translational inhibitory effect, increasing the luciferase activity almost up to the level of the control luciferase gene (L^b and $M1^b$ are 80% and 96% of the control). Double deletion of ATG1 and ATG2 just slightly changed the luciferase activity (L^{a+b} and $M1^{a+b}$ are 93% and 90% of the control, respectively), compared to the single deletion. Similarly, in *in vitro* translation assays, a dramatic increase in translation efficiency was observed when ATG1 was deleted in the L-, M1-, and M2- 5'UTRs (3, 31, and 4-fold higher, respectively) (Figure 2.5.B., C., D.), while the single deletion of ATG2 in the M1-5'UTR only increased translation efficiency slightly (6-fold), and even decreased translation efficiency in the L-5'UTR (80%).

Therefore, it is obvious that the rat Mrp2 mRNA transcripts with the ATG1-containing 5'UTRs (L, M1, and M2) would translate much less efficiently than those without ATG1 (S1 at position -98, comparison shown by B., C.b., D.c., and E.c. in Figure 5.1.). This may partially explain gradually decreasing Mrp2 protein expression in the small intestine from jejunum to ileum [48]. Only the S1 (-98 nt) and M2 (-132 nt) isoforms are observed in the jejunum and ileum, with the other transcripts under detectable limits (Figure 2.2.). However, in the jejunum, the S1 isoform is expressed at a higher level than the M2 isoform, while in the ileum, expression of these two isoforms is reversed. Given the fact that the translation efficiency of the S1 isoform is 1.8-fold higher than that of the M2 isoform as observed in *in vitro* translation assays (Figure 2.5.A.), the 9-fold higher expression of Mrp2 protein in the jejunum than in the ileum may be explainable. Further studies are needed to understand the basis and physiologic implications for use of multiple transcription initiation sites by Mrp2, and why their use varies among tissues, and to a lesser extent, with age (Figure 2.3.). However, altered expression of isoforms is not the reason for the Mrp2 protein changes induced by PCN treatment, or pregnancy in rats, because early studies demonstrated that use of transcription start sites in the rat liver was not altered by treatment with PCN or in pregnancy, implying that this is a fundamental property of the gene that is not readily modified [46].

In this study, we did not investigate the roles of ATG3 (at position -197) or ATG4 (at position -213) in translational regulation. We excluded study ATG4 because it is the first codon at the 5' end of the rat Mrp2 mRNA. Ribosomes

poorly recognize ATG start codons close to the 5' end of an mRNA [97], so it is unlikely that the 40S subunits and the associated initiation factors could recognize ATG4 and initiate translation. The three-codon uORF3 starting at ATG3 is much shorter compared to ATG1 and ATG2. Although ATG3 does not have a Kozak motif its role in translational regulation should be examined in future studies, especially with respect to its interaction with other uORFs. We discuss its importance in the following section.

Interaction of uORFs is involved in translation of the rat Mrp2 mRNA.

We have shown that: 1) ATG1 at position -109 exerts an inhibitory effect on translation; and 2) among the four upstream ATGs, only ATG1 has a flanking Kozak motif (A at -3, and G at +4 relative to ATG1). We therefore hypothesized that ATG1 is able to be recognized efficiently by scanning ribosomes so that uORF1 is translated, according to the scanning model. This hypothesis is confirmed by two experiments in the transcription/translation coupled system. First, a longer luciferase protein (with higher molecular weight) was observed when ATG1 was in-frame with the luciferase ORF in the deL and deM1 (Figure 2.6.). In this same experiment, deletion of ATG1 (deL^b and $deM1^b$) or the absence of ATG1 (S2) abolished expression of the longer luciferase molecule. Second, expression of Pep56 encoded by uORF1 was observed when the pcDNA3.1 vector containing uORF1 was expressed in the TnT system (Figure 3.4.).

Thus, the inhibitory effect exerted by ATG1 on translation of a downstream cistron is due to the fact that only a portion of the scanning ribosomes translate downstream luciferase *in vitro* or Mrp2 *in vivo*, while other ribosomes translate uORF1 when the scanning ribosomes encounter ATG1. Both in the luciferase fusion vector and the *Mrp2* gene, uORF1 terminates within the downstream ORFs. It is known that scanning ribosomes are unable to jump backward to reinitiate at an upstream start codon after translating an uORF [58, 98, 99]. Therefore, it is impossible for scanning ribosomes to reinitiate at ORFs of the luciferase or Mrp2 after translating uORF1. The mechanism of ATG1 modulating expression of both the luciferase and rat Mrp2 mRNA must therefore be a leaky scanning model (shown by C.a., D.a., and L.a. in Figure5.1.)

There are two mechanisms that could explain the fact that uORF2 (starting at ATG2 at -149) or uORF3 (ATG3 at -197) only exert a minor inhibitory effect on translation of a downstream main ORF (like luciferase mRNA *in vitro*, and the Mrp2 mRNA *in vivo*). First, with respect to the leaky scanning model, since neither ATG2 nor ATG3 has a Kozak motif, the association affinity of ATG2 or ATG3 with the scanning ribosomes is weak, leading to their being bypassed by scanning ribosomes. Second, with respect to the reinitiating model, the scanning ribosomes reinitiate translation more efficiently when there is a longer distance between the termination codon of a uORF and the next start codon. This occurs because the 40S ribosomal subunits still associated with the mRNA strand after translating the uORF are believed to have enough time to recruit again the required translation initiation factors [98, 99]. When the intercistronic space is

lengthened from 16 to 64 nucleotides, reinitiation efficiency increases from 16% to 38% [100]. The distances from the termination codons of uORF2 at position -149 and uORF3 at position -197 to ATG0 are 123 and 187 nucleotides, respectively, both of which should be sufficient for the scanning ribosomes to fully reinitiate at ATG0. Either of these two mechanisms leads to only a minor inhibitory effect of uORF2 and -3 on translation of the downstream cistron (shown by D.b. and E.b. in Figure 5.1.).

However, the interaction of ATG2 at position -149 or ATG3 at position -197 with ATG1 may be of importance in terms of exerting a translational regulatory effect. The sequence distances from the termination sites of uORF2 and uORF3 to ATG1 at position -109 are 13 and 79 nucleotides, respectively. Obviously, the 13-nucleotide space is not long enough for ribosomes to reinitiate efficiently at ATG1 if uORF2 is translated, even with poor efficiency. However, because of the space of 79 nucleotides between the termination site of uORF3 and ATG1, reinitiation at uORF1 is efficient after ribosomes translate uORF3. Therefore, uORF1 and ORF0 could be competitors for the reinitiation scanning ribosomes, but this competition depends on whether uORF2 or -3 is translated. A proposed mechanism is that when translation of uORF2 occurs, the scanning ribosomes bypass uORF1 and reinitiate at ORF0; when uORF3 is translated and uORF2 is bypassed, reinitiation occurs at uORF1, not ORF0, resulting in inhibitory translation of ORF0. Therefore, uORF2 could be an activator or repressor of translation of the downstream main ORF, depending on whether or not it is translated.

The distance between the cap site and the initiation codon is very important for recognition of a uORF by 40S subunits. A study of mammalian S-adenosylmethionine de-carboxylase (AdoMetDC) shows that recognition of the single uORF in the AdoMetDC 5'UTR in nonlymphoid cells is increased by extending the space between the cap site and the upstream ATG codon from 14 to 47 nucleotides, leading to suppression of translation of AdoMetDC.[101]. The order of translation efficiencies of the 5'UTRs in Mrp2 from high to low are S1 (-98 nt), M2 (-132 nt), L (-213 nt), and M1 (-163 nt) (Figure 2.5.A.). That translation of S1 is faster than any other one is because S1 does not contain any uORF and the full complement of scanning ribosomes recognizes ORF0. When the space prior to the ATG2 at position -149 is shortened from 64 nucleotides in L to 14 nucleotides in M1, recognition of uORF2 by the scanning ribosomes in L is more efficient than that in M1. Thus when translation of uORF2 occurs in L, reinitiation is not able to occur at uORF1 because of the short intercistronic space of 13 nucleotides, but occurs at ORF0. In contrast, in M1, ribosomes bypass uORF2, and translation of uORF1 occurs, suppressing the translation of ORF0. This provides a likely explanation for why translation efficiency of the luciferase transcript containing L is 15-fold higher than that of M1. Therefore, in terms of translation of ORF0, uORF2 functions as an activator in L, but an inhibitor in M1, which explains two observations in the *in vitro* translation assays: 1) deletion of ATG2 at position -149 of L^a decreased translation efficiency 80% compared to L, while 2) deletion of ATG2 of $M1^a$ increased translation efficiency 6-fold compared to M1.

The distances prior to ATG1 at position -109 in the L (-213 nt), M1 (-163 nt), and M2 (-132 nt) 5'UTRs are 104, 54, and 23 nucleotides, respectively. Therefore, recognition of uORF1 is less efficient in M2 than that in L and M1 (shown by the comparison of C.a. and D.a. in Figure 5.1.), resulting in the increase of translation of ORF0 in M2, compared to L and M1, which explains why translation efficiency of M2 is higher than that of L and M1.

Together, the mechanisms of uORFs-mediated translational regulation in the S1 (-98 nt), M2 (-132 nt), M1 (-163 nt) and L (-213 nt) transcripts are the combination of the leaky scanning model and reinitiation model. That is, interaction of the uORFs influences translation of the downstream main ORF. This kind of interaction depends on the intercistronic distances and the distances between the 5' end and start codons of uORFs. The schematic representation of this mechanic model is shown in Figure 5.1.

We already showed that translation of uORF1 in *in vitro* systems and transiently cotransfected HepG2 cells contributes the majority of translational inhibition. Future studies should focus on the effect of interactions between these uORFs on translation. Thus, do PCN treatment or pregnancy selectively affect translation of alternative uORFs in the Mrp2 5'UTRs, thus changing Mrp2 protein expression? The studies on factors controlling GCN4 translation show that the level of the active form of eIF2 selectively determines the use of uORFs in amino acid-rich or -deprived medium. Future studies should investigate the eIF2 level in relation to the use of Mrp2 uORFs in PCN-treated *vs* pregnant rats.

Finally, the MDM2 transcript has two forms differing in the 5'UTRs: a long form (L-mdm2) which contains two uORFs, and a short form (S-mdm2) without uORFs. Brown and Morris reported that overexpression of MDM2 observed in some tumor cells is related to the elevated ratio of S-mdm2 to L-mdm2. Also, by using sucrose gradient ultracentrifugation to ascertain the extent of ribosome loading on specific mRNA species, they found that L-mdm2 is loaded with ribosomes inefficiently in comparison with S-mdm2 [102]. However, in our case, Jones et. al [46] reported that the relative abundance of the four isoforms of the hepatic Mrp2 mRNA is not altered in PCN-treated, pregnant, and control rats. However, they showed that more Mrp2 mRNAs are loaded with polysomes following PCN treatment than vehicle treatment of the rats. When we ultracentrifuged the total RNAs from the PCN-treated rat liver in sucrose gradients and analyzed by RPA the fractions from these gradients, we did not find an altered relative abundance of these Mrp2 transcript isoforms in each gradient (data not shown). Therefore, the mechanism of Mrp2 translational regulation mediated by uORFs is different from that of MDM2.

uORF1 in controlling translation of the Mrp2 is not a *trans*-acting factor.

As pointed out by Morris [22, 64], nascent peptides encoded by uORFs can mediate regulation through interfering with translation elongation or termination. Ribosomes stall and translation of the downstream ORF is inhibited. These mechanisms are supported by identification of the active roles of the peptide

products of various prokaryotic and eukaryotic uORFs in translational control [103, 104]. The amino acid sequence-dependence of the uORF-encoded peptides has been confirmed in several genes, including *AdoMeDC*, *CPA1*, and *arg-2*, although no conserved amino acids have been found across species or genes [64].

As a major inhibitor among all four uORFs in controlling rat Mrp2 translation and with a perfect flanking Kozak motif, uORF1 was hypothesized to stall ribosomes by association of the nascent encoded peptide with the scanning ribosomes, that is, by an amino acid sequence-dependent mechanism. Efficient translation of uORF1 was confirmed by observing a higher molecular weight of luciferase expressed in the TnT system when uORF1 was in-frame with the luciferase gene (Figure 2.6.). Further, the encoded peptide product, Pep56 (MW=6.5 kDa), was also expressed in the TnT system (Figure 3.4.).

To investigate the amino acid-sequence dependence of inhibition of translation, uORF1 was cloned prior to the luciferase ATG, not overlapping its ORF. The Kozak motif sequence flanking ATG1 in the Mrp2 mRNA was maintained in all tested luciferase fusion vectors. In order to guarantee that reinitiation is fully able to occur at the luciferase ATG, a spacer sequence (from position +62 to +92) was cloned into the vectors. Thus, the distance between the uORF1 termination codon and the luciferase start codon is 71 nucleotides, including the spacer sequence in the control vector. Frame-shifting was used to create a different amino acid sequence, considering 1) the 56 amino acids of uORF1 are too many to mutate one by one, and 2) to keep the nucleotide

sequence unchanged to avoid any effect that the altered nucleotides might have on transcription or mRNA processing (Figure 3.1.).

There was no difference observed in translation efficiency between the native and altered amino acid sequences (r56 and Δr56, respectively, Figure 3.2.E.), but both inhibited translation compared to the luciferase control vector. In addition, deletion of ATG1 at position -109 in r56 did not change translation efficiency (data not shown). Therefore, the translational inhibition by uORF1 in r56 and Δr56 is because of the existence of ATG0 (at position +1) of Mrp2, which is a perfect translation initiation site. This may obscure the effect of amino acid-sequence dependence. Another explanation may be the amino acid similarity between the native and altered forms, because there is not a large difference in their PI values (9.6 for the native, 11.4 for the scrambled). The presence of ATG0 may also explain the difference in translation efficiency of the first (rF), second (rM) and third (rL) 22 amino acid segments, because the second and third segments included ATG0, while the first did not (Figure 3.2.A.). However, the altered sequences of ΔrL and ΔrM dramatically increased translation efficiency in comparison to their native sequences, rL and rM, respectively (Figure 3.2.B and C.). We could not narrow down the amino acids that play the critical roles in the sequence dependence, since no differences in translation efficiency were observed between r11_1, _2, and _3 (Figure 3.2.D.). We propose that all the amino acids in the segment without the first 22 amino acids work together in controlling translation. Future studies should investigate whether ribosome stalling occurs at elongation or termination steps, and how.

However, we determined that association of the amino acids encoded by uORF1 with the scanning ribosomes is *cis*-, not *trans*-acting, since the translation efficiencies of the luciferase mRNAs did not differ when T7Luc_ctrl was incubated alone or when it was incubated under conditions where the peptide encoded by uORF1 in r56_LucAAG could be translated (Figure 3.3.B.). Moreover, addition of the commercially synthesized peptides of the second or third segments (r11aa_2 and r11aa_3) into *in vitro* translation reactions did not change translation efficiency of the control luciferase transcript (data not shown). Although the peptide encoded by uORF1 was expressed in the TnT system (Figure 3.4.), we could not detect its expression by immunoblotting analysis in the rat liver or kidney tissues (shown in Figure 3.5., and 3.6.). These data suggest that the peptide is rapidly degraded *in vivo*. Finally, following transient or stable transfection of HepG2 cells with the pcDNA3.1 vectors containing uORF1, the peptide could not be detected in the cell extracts (data not shown).

The mechanisms involved in controlling translation of the human MRP2 mRNA mediated by 5'UTRs

The data in transiently cotransfected HepG2 cells suggest that the upstream uORF2-7 between position -204 and -99 inhibit expression of the luciferase. The luciferase expression levels of Hu-L (-247 nt) and Hu-M (-204 nt) were the same because there are not any upstream ATGs between position -247 and -204 (Figure 4.3.). Interestingly, the luciferase activities of Hu-L and -M are similar to that of the control luciferase that does not contain any 5'UTR, indicating that the

differing lengths of Hu-L (-247 nt) and Hu-M (-204 nt) 5'UTRs do not affect translation. This is consistent with the observation in the rat Mrp2 5'UTR that the length of the 5'UTRs has no effect on translation. These data also suggest that there are not stable secondary structures in Hu-L or Hu-M 5'UTRs (Figure 4.4.).

The translational inhibitory role of uORF2-7 is also true in *in vitro* translation assays. However, by point mutation of ATG2 at position -105 to AAG, we found that among these uORFs, uORF2 at position -105 is the major player in inhibition of translation, which alone contributes about 50% of the inhibitory effect, with the other uORFs contributing the other 50% of the translational inhibition. This is because among all uORFs, uORF2 is the only one that has a perfect Kozak Motif. Even the sequence flanking the ORF of human MRP2 is not a perfect Kozak Motif. Therefore, according to the scanning model of translation, the scanning ribosomes can efficiently recognize ATG2 at position -105 and initiate translation of uORF2, resulting in down-regulation of translation of the downstream main ORF, the luciferase ORF *in vitro* or the MRP2 ORF *in vivo*, by either the leaky scanning model or the reinitiation model. The effect of the other uORFs and their interactions on translation should be investigated in future studies.

Interestingly, translation efficiency of hS (-99 nt) was higher than that of T7Luc_ctrl in *in vitro* translation assays, consistent with what was observed with Hu-S in transfected HepG2 cells. This suggests 1) the presence of a translational active element between position -99 to -1; 2) uORF1 at position -74 in hS (-99 nt) does not inhibit translation. Given the fact that uORF1 at position -74 is unusually

long and overlaps with the human MRP2 coding gene, the fact that uORF1 does not affect translation of the luciferase is in contrast to the current model in which a uORF overlapping the downstream main ORF suppresses translation of the downstream cistron, because no reinitiation occurs or only a portion of the ribosomes (the leaky scanning model) initiate at the downstream ORF. However, in the hS (-99 nt) 5'UTR, the distance between the capped end to ATG1 (-74 nt) is 25 nucleotides, which may not be long enough for the scanning ribosomes to efficiently recognize ATG1, which also does not have a perfect Kozak Motif. This may explain why ATG1 in the hS has no inhibitory effect on translation of the luciferase. Future studies should investigate the translational regulatory role of ATG1 at position -74 in hL (-247 nt) and hM (-204 nt), because the distances between the capped ends of these two 5'UTRs and ATG1 should be long enough for the scanning ribosomes to initiate translation of uORF1 if ATG1 is recognized.

The inhibitory effect exerted by uROF2 at position -105 on translation is not dependent on the encoded nascent 22-amino acid peptide (Figure 4.5.). Further, there was no *trans*-acting effect of uORF2 observed on translation in *in vitro* translation assays (Figure 4.6.). Finally, the peptide could not be detected when expressed in the transcription/translation coupled system with ^{35}S-Methionine to label the newly synthesized peptide (data not shown). Addition of the commercially synthesized peptide into *in vitro* translation reactions did not change translation efficiency of T7Luc_ctrl (data not shown). Expression of MRP2 protein did not change in transiently or stably transfected HepG2 cells with a pcDNA3.1 vector containing uORF2 (data not shown). In addition, treatment of

HepG2 cells with the synthesized peptide did not change MRP2 expression (data not shown). Therefore, we propose that uORF2 is a *cis*-acting repressor of translation by the mechanism of leaky scanning and reinitiation.

Future studies should investigate the roles of the individual uORFs and their interactions in translational regulation.

Speculations

First, this research provides a framework to understand translational regulation of human MRP2 and rat Mrp2 that could occur under certain conditions (pregnancy, cholestasis, cancer, etc.), i.e., uORF-mediated translational regulatory mechanisms. It was shown in *in vitro* systems that rat uORF1 at position -109 and human uORF2 at position -105 are translational inhibitors. Both the leaky scanning and the reinitiation model are involved in the rat uORFs-mediated mechanisms of translational regulation. Therefore, under certain conditions (pregnancy, cholestasis, cancers), translation of hepatic human MRP2 and rat Mrp2 mRNAs are proposed to be regulated by selective translation of the different uORFs, thus affecting reinitiation or leaky scanning of the downstream ORFs. The level of eIF2 has been shown to affect selective translation of uORFs in the translational regulatory model of *GCN*. Future studies should identify the eIF2 expression levels in PCN-treated and pregnant rats and its correlation with selection of uORFs.

Second, more sensitive methodology should be used to detect expression of Pep56 in the rat liver and kidney. Proteomic analysis [73] found four novel small

peptides encoded by uORFs in human leukemia K562 cells by direct nanoflow liquid chromatography (LC) coupled with the electrospray ionization (ESI)-tandem mass spectrometry (MS/MS) system. This investigation provides the first direct evidence of translation of upstream open reading frames in human cells [73]. In this research, the antibody to Pep56, PAS, failed to detect Pep56 in the rat liver and kidney, although PAS successfully detected the positive control of Pep56, Pep56-His. In the future, small peptides should be separated and concentrated from the rat liver or kidney homogenate by SDS-PAGE separation, acid extraction, or immunoprecipitation by PAS and then nanoflow LC coupled with ESI-MS/MS should be used to detect Pep56.

Physiological and clinical significances

The human MRP2 protein plays an important role in the pharmacokinetics and toxicity of its substrate drugs, because it is localized on the apical membranes of cells of the liver, kidney, small intestine, and brain, and thus affects absorption, disposition, and elimination of the drugs. Some anti-cancer drugs are substrates for human MRP2, including cisplatin, paclitaxel, doxorubicin, vinblastine, sulfinpyrazone, irinotecan SN38, and methotrexate [105]. Changes in MRP2 protein expression may affect transport and/or pharmacokinetics of these substrates. Also, some anti-cancer drugs induce drug-resistance by increasing MRP2 expression. For instance, chemotherapeutic treatment with doxorubicin increases human MRP2 expression in recurrent and

residual tumors of the bladder in comparison with that in untreated primary tumors [106].

Moreover, human MRP2 protein expression differs in normal and tumor tissues. MRP2 protein is expressed at a lower level in the cancerous renal cortex than in the normal cortex [107]. Analysis of regulation of the hamster pgp1 homologue found that transcription initiates at a single site in drug-sensitive cells, while drug-resistance cells utilize several downstream initiation sites [108-110]. Multiple transcription initiation sites are also present in the human *MRP2* gene in the liver (shown in Chapter Four) and placenta [22]. We have shown that the relative abundance of the three MRP2 transcription initiation sites (at position -247, -204, and -99) is similar in the normal liver and HepG2 cells, with -204 nt and -99 nt being the major two sites. But, does transcription of the *MRP2* gene utilize the same initiation sites in cancerous tissues as in normal tissues, or is each initiation site equally used? The MRP2 transcript containing the -99 nt 5'UTR (termed hS in Chapter Four) translates much faster than the other two transcripts containing -204 nt and -247 nt 5'UTRs (termed hM and hL). Therefore, the relative abundance of the three MRP2 transcripts in tumor tissues may differ from that in the normal tissues, or be regulated by anti-cancer drugs, thus leading to regulation of MRP2 protein expression at the translation level. Future investigation should address these issues by RPA.

Interindividual pharmacokinetic variability of anticancer agents is a problem in chemotherapy. Genetic polymorphisms of the *MRP2* gene are one of the factors influencing interindividual pharmacokinetic variability in chemotherapy.

The human *MRP2* gene is shown to have more than 200 naturally occurring mutations. The single nucleotide change at -24C→T is in the 5'UTR [111]. The exchange of -24C→T has been demonstrated to be associated with lower MRP2 mRNA expression in non-cancerous renal cortex tissues compared to that in unaffected tissues [86]. Analysis of organization of the MRP2 uORFs (Figure 4.1) shows that -24C is located in uORF1 of all seven uORFs, and -24C→T is a synonymous mutation for uORF1. Future studies should examine the effect of this single nucleotide polymorphism (SNP) on translation. By *in vitro* assays and transient transfection assays in HepG2 cells, translation efficiency of the transcripts containing -204 nt 5'UTRs should be compared with that of its mutant containing the exchange of -24C→T. The same experiments should also be done with the transcript containing -99 nt 5'UTR and its mutant of -24C→T.

Therefore, investigation of the mechanisms underlying translational regulation of the human MRP2 expression likely provides an additional perspective from which to understand the drug resistance and interindividual variability in chemotherapy in which the human MRP2 protein is involved.

FIGURE AND LEGEND

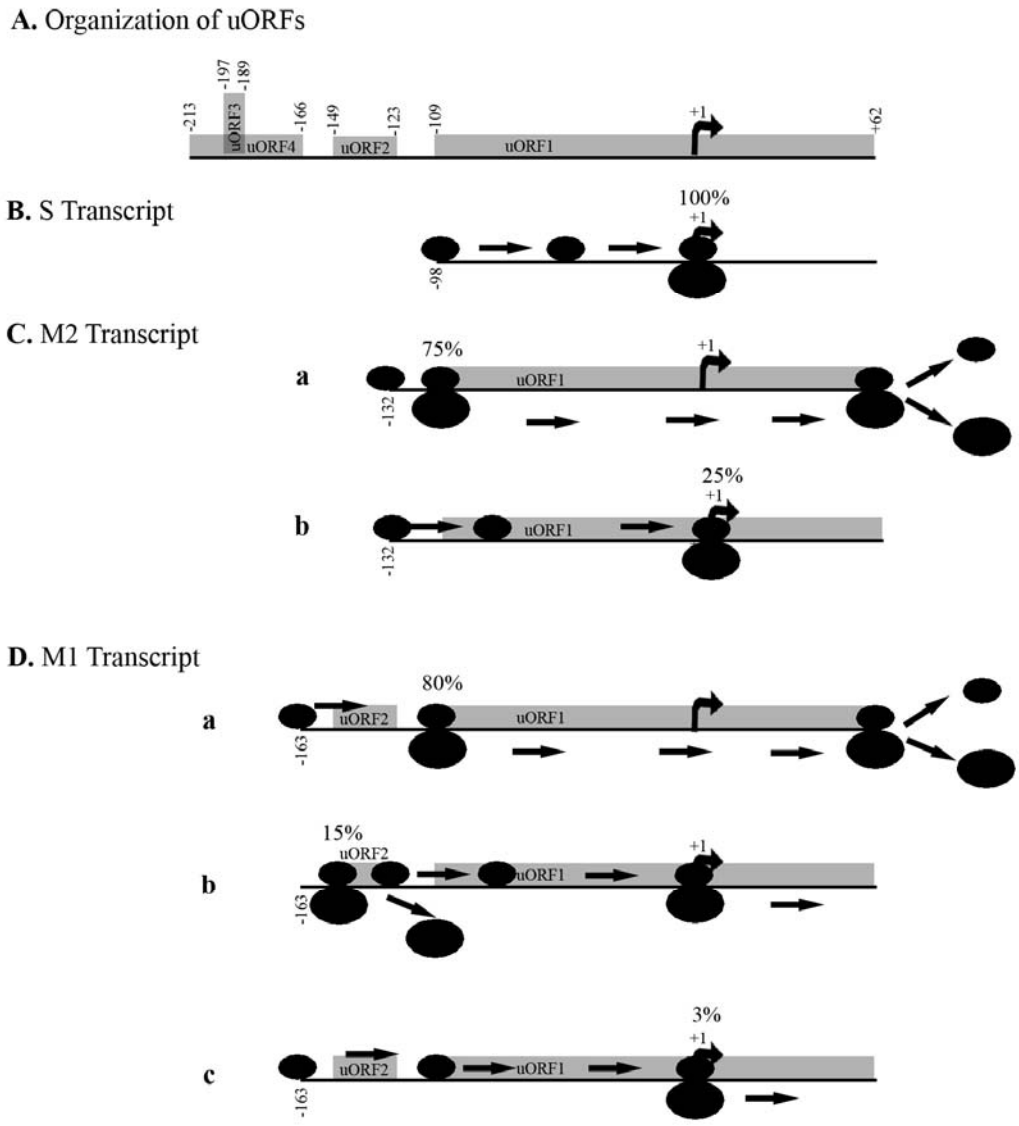

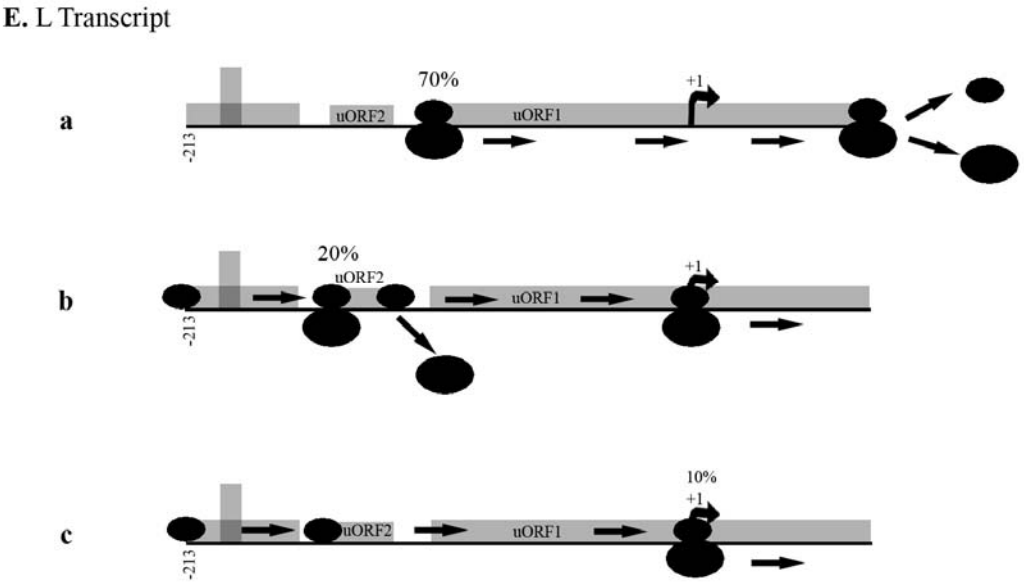

Figure 5.1. A hypothetical mechanistic model of uORFs-mediated translational regulation of the rat Mrp2 mRNA. The percentages of the scanning ribosomes labeled above that initiate translation are predicted values calculated from the data in *in vitro* translation assays. **A.** The schematic representation of organization of uORFs of the rat Mrp2 mRNA. The strand of rat Mrp2 mRNA is represented as a bold line and its start codon is shown as an arrow at position +1. Positions of the start codon and termination codon of each uORF shown as grey rectangles are labeled. **B.** Since there is not any uORF present in the S1 (-98 nt) transcript, 100% of the scanning ribosomes initiate translation of ORF0 at +1 in the -98 nt transcript. **C. I**n the M2 (-132 nt) transcript, only uORF1 is present. **a.** About 75% of the scanning ribosomes initiate translation of uORF1 by leaky scanning ORF1. **b.** About 25% of the scanning ribosomes initiate translation of ORF0 by leaky scanning all of uORFs. **D.** Both of uORF1 and uORF2 are present in the M1 (-163 nt) transcript. **a.** About 82% of the scanning ribosomes initiate translation of uORF1, which is more than

75% in the M2 (-132 nt) transcript, because the distance of 54 nucleotides from the 5' end to the start codon is longer than that in the M2 transcript (23 nucleotides). **b.** About 15% of the scanning ribosomes initiate translation of uORF2. The distance of -123 nucleotides between the termination codon of uORF2 and the start codon of ORF0 is enough for at least a portion of the ribosomes to reinitiate translation of ORF0. **c.** About 3% of the scanning ribosomes initiate translation of ORF0 by leaky scanning all of uORFs. **E.** All uORF1-4 are present in the L (-213 nt) transcript. **a.** After encountering uORF2-4, fewer scanning ribosomes (about 70%) initiate translation of uORF1, compared to that in the M1 (-163 nt) transcript (82%). **b.** About 20% of the scanning ribosomes initiate translation of uORF2 and then reinitiate translation of ORF0. **c.** About 10% of the scanning ribosomes initiate translation of ORF0.

Appendix A

List of abbreviations

2-AAF	2-acetylaminofluorene
AdoMetDC	*S*-Adenosylmethionine decarboxylase
AP1	Activator protein 1
C/EBPα	CCAAT-enhancer binding protein α
CAR	Constitutive androstane receptor
CBF	C-repeat binding factor
CCRCC	Clear-cell renal cell cancer
cDNA	Complementary deoxyribonucleic acid
CMV	Cytomegalovirus
DBcAMP	Dibutyryl-cyclic AMP
$E_2$17G	Estradiol-17β-D-glucuronide
EE2	Ethinylestradiol
EFIA	Enhancer factor IA
ER-8	Everted repeat with 8 bp spacer
FBS	Fetal bovine serum
FXR	Farnesoid X-activated receptor
GRE	Glucocorticoid-responsive element
GSH	Glutathione
HNF1	Hepatic nuclear factor 1
IRF3	Interferon regulatory factor
ISRE	Interferon stimulatory response element
LPS	Lipopolysaccharide
m7G	7-methylguanosine
mRNA	Messenger ribonucleic acid
Mrp2/MRP2	Multidrug resistance-associated protein 2
MSD	Membrane-spanning domain
MW	Molecular weight
NBD	Nucleotide binding domain
PBS	Phosphate buffered saline
PCN	Pregnenolone-16α-carbonitrile
PCR	Polymerase chain reaction
PEA3	Polyomavirus enhancer A binding protein-3
PPRE	Peroxisome proliferators responsive element
PXR	Pregnane X receptor
RARβ2	Retinoic acid receptor-β2
RPA	Ribonuclease protection assay
RXRα	Retinoid X receptor α
SDS	Sodium dodecyle sulfate
SNP	Single nucleotide polymorphism
Sp1	Specificity proteins
uORF	Upstream open reading frame
USF	Upstream stimulatory factor
UTR	Untranslated region

Appendix B

Ribonuclease Protection Assay (RPA) (RPA III Kit, Ambion, Austin)

1. Preparation of the radio-labeled probe (MAXIsript Kit)

a. The vector containing the probe sequence is digested with the restriction enzymes PvuII and BamH I and separated by electrophoresis on 2% agarose gel. A double-stranded 280 bp fragment containing the T7 promoter and the probe sequence is purified using Qiaquick Gel Extraction Kit (Qiagen) and concentrated by vacuum centrifugation at 60ºC. This is the DNA template for *in vitro* transcription reaction.
b. Vortex the reaction buffer and nucleotide solutions until they melt. Keep the reaction buffer at room temperature and nucleotide solutions on ice.
c. Assemble the *in vitro* transcription reaction mix in 0.5 ml tubes at room temperature as following:

Reagents	Volume
DNA template	5 µl
10x reaction buffer	2 µl
10 mM ATP	1 µl
10 mM GTP	1 µl
10 mM CTP	1 µl
α-^{32}P-UTP (800 Ci/mmol, 10 mCi/ml)	5 µl
Enzyme Mix	2 µl
DEPC-treated Water	3 µl
Total volume	20 µl

d. Mix well by flicking the tube or pipetting the mix up and down, and centrifuge briefly to collect all reagents at the bottom.
e. Incubate the reaction mix at 37ºC for 10 min.
f. Add 1 µl DNAse I and incubate at 37ºC for 15 min
g. Add 1 µl 0.5 M EDTA solution and 22 µl loading dye, and then incubate at 95ºC for 3 min.
h. Before loading samples on 6% urea-PAGE gel (Invitrogen), pre-run the gel for 30 min and rinse the wells.
i. Load the sample on the gel and keep running in 1x TBE running buffer at 150 V until the bromophenol blue approaches the bottom of the gel.
j. Take down the gel and carefully separate the plastic plates. The gel will stick to one plate.
k. Cover the gel side with plastic film and wrap the plastic plate
l. Expose the gel to X-ray film with the gel side facing the film. (Note: make sure that it is possible to re-position the gel and film after film development.)
m. Overlap the film and the gel in exactly the same manner as during exposure and mark the band of the probe on the plastic plate.
n. Unwrap the gel and cut out the marked band.

o. Put the gel band in 350 µl elution buffer (RPA III Kit), shred the gel band, and leave it in the hood at room temperature overnight. Do not need to centrifuge to recover the supernatant.
p. 1-2 µl of the elution solution is used for RPA incubation with total RNA.

2. Preparation of the radio-labeled RNA ladders (MAXIscript Kit, Austin)

a. PCR amplification of the DNA templates for the RNA ladder preparation
Assemble the PCR reaction mix as following using (Clontech Advantage 2 PCR Kit)

Reagents	Volume
10X reaction buffer	5 µl
DNA template (Vector T7-Toe1)	1 µl
Forward primer (T7 promoter) (10 µM)	1 µl
Reverse primer (R100, R150, or R200) (10 µM)	1 µl
50x dNTPs	1 µl
Taq polymerase	1 µl
DEPC-treated water	40 µl
Mineral oil	30 µl
Total Volume	50 µl

The first reaction is performed as following:
Step: 1) 95°C for 2 min
2) 95°C for 20 sec
3) 52°C for 20 sec
4) 72°C for 20 sec
Repeat step 2 to 4 33 times and perform a 5- min elongation reaction.

b. The PCR product is separated on 2% agarose gel, purified using Qiaquick Gel extraction Kit (Qiagen), and concentrated by vacuum centrifugation at 60ºC using Vacuumed (Eppendorf).
c. Assemble the reaction mix for *in vitro* translation as following:

Reagents	Volume
DNA templates:	
T100	3 µl
T150	2 µl
T200	2 µl
10x reaction buffer	2 µl
10 mM ATP	1 µl
10 mM GTP	1 µl
10 mM CTP	1 µl
0.5 mM UTP	1 µl
α-^{32}P-UTP (800 Ci/mmol, 10 mCi/ml)	5 µl
Enzyme Mix	2 µl
Total volume	20 µl

d. Flick the tube and mix well, and then spin briefly.
e. Incubate the reaction at 37ºC for 1 hr.
f. Add 1 µl DNAse I and incubate at 37ºC for 15 min.
g. Add 1 µl of 0.5 M EDTA (pH8.0) and 22 µl of loading dye, and then incubate at 95ºC for 3 min
h. Load the sample on 6% urea-PAGE gel to check the quality of the probe. Usually it is good enough to use directly without gel purification.

3. Ribonuclease protection reaction.

a. Assemble the reaction as following on ice

Reagents	Volume
Total RNA	20 µg
Radio-labeled probe	1-2 µl
NH_4Ac (5M)	1 µl

Bring up the total volume of reaction to 50 µl with DEPC-treated water. And add 125 µl (2.5 x volumes) ethanol.

b. Vortex and mix well. Store the reaction at -80ºC for at least 2 hr
c. Precipitate the RNA by centrifugation at maximum speed for 30 min at 4ºC and carefully remove the supernatant.
d. Wash the RNA pellet one with 250 µl of 70% ethanol in DEPC-treated water. Carefully remove the supernatant without touching the pellet. Do not use the 1 ml tips which might suck up the pellet.
e. Spin the tubes after washing and remove the residue of supernatant with 10 µl tips.
f. Add 10 µl Hybridization buffer (RPA III) and pipette up and down to resuspend the RNA pellet.
g. Denature the reaction mix by incubation at 93ºC for 3 min.
h. Incubate the reaction mix at decreasing temperature from 56ºC to 36ºC at the rate of 2ºC per 2 hr per step. Set the final step at 4ºC to keep the reaction mix chilled until the next step after incubation. It takes overnight to finish the incubation.
i. Next day, add 150 µl of diluted RNAse mix (1:100) into the reaction mix, and incubate at 37ºC for 1 hr to digest the single stranded RNA.
j. Stop the reaction by adding 225 µl of RNAse Inactivation & Precipitation Buffer. And then add 2 µl of carrier RNA (1 µg/µl), and 75 µl ethanol.
k. Vortex and mix well the reaction mix. Store at -80ºC for at least 1 hr.
q. Precipitate the RNA by centrifugation at maximum speed for 30 min at 4ºC. There is a tiny blue RNA pellet at the bottom of the tube. Carefully remove the supernatant without touching the pellet.
r. Spin the tube again to collect and carefully remove the residue of supernatant.

s. Resuspend the RNA pellet in 15 µl loading dye. Denature RNA at 95ºC for 3 min, and then the samples are ready for loading on 6% urea-PAGE.

4. Cast 6% urea-PAGE gel before taking out the reactions from incubation,

a. Set up the gel cassette. Two glass plates (size: 16x19.7 cm, and 19x19.7 cm) are washed by detergent and the insides wiped with Methanol. Let them air dry. Then wipe inside of the big plate with Sigmacote and dry in the hood (Note: Sigmacote is toxic and volatile, so the operation should be in the hood). The thickness of two side spacers and one bottom spacer used is 0.5 mm. The two plates are clipped together tightly with big binder clips on both sides and bottom.
b. Reagents, buffers and gel casting

10xTBE buffer

Tris-base	110 g
Boric acid	55 g
EDTA	5.8 g

Dissolve in 1L DEPC-treated water.

30% Acrylamide : Bis Mix (19:1)

Acrylamide	150 g
N.N'-Bis-methylene Acrylamide	4 g

Bring up to 500 ml with DEPC-treated water
Filter and store at 4ºC.

6% urea-PAGE gel

Urea	12 g
10X TBE	2.5 ml
30% Acrylamide: Bis Mix (19:1)	5 ml
H_2O	8 ml
TEMED	15 µl
10% ammonium persulfate	200 µl

Before adding TEMED and 10% ammonium persulfate, stir at room temperature till urea is completely dissolved. Then, mix and pipette the gel medium slowly into the gel cassette, trying not to leave any air bubbles. If there is any bubble, use a spacer to push it out. Then insert the 0.5 mm comb on the top of the gel. ¾ of the length of the comb teeth, not the whole teeth, should be in the gel medium, otherwise, it is hard to rinse the bottom of the wells. Still try not to produce any bubble. Wrap the gel cassette up and let it dry at room temperature for 2-3 hrs until use.

5. Load the gel cassette into the Vertical Gel Electrophoresis System (Bethesda Research Laboratories, Life Technologies, Inc. Gaithersburg). Fill the top tank and the bottom tank with 1x TBE buffer. Before loading the sample on the gel, pre-run the gel for at least 30 min. Rinse the wells and blow off the air bubbles at the bottom of the gel using a syringe right before loading.

6. Load samples on the gel and run at 250 V for about 3-4 hr until the blue dye approaches the bottom.

7. Take down the gel cassette and take off the binder clips. Use a spacer to separate the glass plates. The gel will stick to the big piece of plate that is wiped with Sigmacote. Cover the gel with a 3 mm Whatman paper and carefully peel the gel from the glass plate. Wrap the gel and paper with plastic film.

8. Dry the gel in a vacuum gel dryer (Bio-Rad) at 80ºC for 2 hr and expose it to X-ray film and store at -80ºC overnight.

Appendix C

In Vitro Translation Assay

1. m7G capped mRNA preparation by in vitro transcription (mMESSAGE mMACHINE T7 kit, Ambion, Austin).

a. Plasmids of 20 – 40 µg are digested with the restriction enzymes PvuII and Sac I in a 100 µl reaction mixture.
b. Digestion products are separated on 1% agarose gel and the ~1.8 kb fragments are cut out under UV light and purified using Qiaquick Gel Extraction Kit (Qiagen).
c. The volume of the gel-purified fragment is decreased to about 10 µl by vacuum concentration at 60ºC for about 25 min, and the fragments are used as DNA template in *in vitro* transcription reactions.
d. Assemble the *in vitro* transcription reaction mixtures in 0.5 ml tubes as follows:

Reagents	Volume
DNA template	5 µl
2x NTP	10 µl
α- ^{32}P- UTP	1 µl
10* buffer	2 µl
Enzyme Mix	2 µl
Total volume	20 µl

e. Gently flick to mix and spin to collect all at the bottom of the tubes. The reaction mixtures are incubated in heat block at 37ºC for 1 hr.
f. Stop the reactions on ice and remove 2 µl of the products for yield quantitation.
g. Add 1 µl of DNAout enzyme to degrade the DNA templates and incubate the mix at 37ºC for 15 min.
h. Stop the reactions by adding 20 µl of RNAse-free water and 25 µl of lithium chloride precipitation solution, and mix thoroughly and store at -80ºC for at least 1 hr for RNA precipitation.

2. Lithium chloride precipitation of mRNA.

a. Centrifuge the chilled mRNA solutions at 4 °C for 30 min at maximum speed to pellet the RNAs.
b. Carefully remove the supernatants. Wash the pellets twice with 250 µl of the mixture of DEPC-treated water and ethanol (30:70), and re-centrifuge to maximize removal of unincorporated nucleotides.
c. Carefully remove the supernatants and dry the mRNA pellets for 2-5 min
d. Resuspend the mRNAs in an appropriate volume of DEPC-H_2O to make 1 µg/ µl RNA concentration according to the yield calculated.

3. Quantitation of the mRNA yield by trace radiolabeling

a. The in vitro transcription reaction products of 2 µl of are added into 198 µl of a carrier DNA solution (1 µg/µl of shredded salmon DNA, Ambion, Austin).

b. Half of the carrier DNA solution passes through NucAway Spin Columns (Ambion, Austin) to remove free nucleotides. Briefly, tap NucAway Spin Columns on bench to collect all beads. Add 650 µl of DEPC-treated water into columns and vortex for one minute to get rid of any air bubbles. Columns are incubated at room temperature for 10 -15 min and chilled at 4ºC till use. Five minutes before use, columns are centrifuged at 800x g for 2 min at 4 ºC to remove the solution. After adding 100µl of the carrier DNA solution plus reaction product, columns are centrifuged again at 800x g for 2 min at 4 ºC to remove free nucleotide. The elution solution is used for scintillation counting.

c. Scintillation counts the half of the carrier DNA solution and the elution solution from the NucAway Spin Column.

d. Calculate the incorporation efficiency of α- ^{32}P- UTP into mRNA which is the percentage determined by the following formula:

$$\frac{\text{CPM of elution solution (without free radio-labeled nucleot}}{\text{CPM of solution before elution (with free radio-labeled nucleotide)}} \text{ X } 100\%$$

e. Calculation of the yield of mRNA: 1% incorporation corresponds to 2 µg of mRNA.

4. *In vitro* translation reaction

a. Prepare mRNA solutions of 100, 20, 10, and 2 ng/µl by series dilution: 5 µl of the stock solution (1 µg/µl) into 45 µl DEPC-treated water to make 100 ng/ µl; 10 µl of 100 ng/µl solution into 40 µl DEPC-treated water to make 20 ng/µl; 5 µl of 100 ng/µl solution into 45 µl water to make 10 ng/µl; and 5 µl of 20 ng/µl solution into 45 µl water to make 2 ng/µl.

b. Assemble *in vitro* translation reaction mixtures in 0.5 tubes as follows:

Reagents	Volume
Rabbit reticulocyte lysate	22 µl
Amino acids mix minus leucine	0.5 µl
Amino acids mix minus Methionine	0.5 µl
RNasin ribonuclease inhibitor (40 U/µl)	1 µl
mRNA	1 or 2 µl
DEPC-treated water	7 or 6 µl
Total volume	30 µl

c. Incubate the reaction mix at 30ºC for 1 hr and stop the reaction on ice

d. Measure the firefly luciferase activity using the Luciferase Assay System.

Appendix D

Site-directed mutagenesis (QuikChange II Site-directed Mutagenesis Kit, Stratagene)

1. Design primers. Primers must be longer than 27 nucleotides. Point mutation must be in the middle of the primer. Tm of primers calculated Stratagene QuickChange Tm Calculator must be higher than 75ºC for point mutation. Primers are better if they end with 1 or 2 G or C.

2. Assemble the PCR reactions as follows:

Reagents	Volume or amount
10X reaction buffer	5 µl
Plasmid	10 to 50 ng
Forward primer	125 ng
Reverse primer	125 ng
dNTP mixture	1 µl
DEPC-treated water	Up to 50 µl

Then add 1 µl of *PfuTurbo* DNA polymerase.

3. PCR amplification.
   The first cycle
   Step: 1) 95°C for 30 sec
   2) 95 °C for 30 sec
   3) 55 °C for 1 min
   4) 68 °C for 1 min/kb of plasmid length

Repeat step 2 to 4 12 times if it is a point mutation, 18 times if a multiple amino acid deletion or insertion.

4. Following the temperature cycling, place the reaction on ice for 2 minutes.
5. Add 1 µl of the Dpn I restriction enzyme (10 U/µl) to the amplification reaction. Then incubate the reaction at 37 °C for 1 hr to digest the parental supercoiled dsDNA.
6. After the competent cells have melted on ice slowly, add 1 µl of the Dpn I treated DNA reaction product into 50 µl of the competent cells, gently flip the tube, and keep the transformation reaction on ice for 30 min. Then heatshock the transformation reaction at 42ºC in a waterbath for 45 sec, and place on ice for 2 min.
7. Add 500 µl of S.O.C medium (Invitrogen) into the transformation reaction and incubate for exactly 1 hr at 37ºC at 250 rpm in shaker.
8. Inoculate 100 to 200 µl of culture solution of Step 7 onto Agarose-LB plate containing 100ng/ml ampicillin and incubate at 37ºC overnight.

Appendix E

The first strand of cDNA preparation (SuperScript III First-Strand Synthesis for RT-PCR).

1. Prepare RNA/primer Mix as following

Reagents	Volume
Total RNA (1µg/µl)	1 µl
50 ng/ µl random hexamers	1 µl
10 mM dNTP	1 µl
DEPC-ddH2O	7 µl
Total Volume	10 µl

Incubate RNA/primer Mix at 65°C for 5 minutes.

2. Prepare cDNA synthesis Mix as following

Reagents	Volume
10X RT buffer	2 µl
25 mM MgCl2	4 µl
0.1 M DTT	2 µl
RNaseOUT (40 U/µl)	1 µl
SuperScript III RT (200 U/µl)	1 µl
Total Volume	10 µl

3. Combine 10 µl cDNA syntheses Mix and RNA/primer Mix.
4. Incubate the combined Mix at 25°C for 10 min, 50°C for 50 min, and then 85°C for 5 min. Keep the reaction at 4°C.
5. Add 1 µl of RNAse H into the reaction and incubate for 20 min.
6. Store cDNA at -20°C till use.

Appendix F

Online programs

1. Translate Tool: a tool which allows the translation of a nucleotide (DNA/RNA) sequence to a protein sequence.
http://www.expasy.org/tools/dna.html

2. RestrictionMapper: maps sites for restriction enzymes in DNA sequences.
http://www.restrictionmapper.org/

3. Oligonucleotide Properties Calculator: calculates Tm and checks self-complementarity.
http://www.basic.northwestern.edu/biotools/oligocalc.html

4. RNA mfold: predicts RNA secondary structure.
http://frontend.bioinfo.rpi.edu/applications/mfold/cgi-bin/rna-form1.cgi

5. Stratagene Quikchange Primer Tm Calculator: calculates the Tm of oligos specially for QuikChange® Site-Directed Mutagenesis kits
http://www.stratagene.com/QPCR/tmCalc.aspx

REFERENCES

[1] M. Dean, and T. Annilo, Evolution of the ATP-binding cassette (ABC) transporter superfamily in vertebrates, Annu Rev Genomics Hum Genet 6 (2005) 123-142.

[2] D. Keppler, and J. Kartenbeck, The canalicular conjugate export pump encoded by the cmrp/cmoat gene, Prog Liver Dis 14 (1996) 55-67.

[3] M. Kool, M. de Haas, G. L. Scheffer, R. J. Scheper, M. J. van Eijk, J. A. Juijn, F. Baas, and P. Borst, Analysis of expression of cMOAT (MRP2), MRP3, MRP4, and MRP5, homologues of the multidrug resistance-associated protein gene (MRP1), in human cancer cell lines, Cancer Res 57 (1997) 3537-3547.

[4] M. Buchler, J. Konig, M. Brom, J. Kartenbeck, H. Spring, T. Horie, and D. Keppler, cDNA cloning of the hepatocyte canalicular isoform of the multidrug resistance protein, cMrp, reveals a novel conjugate export pump deficient in hyperbilirubinemic mutant rats, J Biol Chem 271 (1996) 15091-15098.

[5] C. C. Paulusma, M. Kool, P. J. Bosma, G. L. Scheffer, F. ter Borg, R. J. Scheper, G. N. Tytgat, P. Borst, F. Baas, and R. P. Oude Elferink, A mutation in the human canalicular multispecific organic anion transporter gene causes the Dubin-Johnson syndrome, Hepatology 25 (1997) 1539-1542.

[6] T. P. Schaub, J. Kartenbeck, J. Konig, O. Vogel, R. Witzgall, W. Kriz, and D. Keppler, Expression of the conjugate export pump encoded by the mrp2 gene in the apical membrane of kidney proximal tubules, J Am Soc Nephrol 8 (1997) 1213-1221.

[7] T. P. Schaub, J. Kartenbeck, J. Konig, H. Spring, J. Dorsam, G. Staehler, S. Storkel, W. F. Thon, and D. Keppler, Expression of the MRP2 gene-encoded conjugate export pump in human kidney proximal tubules and in renal cell carcinoma, J Am Soc Nephrol 10 (1999) 1159-1169.

[8] M. F. Fromm, H. M. Kauffmann, P. Fritz, O. Burk, H. K. Kroemer, R. W. Warzok, M. Eichelbaum, W. Siegmund, and D. Schrenk, The effect of rifampin treatment on intestinal expression of human MRP transporters, Am J Pathol 157 (2000) 1575-1580.

[9] G. E. Sandusky, K. S. Mintze, S. E. Pratt, and A. H. Dantzig, Expression of multidrug resistance-associated protein 2 (MRP2) in normal human tissues and carcinomas using tissue microarrays, Histopathology 41 (2002) 65-74.

[10] A. D. Mottino, T. Hoffman, L. Jennes, J. Cao, and M. Vore, Expression of multidrug resistance-associated protein 2 in small intestine from pregnant and

postpartum rats, Am J Physiol Gastrointest Liver Physiol 280 (2001) G1261-1273.

[11] J. Konig, Nies AT, Cui Y, Keppler D., in London: Academic Press, 2003 pp. pp 423-443.

[12] D. Rost, J. Konig, G. Weiss, E. Klar, W. Stremmel, and D. Keppler, Expression and localization of the multidrug resistance proteins MRP2 and MRP3 in human gallbladder epithelia, Gastroenterology 121 (2001) 1203-1208.

[13] A. Soontornmalai, M. L. Vlaming, and J. M. Fritschy, Differential, strain-specific cellular and subcellular distribution of multidrug transporters in murine choroid plexus and blood-brain barrier, Neuroscience 138 (2006) 159-169.

[14] H. E. Meyer zu Schwabedissen, G. Jedlitschky, M. Gratz, S. Haenisch, K. Linnemann, C. Fusch, I. Cascorbi, and H. K. Kroemer, Variable expression of MRP2 (ABCC2) in human placenta: influence of gestational age and cellular differentiation, Drug Metab Dispos 33 (2005) 896-904.

[15] J. Kartenbeck, U. Leuschner, R. Mayer, and D. Keppler, Absence of the canalicular isoform of the MRP gene-encoded conjugate export pump from the hepatocytes in Dubin-Johnson syndrome, Hepatology 23 (1996) 1061-1066.

[16] C. C. Paulusma, P. J. Bosma, G. J. Zaman, C. T. Bakker, M. Otter, G. L. Scheffer, R. J. Scheper, P. Borst, and R. P. Oude Elferink, Congenital jaundice in rats with a mutation in a multidrug resistance-associated protein gene, Science 271 (1996) 1126-1128.

[17] K. Ito, H. Suzuki, T. Hirohashi, K. Kume, T. Shimizu, and Y. Sugiyama, Molecular cloning of canalicular multispecific organic anion transporter defective in EHBR, Am J Physiol 272 (1997) G16-22.

[18] P. Borst, R. Evers, M. Kool, and J. Wijnholds, The multidrug resistance protein family, Biochim Biophys Acta 1461 (1999) 347-357.

[19] J. Konig, A. T. Nies, Y. Cui, I. Leier, and D. Keppler, Conjugate export pumps of the multidrug resistance protein (MRP) family: localization, substrate specificity, and MRP2-mediated drug resistance, Biochim Biophys Acta 1461 (1999) 377-394.

[20] Y. Cui, J. Konig, J. K. Buchholz, H. Spring, I. Leier, and D. Keppler, Drug resistance and ATP-dependent conjugate transport mediated by the apical multidrug resistance protein, MRP2, permanently expressed in human and canine cells, Mol Pharmacol 55 (1999) 929-937.

[21] H. M. Kauffmann, D. Keppler, J. Kartenbeck, and D. Schrenk, Induction of cMrp/cMoat gene expression by cisplatin, 2-acetylaminofluorene, or cycloheximide in rat hepatocytes, Hepatology 26 (1997) 980-985.

[22] T. Tanaka, T. Uchiumi, E. Hinoshita, A. Inokuchi, S. Toh, M. Wada, H. Takano, K. Kohno, and M. Kuwano, The human multidrug resistance protein 2 gene: functional characterization of the 5'-flanking region and expression in hepatic cells, Hepatology 30 (1999) 1507-1512.

[23] H. R. Kast, B. Goodwin, P. T. Tarr, S. A. Jones, A. M. Anisfeld, C. M. Stoltz, P. Tontonoz, S. Kliewer, T. M. Willson, and P. A. Edwards, Regulation of multidrug resistance-associated protein 2 (ABCC2) by the nuclear receptors pregnane X receptor, farnesoid X-activated receptor, and constitutive androstane receptor, J Biol Chem 277 (2002) 2908-2915.

[24] T. A. Vos, G. J. Hooiveld, H. Koning, S. Childs, D. K. Meijer, H. Moshage, P. L. Jansen, and M. Muller, Up-regulation of the multidrug resistance genes, Mrp1 and Mdr1b, and down-regulation of the organic anion transporter, Mrp2, and the bile salt transporter, Spgp, in endotoxemic rat liver, Hepatology 28 (1998) 1637-1644.

[25] R. Kubitz, M. Wettstein, U. Warskulat, and D. Haussinger, Regulation of the multidrug resistance protein 2 in the rat liver by lipopolysaccharide and dexamethasone, Gastroenterology 116 (1999) 401-410.

[26] M. Trauner, M. Arrese, C. J. Soroka, M. Ananthanarayanan, T. A. Koeppel, S. F. Schlosser, F. J. Suchy, D. Keppler, and J. L. Boyer, The rat canalicular conjugate export pump (Mrp2) is down-regulated in intrahepatic and obstructive cholestasis, Gastroenterology 113 (1997) 255-264.

[27] L. A. Denson, A. Bohan, M. A. Held, and J. L. Boyer, Organ-specific alterations in RAR alpha:RXR alpha abundance regulate rat Mrp2 (Abcc2) expression in obstructive cholestasis, Gastroenterology 123 (2002) 599-607.

[28] L. A. Denson, K. L. Auld, D. S. Schiek, M. H. McClure, D. J. Mangelsdorf, and S. J. Karpen, Interleukin-1beta suppresses retinoid transactivation of two hepatic transporter genes involved in bile formation, J Biol Chem 275 (2000) 8835-8843.

[29] K. Hisaeda, A. Inokuchi, T. Nakamura, Y. Iwamoto, K. Kohno, M. Kuwano, and T. Uchiumi, Interleukin-1beta represses MRP2 gene expression through inactivation of interferon regulatory factor 3 in HepG2 cells, Hepatology 39 (2004) 1574-1582.

[30] H. Roelofsen, C. T. Bakker, B. Schoemaker, M. Heijn, P. L. Jansen, and R. P. Elferink, Redistribution of canalicular organic anion transport activity in isolated and cultured rat hepatocytes, Hepatology 21 (1995) 1649-1657.

[31] P. Zhang, X. Tian, P. Chandra, and K. L. Brouwer, Role of glycosylation in trafficking of Mrp2 in sandwich-cultured rat hepatocytes, Mol Pharmacol 67 (2005) 1334-1341.

[32] D. Rost, J. Kartenbeck, and D. Keppler, Changes in the localization of the rat canalicular conjugate export pump Mrp2 in phalloidin-induced cholestasis, Hepatology 29 (1999) 814-821.

[33] F. Dombrowski, R. Kubitz, A. Chittattu, M. Wettstein, N. Saha, and D. Haussinger, Electron-microscopic demonstration of multidrug resistance protein 2 (Mrp2) retrieval from the canalicular membrane in response to hyperosmolarity and lipopolysaccharide, Biochem J 348 Pt 1 (2000) 183-188.

[34] D. Haussinger, M. Schmitt, O. Weiergraber, and R. Kubitz, Short-term regulation of canalicular transport, Semin Liver Dis 20 (2000) 307-321.

[35] A. D. Mottino, T. Hoffman, F. A. Crocenzi, E. J. Sanchez Pozzi, M. G. Roma, and M. Vore, Disruption of function and localization of tight junctional structures and Mrp2 in sustained estradiol-17beta-D-glucuronide-induced cholestasis, Am J Physiol Gastrointest Liver Physiol 293 (2007) G391-402.

[36] J. Shoda, M. Kano, K. Oda, J. Kamiya, Y. Nimura, H. Suzuki, Y. Sugiyama, H. Miyazaki, T. Todoroki, S. Stengelin, W. Kramer, Y. Matsuzaki, and N. Tanaka, The expression levels of plasma membrane transporters in the cholestatic liver of patients undergoing biliary drainage and their association with the impairment of biliary secretory function, Am J Gastroenterol 96 (2001) 3368-3378.

[37] H. Kojima, A. T. Nies, J. Konig, W. Hagmann, H. Spring, M. Uemura, H. Fukui, and D. Keppler, Changes in the expression and localization of hepatocellular transporters and radixin in primary biliary cirrhosis, J Hepatol 39 (2003) 693-702.

[38] H. Kipp, and I. M. Arias, Intracellular trafficking and regulation of canalicular ATP-binding cassette transporters, Semin Liver Dis 20 (2000) 339-351.

[39] Z. C. Gatmaitan, A. T. Nies, and I. M. Arias, Regulation and translocation of ATP-dependent apical membrane proteins in rat liver, Am J Physiol 272 (1997) G1041-1049.

[40] S. Kikuchi, M. Hata, K. Fukumoto, Y. Yamane, T. Matsui, A. Tamura, S. Yonemura, H. Yamagishi, D. Keppler, and S. Tsukita, Radixin deficiency causes

conjugated hyperbilirubinemia with loss of Mrp2 from bile canalicular membranes, Nat Genet 31 (2002) 320-325.

[41] H. Kojima, S. Sakurai, H. Yoshiji, M. Uemura, M. Yoshikawa, and H. Fukui, The role of radixin in altered localization of canalicular conjugate export pump Mrp2 in cholestatic rat liver, Hepatol Res 38 (2008) 202-210.

[42] H. Kojima, S. Sakurai, M. Uemura, K. Kitamura, H. Kanno, Y. Nakai, and H. Fukui, Disturbed colocalization of multidrug resistance protein 2 and radixin in human cholestatic liver diseases, J Gastroenterol Hepatol (2007).

[43] Q. Yang, R. Onuki, C. Nakai, and Y. Sugiyama, Ezrin and radixin both regulate the apical membrane localization of ABCC2 (MRP2) in human intestinal epithelial Caco-2 cells, Exp Cell Res 313 (2007) 3517-3525.

[44] J. Cao, L. Huang, Y. Liu, T. Hoffman, B. Stieger, P. J. Meier, and M. Vore, Differential regulation of hepatic bile salt and organic anion transporters in pregnant and postpartum rats and the role of prolactin, Hepatology 33 (2001) 140-147.

[45] J. Cao, B. Stieger, P. J. Meier, and M. Vore, Expression of rat hepatic multidrug resistance-associated proteins and organic anion transporters in pregnancy, Am J Physiol Gastrointest Liver Physiol 283 (2002) G757-766.

[46] B. R. Jones, W. Li, J. Cao, T. A. Hoffman, P. M. Gerk, and M. Vore, The role of protein synthesis and degradation in the post-transcriptional regulation of rat multidrug resistance-associated protein 2 (Mrp2, Abcc2), Mol Pharmacol 68 (2005) 701-710.

[47] D. R. Johnson, S. S. Habeebu, and C. D. Klaassen, Increase in bile flow and biliary excretion of glutathione-derived sulfhydryls in rats by drug-metabolizing enzyme inducers is mediated by multidrug resistance protein 2, Toxicol Sci 66 (2002) 16-26.

[48] A. D. Mottino, T. Hoffman, L. Jennes, and M. Vore, Expression and localization of multidrug resistant protein mrp2 in rat small intestine, J Pharmacol Exp Ther 293 (2000) 717-723.

[49] G. Zollner, P. Fickert, R. Zenz, A. Fuchsbichler, C. Stumptner, L. Kenner, P. Ferenci, R. E. Stauber, G. J. Krejs, H. Denk, K. Zatloukal, and M. Trauner, Hepatobiliary transporter expression in percutaneous liver biopsies of patients with cholestatic liver diseases, Hepatology 33 (2001) 633-646.

[50] J. Lee, and J. L. Boyer, Molecular alterations in hepatocyte transport mechanisms in acquired cholestatic liver disorders, Semin Liver Dis 20 (2000) 373-384.

[51] M. G. Elferink, P. Olinga, A. L. Draaisma, M. T. Merema, K. N. Faber, M. J. Slooff, D. K. Meijer, and G. M. Groothuis, LPS-induced downregulation of MRP2 and BSEP in human liver is due to a posttranscriptional process, Am J Physiol Gastrointest Liver Physiol 287 (2004) G1008-1016.

[52] G. Lee, and M. Piquette-Miller, Cytokines alter the expression and activity of the multidrug resistance transporters in human hepatoma cell lines; analysis using RT-PCR and cDNA microarrays, J Pharm Sci 92 (2003) 2152-2163.

[53] M. Kozak, Point mutations define a sequence flanking the AUG initiator codon that modulates translation by eukaryotic ribosomes, Cell 44 (1986) 283-292.

[54] Y. Furuichi, and A. J. Shatkin, Viral and cellular mRNA capping: past and prospects, Adv Virus Res 55 (2000) 135-184.

[55] A. C. Gingras, B. Raught, and N. Sonenberg, eIF4 initiation factors: effectors of mRNA recruitment to ribosomes and regulators of translation, Annu Rev Biochem 68 (1999) 913-963.

[56] T. von der Haar, J. D. Gross, G. Wagner, and J. E. McCarthy, The mRNA cap-binding protein eIF4E in post-transcriptional gene expression, Nat Struct Mol Biol 11 (2004) 503-511.

[57] K. Berthelot, M. Muldoon, L. Rajkowitsch, J. Hughes, and J. E. McCarthy, Dynamics and processivity of 40S ribosome scanning on mRNA in yeast, Mol Microbiol 51 (2004) 987-1001.

[58] M. Kozak, Regulation of translation via mRNA structure in prokaryotes and eukaryotes, Gene 361 (2005) 13-37.

[59] J. D. Short, and C. M. Pfarr, Translational regulation of the JunD messenger RNA, J Biol Chem 277 (2002) 32697-32705.

[60] M. Kozak, Circumstances and mechanisms of inhibition of translation by secondary structure in eucaryotic mRNAs, Mol Cell Biol 9 (1989) 5134-5142.

[61] A. W. van der Velden, K. van Nierop, H. O. Voorma, and A. A. Thomas, Ribosomal scanning on the highly structured insulin-like growth factor II-leader 1, Int J Biochem Cell Biol 34 (2002) 286-297.

[62] A. G. Hinnebusch, Translational regulation of GCN4 and the general amino acid control of yeast, Annu Rev Microbiol 59 (2005) 407-450.

[63] M. Kozak, Effects of intercistronic length on the efficiency of reinitiation by eucaryotic ribosomes, Mol Cell Biol 7 (1987) 3438-3445.

[64] D. R. Morris, and A. P. Geballe, Upstream open reading frames as regulators of mRNA translation, Mol Cell Biol 20 (2000) 8635-8642.

[65] A. Gaba, Z. Wang, T. Krishnamoorthy, A. G. Hinnebusch, and M. S. Sachs, Physical evidence for distinct mechanisms of translational control by upstream open reading frames, EMBO J 20 (2001) 6453-6463.

[66] C. Vilela, and J. E. McCarthy, Regulation of fungal gene expression via short open reading frames in the mRNA 5'untranslated region, Mol Microbiol 49 (2003) 859-867.

[67] J. Cao, and A. P. Geballe, Translational inhibition by a human cytomegalovirus upstream open reading frame despite inefficient utilization of its AUG codon, J Virol 69 (1995) 1030-1036.

[68] J. R. Hill, and D. R. Morris, Cell-specific translational regulation of S-adenosylmethionine decarboxylase mRNA. Dependence on translation and coding capacity of the cis-acting upstream open reading frame, J Biol Chem 268 (1993) 726-731.

[69] G. J. Mize, H. Ruan, J. J. Low, and D. R. Morris, The inhibitory upstream open reading frame from mammalian S-adenosylmethionine decarboxylase mRNA has a strict sequence specificity in critical positions, J Biol Chem 273 (1998) 32500-32505.

[70] J. Cao, and A. P. Geballe, Ribosomal release without peptidyl tRNA hydrolysis at translation termination in a eukaryotic system, Rna 4 (1998) 181-188.

[71] F. Diba, C. S. Watson, and B. Gametchu, 5'UTR sequences of the glucocorticoid receptor 1A transcript encode a peptide associated with translational regulation of the glucocorticoid receptor, J Cell Biochem 81 (2001) 149-161.

[72] A. Raney, A. C. Baron, G. J. Mize, G. L. Law, and D. R. Morris, In vitro translation of the upstream open reading frame in the mammalian mRNA encoding S-adenosylmethionine decarboxylase, J Biol Chem 275 (2000) 24444-24450.

[73] M. Oyama, C. Itagaki, H. Hata, Y. Suzuki, T. Izumi, T. Natsume, T. Isobe, and S. Sugano, Analysis of small human proteins reveals the translation of upstream open reading frames of mRNAs, Genome Res 14 (2004) 2048-2052.

[74] P. L. Jansen, W. H. Peters, and D. K. Meijer, Hepatobiliary excretion of organic anions in double-mutant rats with a combination of defective canalicular

transport and uridine 5'-diphosphate-glucuronyltransferase deficiency, Gastroenterology 93 (1987) 1094-1103.

[75] P. M. Gerk, and M. Vore, Regulation of expression of the multidrug resistance-associated protein 2 (MRP2) and its role in drug disposition, J Pharmacol Exp Ther 302 (2002) 407-415.

[76] N. Ballatori, and A. T. Truong, Glutathione as a primary osmotic driving force in hepatic bile formation, Am J Physiol 263 (1992) G617-624.

[77] M. Wagner, E. Halilbasic, H. U. Marschall, G. Zollner, P. Fickert, C. Langner, K. Zatloukal, H. Denk, and M. Trauner, CAR and PXR agonists stimulate hepatic bile acid and bilirubin detoxification and elimination pathways in mice, Hepatology 42 (2005) 420-430.

[78] J. M. Maher, X. Cheng, A. L. Slitt, M. Z. Dieter, and C. D. Klaassen, Induction of the multidrug resistance-associated protein family of transporters by chemical activators of receptor-mediated pathways in mouse liver, Drug Metab Dispos 33 (2005) 956-962.

[79] D. R. Johnson, G. L. Guo, and C. D. Klaassen, Expression of rat Multidrug Resistance Protein 2 (Mrp2) in male and female rats during normal and pregnenolone-16alpha-carbonitrile (PCN)-induced postnatal ontogeny, Toxicology 178 (2002) 209-219.

[80] D. R. Johnson, and C. D. Klaassen, Regulation of rat multidrug resistance protein 2 by classes of prototypical microsomal enzyme inducers that activate distinct transcription pathways, Toxicol Sci 67 (2002) 182-189.

[81] N. K. Gray, and M. Wickens, Control of translation initiation in animals, Annu Rev Cell Dev Biol 14 (1998) 399-458.

[82] A. W. van der Velden, and A. A. Thomas, The role of the 5' untranslated region of an mRNA in translation regulation during development, Int J Biochem Cell Biol 31 (1999) 87-106.

[83] K. Reynolds, A. M. Zimmer, and A. Zimmer, Regulation of RAR beta 2 mRNA expression: evidence for an inhibitory peptide encoded in the 5'-untranslated region, J Cell Biol 134 (1996) 827-835.

[84] J. P. Alderete, S. Jarrahian, and A. P. Geballe, Translational effects of mutations and polymorphisms in a repressive upstream open reading frame of the human cytomegalovirus UL4 gene, J Virol 73 (1999) 8330-8337.

[85] C. R. Degnin, M. R. Schleiss, J. Cao, and A. P. Geballe, Translational inhibition mediated by a short upstream open reading frame in the human cytomegalovirus gpUL4 (gp48) transcript, J Virol 67 (1993) 5514-5521.

[86] S. Haenisch, U. Zimmermann, E. Dazert, C. J. Wruck, P. Dazert, W. Siegmund, H. K. Kroemer, R. W. Warzok, and I. Cascorbi, Influence of polymorphisms of ABCB1 and ABCC2 on mRNA and protein expression in normal and cancerous kidney cortex, Pharmacogenomics J 7 (2007) 56-65.

[87] C. G. Dietrich, A. Geier, N. Salein, F. Lammert, E. Roeb, R. P. Oude Elferink, S. Matern, and C. Gartung, Consequences of bile duct obstruction on intestinal expression and function of multidrug resistance-associated protein 2, Gastroenterology 126 (2004) 1044-1053.

[88] Y. Zhang, W. Li, and M. Vore, Translational regulation of rat multidrug resistance-associated protein 2 expression is mediated by upstream open reading frames in the 5' untranslated region, Mol Pharmacol 71 (2007) 377-383.

[89] I. B. Rogozin, A. V. Kochetov, F. A. Kondrashov, E. V. Koonin, and L. Milanesi, Presence of ATG triplets in 5' untranslated regions of eukaryotic cDNAs correlates with a 'weak' context of the start codon, Bioinformatics 17 (2001) 890-900.

[90] A. V. Kochetov, A. Sarai, I. B. Rogozin, V. K. Shumny, and N. A. Kolchanov, The role of alternative translation start sites in the generation of human protein diversity, Mol Genet Genomics 273 (2005) 491-496.

[91] H. A. Meijer, and A. A. Thomas, Control of eukaryotic protein synthesis by upstream open reading frames in the 5'-untranslated region of an mRNA, Biochem J 367 (2002) 1-11.

[92] A. V. Kochetov, [Alternative translation start sites and their significance for eukaryotic proteome], Mol Biol (Mosk) 40 (2006) 788-795.

[93] D. E. Neafsey, and J. E. Galagan, Dual modes of natural selection on upstream open reading frames, Mol Biol Evol 24 (2007) 1744-1751.

[94] M. Cvijovic, D. Dalevi, E. Bilsland, G. J. Kemp, and P. Sunnerhagen, Identification of putative regulatory upstream ORFs in the yeast genome using heuristics and evolutionary conservation, BMC Bioinformatics 8 (2007) 295.

[95] M. Matsui, N. Yachie, Y. Okada, R. Saito, and M. Tomita, Bioinformatic analysis of post-transcriptional regulation by uORF in human and mouse, FEBS Lett 581 (2007) 4184-4188.

[96] R. J. Jackson, Alternative mechanisms of initiating translation of mammalian mRNAs, Biochem Soc Trans 33 (2005) 1231-1241.

[97] M. Kozak, A short leader sequence impairs the fidelity of initiation by eukaryotic ribosomes, Gene Expr 1 (1991) 111-115.

[98] M. Kozak, Constraints on reinitiation of translation in mammals, Nucleic Acids Res 29 (2001) 5226-5232.

[99] A. V. Kochetov, S. Ahmad, V. Ivanisenko, O. A. Volkova, N. A. Kolchanov, and A. Sarai, uORFs, reinitiation and alternative translation start sites in human mRNAs, FEBS Lett 582 (2008) 1293-1297.

[100] B. G. Luukkonen, W. Tan, and S. Schwartz, Efficiency of reinitiation of translation on human immunodeficiency virus type 1 mRNAs is determined by the length of the upstream open reading frame and by intercistronic distance, J Virol 69 (1995) 4086-4094.

[101] H. Ruan, J. R. Hill, S. Fatemie-Nainie, and D. R. Morris, Cell-specific translational regulation of S-adenosylmethionine decarboxylase mRNA. Influence of the structure of the 5' transcript leader on regulation by the upstream open reading frame, J Biol Chem 269 (1994) 17905-17910.

[102] C. Y. Brown, G. J. Mize, M. Pineda, D. L. George, and D. R. Morris, Role of two upstream open reading frames in the translational control of oncogene mdm2, Oncogene 18 (1999) 5631-5637.

[103] J. Cao, and A. P. Geballe, Coding sequence-dependent ribosomal arrest at termination of translation, Mol Cell Biol 16 (1996) 603-608.

[104] P. S. Lovett, and E. J. Rogers, Ribosome regulation by the nascent peptide, Microbiol Rev 60 (1996) 366-385.

[105] T. M. Bosch, I. Meijerman, J. H. Beijnen, and J. H. Schellens, Genetic polymorphisms of drug-metabolising enzymes and drug transporters in the chemotherapeutic treatment of cancer, Clin Pharmacokinet 45 (2006) 253-285.

[106] Y. Tada, M. Wada, T. Migita, J. Nagayama, E. Hinoshita, Y. Mochida, Y. Maehara, M. Tsuneyoshi, M. Kuwano, and S. Naito, Increased expression of multidrug resistance-associated proteins in bladder cancer during clinical course and drug resistance to doxorubicin, Int J Cancer 98 (2002) 630-635.

[107] E. Hinoshita, T. Uchiumi, K. Taguchi, N. Kinukawa, M. Tsuneyoshi, Y. Maehara, K. Sugimachi, and M. Kuwano, Increased expression of an ATP-binding cassette superfamily transporter, multidrug resistance protein 2, in human colorectal carcinomas, Clin Cancer Res 6 (2000) 2401-2407.

[108] K. W. Scotto, Transcriptional regulation of ABC drug transporters, Oncogene 22 (2003) 7496-7511.

[109] T. A. Ince, and K. W. Scotto, Differential utilization of multiple transcription start points accompanies the overexpression of the P-glycoprotein-encoding gene in Chinese hamster lung cells, Gene 156 (1995) 287-290.

[110] T. A. Ince, and K. W. Scotto, Stable transfection of the P-glycoprotein promoter reproduces the endogenous overexpression phenotype: the role of MED-1, Cancer Res 56 (1996) 2021-2024.

[111] A. T. Nies, and D. Keppler, The apical conjugate efflux pump ABCC2 (MRP2), Pflugers Arch 453 (2007) 643-659.

VITA

Yuanyuan Zhang

Date of Birth: February 16, 1977
Place of Birth: Nanchong, Sichuan, People's Republic of China

Education

09/1999– 08/2002 Institute for Nutrition and Food Safety, Chinese Center for Disease Control and Prevention, Beijing, China
Degree: M.S.
Major: Analytical Toxicology:
Mentor: Dr. Yongning Wu

09/1995 – 08/1999 College of Pharmacy, Health Science Center, Peking University, Beijing, China
Degree: B.S.
Major: Pharmacy

Professional Positions

Graduate Research Assistant: 08/2002 – 07/2008
Graduate Center for Toxicology, College of Medicine, University of Kentucky, Lexington, KY

Graduate Research Assistant: 09/1999– 08/2002
Institute for Nutrition and Food Safety, Chinese Center for Disease Control and Prevention, Beijing, China

Publications

Zhang Y, Li W, Vore M. Translational Regulation of Rat Multidrug Resistance-associated Protein 2 Expression is Mediated by Upstream Open Reading Frames in the 5' Untranslated Region. *Mol Pharmacol 71: 377-388, 2007.*

Zhang Y, Wu Y. Toxicological Effect of Clenbuterol in Human and Animals. *Wei Sheng Yan Jiu 31(4): 328-30, 2002. Review.*

Poster Presentations

Zhang Y, Li W, Vore M. Translation of Human Multidrug Resistance Protein 2 (*MRP2*) Gene is under 5' Untranslated Regions (UTRs)-mediated Regulation. *The 3rd Annual Meeting of the Great Lakes Drug Metabolism Discussion Group, 2008, Indianapolis, Indiana.*

Zhang Y, Li W, Vore M. Translation of Human Multidrug Resistance Protein 2 (*MRP2*) Gene is under 5' Untranslated Regions (UTRs)-mediated Regulation. *Keystone symposia: translational regulatory mechanism, 2008, Coeur d'Alene, Idaho.*

Zhang Y, Li W, Vore M. 5' Untranslated Regions (UTRs) of Human Multidrug Resistance Protein 2 (*MRP2*) Gene Regulate in vitro Translation. *The 58th Annual Meeting of the American Association for the Study of Liver Disease (AASLD), 2007, Boston, Massachusetts.*

Zhang Y, Li W, Vore M. Translational Regulation of Human MRP2 Expression. *AAPS workshop on drug transporter in ADME: from the bench to the bedside, 2007, Bethesda, Maryland.*

Zhang Y, Li W, Vore M. Translational Regulation of Rat Mrp2 Protein Expression. *The 56th Annual Meeting of the American Association for the Study of Liver Disease (AASLD), 2005, San Francisco, California.*

Zhang Y, Li W. Vore M, Post-transcriptional Regulation of Rat Mrp2 Expression. *Experimental Biology Meeting (EB), 2005, San Diego, California.*

Zhang Y, Li W, Vore M. Translational Regulation of Human MRP2 Expression. *Clinical and Translational Science Spring Conference, 2007, University of Kentucky, Lexington, Kentucky.*

Zhang Y, Li W, Vore M. Post-transcriptional Regulation of Rat Mrp2 Expression. *The Ohio Valley Chapter Society of Toxicology (OVSOT) Annual Meeting, 2004, University of Kentucky, Lexington, Kentucky.*

Memberships

The American Association for the Advancement of Science (AAAS), 2008

The American Association of Pharmaceutical Scientists (AAPS), 2007.

The American Society for Pharmacology and Experimental Therapeutics (ASPET), 2005.